

## Curriculum Vitae

DAVID P. LANGAN  
davidlangan26@gmail.com

### EDUCATION

**University of Maryland, Baltimore**, Baltimore, MD **July 2016 – Summer 2021**  
School of Medicine, Department of Microbiology and Immunology  
Immunology concentrated PhD  
Graduate Advisor: Kamal D. Moudgil

**Hood College**, Frederick, MD **Aug 2010 – May 2014**  
Bachelor of Arts in Biochemistry

### PROFESSIONAL WORK EXPERIENCE

**University of Maryland, Baltimore**, Baltimore, MD **Mar 2017 – July 2021**  
**PhD Thesis Project** (Mentor: KD Moudgil, MD, PhD)  
“Modulation of inflammation and stromal remodeling processes in autoimmune arthritis by microbial indole derivatives”

- Defined mechanisms of action of microbiota metabolites on key cellular processes in autoimmune arthritis as Lead Project Developer.
- Optimized the protocol (drug solubility, delivery, serum extraction) to assess disease modulation and therapeutic efficacy by my lead metabolites in a rat model of RA.
- Created SOPs for cell assays of inflammation, angiogenesis, and bone remodeling.
- Supported preclinical rodent studies on MS and RA by drug administration, immunohistochemistry, tissue homing analysis, and *ex vivo* studies on lymphocytes.
- Revamped workflows for 96-well formatted assays and qRT-PCR SOP.
- My contributions are noted in high impact articles, local and national conferences.

**Graduate Research Rotation** (Mentor: NJ Singh, PhD) **Jan 2017 – Mar 2017**  
• Characterized s100A4 association with chronic T cell activation using transgenic mouse lymphocytes and by immunophenotyping with Flow cytometry analysis.

**Graduate Research Rotation** (Mentor: SN Vogel, PhD) **July 2016 – Sept 2016**  
• Characterized M1-M2 macrophage plasticity by assessing peritoneal macrophage transcriptional phenotype in response to distinct differentiation conditions.

**United States Army Medical Research Institute of Infectious Diseases**, Frederick MD  
**Research Fellowship** (Mentor: CL Cooper, PhD) **May 2014 – July 2016**

- Developed a fluorescent, confocal microscopy-based high-throughput screening assay with which I screened candidate anti-viral monoclonal antibodies and small molecules.
- Produced antibodies from hybridomas and conducted neutralization screens.
- Made knockdown cells from an shRNAi library to characterize Alphavirus infection.
- Analyzed GP-specific antibody titers from EBOLA vaccine mouse studies.
- My contributions are recognized in the support of two high impact manuscripts.

**Undergraduate Research Internship** (Mentor: CL Cooper, PhD) **June 2013 – May 2014**  
• Constructed plasmids and scaled-up production of GFP-reporter VSV pseudoparticles.  
• Created stable knockdown human THP-1 cells lines by lentivirus shRNAi transduction.

## **RELEVANT SKILLS**

- **Molecular and Immunological techniques** – Highly trained in cell line and primary cell culture, qRT-PCR, DNA/RNA purification, primer design, protein analysis (immuno-blotting & -histochemistry), microscopy, molecular cloning, transfections, transductions, immune functional assays, and multicolor Flow cytometry, ELISAs, and neutralization assays. Versed in serum metabolite extraction and HPLC-UV.
- **Animal Handling and Husbandry** – Capable in bleeding, tissue dissection, drug administration, primary cell isolation, animal husbandry, and rodent disease models.
- **Computational Skills** –ImageJ, FlowJo, GraphPad Prism, NCBI primer-blast, Microsoft Suite, Photoshop, as well as R and Linux for biological application.
- **Lab & Data management** – Lab manager at UMB. Record keeping. SOP creation.
- **Analytical Rigor** – High impact publications. Expertise in ANOVA and *t* tests.
- **Science Communication** –Presented at local and national conferences and seminars.
- **Leadership & Integrity** – I oversaw components of conference organization as the Graduate Research Conference (GRC) student coordinator. Lastly, I am a prospective PhD student interviewer.

## **LEADERSHIP/TEACHING POSITIONS**

**University of Maryland, Baltimore, Baltimore, MD**

*PhD Student Admission Interviewer*

**Feb 2021 – Present**

*2<sup>nd</sup> Year Medical Student Immunology Section Proctor*

**Nov 2020**

*M&I Annual Research Symposium Co-Manager*

**Feb – June 2020**

*Lab Manager (PhD Lab)*

**Dec 2019 – Present**

*Graduate Research Conference Student Coordinator*

**July 2019 – Present**

*Immunology Journal Club Co-Manager*

**Aug 2018 – 2019**

*Session Moderator for OSR GRC*

**July 2018 – Present**

*Qualification Exam Preparation Proctor and/or Tester*

**Feb 2018 – Present**

**USAMRIID, Frederick MD**

*Oversaw the work of high school interns in the lab*

**2014 – 2016**

## **ACADEMIC HONORS/AWARDS**

**University of Maryland, Baltimore, Baltimore, MD**

T32 AI095190 (Aug 2019 – Present) (PI: SN Vogel, PhD)

2020 AARDA Colloquium Scribe (International meeting organized by Noel Rose, MD, PhD and Kamal D Moudgil, MD, PhD)

Aug 2019 MMI SPARK (*Stimulating Participation in Academically Rigorous Kinship*)

**Hood College, Frederick, MD**

Hood College Leadership Award

Mortar Board, National Senior Academic Honors Society

Gamma Sigma Epsilon, Chemistry National Honors Society

## **PROFESSIONAL ORGANIZATIONS:**

FOCIS Member (Nov 2019 – present)

AAI Member (Dec 2019 – present)

## **PEER-REVIEWED PUBLICATIONS**

- 1) **Langan D**, Perkins DJ, Vogel SN, Moudgil KD. Microbiota-Derived Metabolites, Indole-3-aldehyde and Indole-3-acetic Acid, Differentially Modulate Innate Cytokines and Stromal Remodeling Processes Associated with Autoimmune Arthritis. *Int. J. Mol. Sci.* 2021 Feb; 18, 22:4. [Research]
- 2) **Langan D**, Rose NR, Moudgil KD. Common innate pathways to autoimmune disease. *Clin Immunol.* 2020 Feb; 212:108361 [Review]
- 3) **Langan D**, Kim EY, Moudgil KD. Modulation of autoimmune arthritis by environmental 'hygiene' and commensal microbiota. *Cell Immunol.* 2019 May; 339:59-67 [Review]
- 4) Cooper CL, Martins KA, Stronsky SM, **Langan DP**, Steffens J, Van Tongeren S, Bavari S. T-cell-dependent mechanisms promote Ebola VLP-induced antibody responses, but are dispensable for vaccine-mediated protection. *Emerg Microbes Infect.* 2017 Jun; 6(6): e46 [Research]
- 5) Radoshitzky SR, Pegoraro G, Chī XO, D Ng L, Chiang CY, Jozwick L, Clester JC, Cooper CL, Courier D, **Langan DP**, Underwood K, Kuehl KA, Sun MG, Cai Y, Yú SQ, Burk R, Zamani R, Kota K, Kuhn JH, Bavari S. siRNA Screen Identifies Trafficking Host Factors that Modulate Alphavirus Infection. *PLoS Pathog.* 2016 Mar; 12(3): e1005466 [Research]

## **SCIENTIFIC PRESENTATIONS**

- 1) **Langan DP**, Perkins DJ, Vogel SN, Moudgil KD. Microbiota-derived indole derivatives regulate key cellular processes involved in arthritis pathogenesis. [Poster] Virtual Symposium: 2021 Federation of Clinical Immunology Societies; 2021
- 2) **Langan D**, Meka RR, Moudgil KD. Modulation of Pathophysiological Processes of Autoimmune Arthritis by Indole-3-Acetic Acid and Indole-3-Aldehyde. [Poster]. UMB Graduate Research Conference 2020, Baltimore MD
- 3) Langan D, Martins K, Silverstein R, Cooper CL, Bavari S. Generation of THP-1 human monocyte cell lines with RIG-I or MDA-5 receptor knockdown for viral immune response modeling. [Poster]. Dallas, TX: 2014 ACS National Symposium; 2014.

NCBI Bibliography:

<https://www.ncbi.nlm.nih.gov/myncbi/12kt8yzknja5p/bibliography/public/>

## **Abstract**

Title of Dissertation: Modulation of Inflammation and Stromal Remodeling Processes in Autoimmune Arthritis by Microbial Indole Derivatives

David Patrick Langan, Doctor of Philosophy, 2021

Dissertation Directed by: Dr. Kamal D. Moudgil, MD, PhD, Molecular Microbiology and Immunology

Rheumatoid arthritis (RA) is an autoimmune disease characterized by chronic inflammation of the synovial tissue that can lead to joint damage and deformities. Inflammation, new blood vessel formation (angiogenesis), and bone resorption (osteoclastogenesis) are three key processes of the pathophysiology of RA. ‘Dysbiosis’ of the gut microbiota is implicated in RA pathogenesis because it can cause an imbalance in the microbial metabolites that regulate host health and disease. However, there is little information about the impact of two such indole derivatives, indole-3-aldehyde (IAld) and indole-3-acetic acid (I3AA), on arthritis-related processes. Using established cell-based models and the adjuvant-induced arthritis animal model, we conducted a comparative analysis of IAld and I3AA to understand how these metabolites might impact RA pathogenesis. To our surprise, despite their structural similarities, the bioactivities of these two metabolites were profoundly different. IAld, but not I3AA, altered the expression of genes encoding arthritis-associated cytokines (IL-1 $\beta$ , IL-6, VEGF) in RAW 264.7 (murine macrophage) cells stimulated with heat-killed *M. tuberculosis*. Further investigation of this anti-inflammatory activity of IAld suggested that inhibition of the MyD88-dependent

activation of NF- $\kappa$ B and MAPK pathways was unlikely to be involved. IAld also exhibited pro-osteoclastogenic and pro-angiogenic activity. In contrast, I3AA exhibited only anti-angiogenic activity. Both IAld and I3AA are proposed agonists of the aryl hydrocarbon receptor (AhR). However, AhR inhibitor CH-223191 suppressed the anti-angiogenic activity of I3AA, but failed to mitigate any of the effects of IAld. There is a cross-talk between the AhR and Nrf2 pathways, and some plant-derived phytochemicals are multifunctional ligands of both pathways. Our findings show that IAld, unlike I3AA, can suppress the Nrf2-dependent antioxidant response of macrophages to an Nrf2 agonist, but that IAld also potentially reduces intracellular ROS levels during osteoclast differentiation. Furthermore, oral administration of IAld to rats resulted in the reduction of arthritis severity compared to the arthritic control group. Taken together, our findings suggest that the relative bioavailability of these microbial indole derivatives has the potential to influence their immunomodulatory effects in healthy individuals as well as patients with RA.

Modulation of Inflammation and Stromal Remodeling Processes in Autoimmune  
Arthritis by Microbial Indole Derivatives

by  
David P Langan

Dissertation submitted to the faculty of the Graduate School of the  
University of Maryland, Baltimore in partial fulfillment  
of the requirements for the degree of  
Doctor of Philosophy  
2021

## Acknowledgements

Thanks to all those colleagues and mentors that have provided help and resources during my graduate studies at the University of Maryland, Baltimore. A special thanks to my PhD advisor, Dr. Kamal Moudgil, for being highly supportive and for feeding my inquisitive nature. He was very supportive of me developing a novel project for my thesis work and in supporting my aspirational goals. Additionally, I would like to thank the Moudgil lab members with whom I began my dissertation work. Before leaving for other positions, Dr. Rakeshchandra Meka, Dr. Shivaprasad Venkatesha, and Dr. Steven Dudics each provided valuable insights and a helping hand.

Conceptualization of the project and troubleshooting was made easier by having an incredible body of individuals in the Department of Microbiology and Immunology. With the expertise of Dr. Darren Perkins, I quickly incorporated the use of immunoblotting into my technical toolkit. Dr. Katharina Richard and Dr. Kari Ann Shirey gave me insights and the knowledge to run qRT-PCR, analyze these data, and run statistical testing. Thanks to Dr. Apurva Borcar (STAR) and Dr. Daniel Prantner for help in conceptualizing my experimental design for testing how my compounds may regulate Nrf2 activity and the antioxidant response. I would also like to thank Nevil Singh for always having the door open for discussion. These individuals were always there to lend their expertise and insights when asked.

I cannot go without thanking my incredible committee of amazingly accomplished scientists. I have had wonderful discussions with Dr. Brian Polster about building the strongest hypothesis-driven experiments. Dr. Stefanie Vogel was instrumental from start

to finish as a rotation advisor, for believing in me enough to support my training by placing me on her NIH T32 grant (Signaling Pathways in Innate Immunity), and offering resources that made my dissertation possible. Thanks to Dr. Tonya Webb for teaching me the lessons of clarity in my approach to science and ability to communicate my work to ensure success in the future. Additionally, special thanks to Dr. Abdel Hamad for being the outside member of my committee and helping me to rationalize a project that was relevant for translational medicine.

Also, I would like to remember the late Dr. Noel Rose (Department of Pathology at Brigham and Women's Hospital in Boston, MA, USA). I had the pleasure of meeting and working with him on the occasion of an international colloquium on “Common innate pathways to autoimmune disease” (2019) that he had organized in collaboration with Kamal Moudgil and Virginia Ladd (President and Executive Director, the American Autoimmune Related Diseases Association (AARDA)). I will cherish the proceedings of that colloquium that I wrote with Dr. Rose as a coauthor.

Lastly, but not least, thanks to my friends, family, and previous mentors. They are strong sources of moral support and have always been the biggest supporters of my endeavors. My wife Natalie is the rock that grounds me and she has always offered the moral support that kept me going through the lows, and that took great celebration in all my accomplishments.

Because of all of you, I am now ready to turn the page to the next chapter of my career.

# Table of Contents

<b>Acknowledgements</b> .....	iii
<b>List of Tables</b> .....	ix
<b>List of Figures</b> .....	x
<b>List of Abbreviations</b> .....	xii
<b>Chapter 1. Scope of Dissertation</b> .....	1
<b>Chapter 2: General Introduction</b> .....	4
2.1 Introduction to Autoimmune Diseases .....	4
2.2 The Prevalence of Autoimmune Diseases in the United States.....	5
<b>Chapter 3: Rheumatoid Arthritis (RA)</b> .....	7
3.1 The Epidemiology of RA .....	7
3.2 RA Risk Factors.....	9
3.2.1 Genetic Risk Factors for RA.....	9
3.2.2 Environmental Risk Factors for RA .....	10
3.3 Pathophysiology of RA .....	15
3.4 The Role of the Immune System in RA .....	17
3.4.1 Innate Immune Processes Involved in RA Pathogenesis.....	17
3.4.2 Adaptive Immune Processes Involved in RA Pathogenesis .....	21
3.5 Stromal Remodeling in Arthritis .....	24
3.6 Adjuvant-Induced Arthritis (AA): An Animal Model of RA.....	26
3.7 Therapeutic Options for RA .....	29
3.7.1 Corticosteroids .....	31
3.7.2 Non-Steroidal Anti-inflammatory Drugs (NSAIDs) .....	31

3.7.3 Disease-modifying Anti-rheumatic Drugs (DMARDs).....	32
3.7.4 Biologics .....	33
<b>Chapter 4: Microbiome and ‘Hygiene Hypothesis’: Implications for</b>	
<b>Autoimmunity, Including RA.....</b>	<b>34</b>
4.1 ‘Dysbiosis’ in RA and Microbiota Correlates of Disease .....	36
4.2 Beneficial Commensals and Their Bioactive Metabolites .....	38
4.2.1 Short-chain Fatty Acid-metabolizers and SCFAs.....	40
4.2.2 Catabolites of Tryptophan (Indole Derivatives) .....	41
4.2.3 Other Microbiota-derived Immunoregulatory Metabolites that Influence	
Arthritis .....	44
<b>Chapter 5: The Xenobiotic and Antioxidant Responses.....</b>	<b>45</b>
<b>Chapter 6: Materials and Methods.....</b>	<b>49</b>
6.1 Cell Culture.....	49
6.2 Chemicals and Reagents .....	49
6.3 Cytotoxicity Assessment by MTT Assay .....	50
6.4 Quantitative Real-time Polymerase Chain Reaction .....	51
6.5 Determination of the Immunomodulatory Effect of Indole Derivatives on the	
Response of RAW Cells to Mtb-sonicate or LPS.....	52
6.6 Analysis of Cell Signaling by Immunoblot Analysis .....	52
6.7 Osteoclast Generation and Subsequent Testing of the Effect of IAld and I3AA	53
6.8 Analysis of a Role for Nrf2 in Mediating the Effect of IAld on Mφ.....	54
6.9 Intracellular ROS in RANKL-treated RAW Cells and Impact of IAld.....	55

6.10 2D-Matrigel Tube Formation Assay with HUVEC and Subsequent Assessment of the Effect of Indole Derivatives .....	56
6.11 Induction of AA, Disease Evaluation, and IAld Treatment .....	58
6.12 Extraction of Indole Derivatives and Standard Spike Analysis by HPLC-UV .	58
6.13 Statistical Analysis .....	59
<b>Chapter 7: Results</b> .....	<b>60</b>
7.1 Assessment of Cytotoxicity of IAld and I3AA on RAW Cells and HUVEC. ....	60
7.2 IAld, but not I3AA, Inhibits Expression of Several Pro-inflammatory Cytokines by M $\phi$ in Response to Mtb .....	61
7.3 Inhibition of Mtb-induced IL-1 $\beta$ and IL-6 Expression by IAld was Only Partially Reversed by AhR Antagonist CH-223191 .....	62
7.4 IAld-mediated Inhibition of Pro-inflammatory Cytokine Production by RAW Cells Was Not Associated with MyD88-dependent Activation of Canonical NF- $\kappa$ B or MAPK Pathways.....	64
7.5 Modulation of RANKL-induced Differentiation of RAW Cells into Osteoclasts by IAld, but Not I3AA.....	67
7.6 Differential Regulation of Endothelial Cell Tube Formation by IAld and I3AA	71
7.7 AhR Antagonist Inhibited the Anti-angiogenic Effect of I3AA, but Not the Stomal Remodeling Effects of IAld on Endothelial Cells and Osteoclasts.....	75
7.8 Nrf2 Agonism Reverses the Effect of IAld on Osteoclastogenesis. ....	78
7.9 Treatment of AA with IAld. ....	84
<b>Chapter 8. Discussion</b> .....	<b>86</b>
<b>Chapter 9: Summary and Concluding Remarks</b> .....	<b>96</b>

<b>Chapter 10: Future Directions</b> .....	100
<b>Appendices</b> .....	102
<b>References</b> .....	104

## List of Tables

Table 1. USFDA-approved, commonly prescribed drugs for RA. ....	30
Table 2. The impact of exposure to microbes or helminths on disease susceptibility and severity in animal models of autoimmunity.....	35
Table 3. Sequences of in-house designed primers .....	51
Table 4. Summary of results from the completion of Aim 1 .....	98
Table 5. Summary of results from the completion of Aim 2 .....	98
Table 6. Summary of results from the completion of Aim 3 .....	98

## List of Figures

Figure 1. Age-standardized prevalence rate (per 100,000), both sexes 2017. ....	8
Figure 2. The ‘Hygiene hypothesis’ .....	13
Figure 3. Key mediators of RA pathogenesis. ....	18
Figure 4. Adjuvant-induced arthritis (AA): An animal model of RA.....	28
Figure 5. The impact of diet and exposure to exogenous compounds through the gut has critical implication for health and disease. ....	39
Figure 6. Microbiota-derived catabolites of tryptophan (indole derivatives).....	43
Figure 7. The environment is a source of exogenous AhR and Nrf2 ligands that regulate RA pathology. ....	48
Figure 8. The generation of osteoclasts from RAW cells. ....	54
Figure 9. Experimental design of how a potential role for the AhR and Nrf2 pathways in mediating the observed effects of the indole derivatives were tested.....	56
Figure 10. The 2D-Matrigel tube formation assay using HUVEC. ....	57
Figure 11. Assessment of cellular cytotoxicity of I3AA and IAld by MTT assay. ....	60
Figure 12. IAld inhibits the production of subsets of pro-inflammatory cytokines and other mediators by RAW cells in response to Mtb. ....	62
Figure 13. AhR antagonist CH-223191 partially reversed IAld-induced inhibition of the IL-1 $\beta$ , but not IL-6 response of Mtb-treated M $\phi$ . ....	63
Figure 14. IAld-mediated inhibition of pro-inflammatory cytokines apparently was not induced via the MyD88-dependent signaling pathway.....	66
Figure 15. Osteoclast numbers and cell morphology are altered in the presence of IAld.	68
Figure 16. IAld enhances the bone remodeling process of osteoclastogenesis. ....	70

Figure 17. HUVEC tube morphology in the presence of IAld and I3AA in a 2D-Matrigel tube formation assay. .... 72

Figure 18. IAld and I3AA differentially influence angiogenesis. .... 74

Figure 19. AhR antagonist CH-223191 inhibits the disruption of angiogenesis by I3AA but fails to alter the effect of IAld on angiogenesis and osteoclastogenesis..... 77

Figure 20. IAld inhibits the induction of antioxidant gene expression by the Nrf2 agonist CDDO-IM..... 79

Figure 21. Nrf2 agonist CDDO-IM partially reverses IAld-mediated potentiation of osteoclastogenesis..... 80

Figure 22. IAld reduces intracellular ROS levels in RAW cells treated with RANKL.... 82

Figure 23. Nrf2 agonist CDDO-IM does not alter IAld-mediated inhibition of Mtb-induced proinflammatory cytokine genes. .... 83

Figure 24. Pilot experiment to assess the effect of oral treatment with IAld on arthritis progression..... 85

Figure 25. The bioavailability of IAld and I3AA may impact pathophysiological processes that occur in the arthritic joint during RA. .... 99

Appendix I. Experimental design illustrating how the therapeutic potential of indole derivatives for autoimmune arthritis will be assessed using the AA rat..... 102

Appendix II. Optimization of indole derivative extraction from serum ..... 103

## List of Abbreviations

AA	Adjuvant-induced arthritis
AARDA	American Autoimmune Related Diseases Association
ACR	American College of Rheumatology
ACPAs	Anti-citrullinated protein antibodies
AhR	Aryl hydrocarbon receptor
ANA	Antinuclear antibodies
APC	Antigen presenting cell
BMM	Bone marrow macrophage
CatK	Cathepsin K
CIA	Collagen-induced arthritis
COX	Cyclooxygenase
CRP	C-reactive protein
CXCL	CXC chemokine ligand
CXCR	CXC chemokine receptor
DAMP	Danger-associated molecular pattern
DAS28	Disease activity score-28
DC	Dendritic cell
DHFR	Dihydrofolate reductase
DHODH	Dihydroorotate dehydrogenase
DMARD	Disease modifying anti-rheumatic drug
DMEM	Dulbecco's modified eagle media
DNA	Deoxyribonucleic acid

EAE	Experimental autoimmune encephalomyelitis
ERK1/2	Extracellular signal-regulated kinases 1 and 2
EULAR	European League Against Rheumatism
FBS	Fetal bovine serum
Foxp3	Forkhead box P3
GIT	Gastrointestinal tract
GPR43	G protein-coupled receptor 43
H <sub>2</sub> O <sub>2</sub>	Hydrogen peroxide
HLA	Human leukocyte antigen
HMGB1	High mobility group box 1
HMOX1	Heme oxygenase 1
Hsp	Heat shock protein
HUVEC	Human umbilical vein endothelial cell
I3AA	Indole-3-acetic acid
IAlD	Indole-3-aldehyde
iNos	Inducible nitric oxide synthases
IFN $\gamma$	Interferon gamma
IL	Interleukin
K/BxN	T cell receptor transgene KRN and the MHC class II molecule A (g7)
Lox	Lipoxygenase
LPS	Lipopolysaccharide
LTB4	Leukotriene B4

M $\phi$	Macrophage
MAPK	Mitogen-activated protein kinase
MHC	Major histocompatibility complex
MK	Menaquinones
MMP	Matrix metalloproteinase
mRNA	Messenger ribonucleic acid
MS	Multiple sclerosis
Mtb	<i>Mycobacterium tuberculosis</i> H37Ra
MTT	3-(4,5-dimethylthiazol-2-yl)-2,5-diphenyltetrazolium bromide
MTX	Methotrexate
MyD88	Myeloid differentiation primary response 88
NF- $\kappa$ B	Nuclear factor kappa-light-chain-enhancer of activated B cells
NIAID	National Institute of Allergy and Infectious Diseases
NIEHS	National Institute of Environmental Health Sciences
NIH	National Institutes of Health
NO	Nitric oxide
NOX1	NADPH oxidase 1
Nrf2	Nuclear factor erythroid 2-related factor 2
NSAID	Non-steroidal anti-inflammatory drug
NQO1	NADPH dehydrogenase [quinone] 1
O $_2^{\cdot-}$	Superoxide
OA	Osteoarthritis
p38	Mitogen-activated protein kinase subunit 38

p60/p65	Nuclear factor kappa-light-chain-enhancer of activated B cells subunits p60 and p65
PAD	Peptidyl arginine deiminase
PAMP	Pathogen-associated molecular pattern
PD	Periodontal disease
PG	Prostaglandin
PPAD	<i>P. gingivalis</i> peptidyl arginine deiminase
PXR	Pristane X receptor
qRT-PCR	Quantitative real-time polymerase chain reaction
RA	Rheumatoid arthritis
RANKL	Receptor-activated nuclear factor-kappa beta ligand
Res	Resveratrol
RF	Rheumatoid factor
RNA	Ribonucleic acid
ROR $\gamma$	RAR-related orphan receptor gamma
SCFA	Short-chain fatty acid
SE	Shared-epitope
SFB	Segmented filamentous bacteria
sIL-6R	Soluble interleukin-6 receptor
sIL-1Ra	Soluble interleukin-1 receptor antagonist
SLE	Systemic lupus erythematosus
STAT	Signal transducer and activator of transcription
T1D	Type 1 diabetes

T-bet	T-box transcription factor
TBST	Tris-buffer saline containing Tween 20
TCDD	2,3,7,8-Tetrachlorodibenzo-p-dioxin
TCR	T cell receptor
Th	T helper cell
TGF $\beta$	Transforming growth factor beta
TLR	Toll-like receptor
TNF $\alpha$	Tumor-necrosis factor alpha
TRAP	Tartrate-resistant acid phosphatase
Treg	Foxp3 <sup>+</sup> T regulatory cell
U.S.A.	United States of America
VEGF	Vascular endothelial growth factor
XRE	Xenobiotic response element

## Chapter 1. Scope of Dissertation

Rheumatoid arthritis (RA) affects approximately 0.3 – 1% of the population worldwide (1–4). Despite several advances made in the management of this disease, many challenges remain. These include significant side effects that are associated with many of the currently used drugs for RA (5–7), and the lack of adequate disease control in about 30-40 % of RA patients. For these reasons, there remains a significant need to identify new agents with defined mechanisms of action that possess therapeutic potential. The influence of the gut microbiota on health and disease is largely mediated by bioactive metabolites that the organisms produce (8–10). Some metabolites get absorbed by the host and regulate many aspects of health and disease; however, little is known about the potential impact of indole derivatives on arthritis-related processes. In addition, mechanistic investigation of the bioactivity of these metabolites is important for understanding the potential contribution of ‘dysbiosis’ to the pathophysiology of RA. This study is centered on an analysis of two indole derivatives, indole-3-aldehyde (IAld) and indole-3-acetic acid (I3AA), that are produced by gut microbiota (11).

**We hypothesized** that IAld and I3AA differential effect arthritis-associated processes that contribute to inflammation and stromal remodeling. Furthermore, that these indole derivatives might have anti-arthritic activities that can potentially be harnessed in a therapeutic setting to manage disease. To address these propositions, we developed three Specific Aims:

**Aim 1.** To define the bioactivities of IAld and I3AA on three of the key arthritis processes, namely the inflammatory response of macrophage, new blood vessel formation (angiogenesis), and bone resorption (osteoclastogenesis) using cell-based assays.

**Aim 2.** To investigate the likely cell-signaling pathways that are regulated by IAld and I3AA and may contribute to the above bioactivities.

**Aim 3.** To test the disease-modulating activity of these indole derivatives in the rat adjuvant arthritis (AA) model.

The first Specific Aim of our project was to determine the bioactivities of IAld and I3AA on three key cellular processes that contribute to the pathophysiology of RA. This was accomplished by testing the effect of both metabolites using standard cell-based models: i) TLR-activated RAW 264.7 (RAW; murine macrophage) cells using heat-killed *M. tuberculosis* and lipopolysaccharide (LPS), ii) RANKL-induced generation of osteoclasts from RAW cells, and iii) 2-D Matrigel tube formation assay using human umbilical vein endothelial cells (HUVECs). We measured the effect of these two indole derivatives on the expression by RAW cells of genes encoding inflammatory mediators or osteoclast-associated bone-resorbing enzymes using quantitative real-time polymerase chain reaction (qRT-PCR). Additionally, we measured the effects of these indole derivatives on osteoclast formation by RAW cells and loop formation by HUVEC cells.

The second Specific Aim of our project was to investigate the cell signaling pathways regulated by these indoles derivatives that may contribute to the bioactivities characterized in Aim 1. Specifically, we tested whether IAld and I3AA regulate MyD88-

dependent activation of NF- $\kappa$ B and MAPK pathways by using LPS to activate these pathways in RAW cells and performing Western blot analyses for cytoplasmic indicators of pathway intermediate activation. Additionally, the involvement of the AhR (xenobiotic) and Nrf2 (antioxidant) pathways in mediating the observed effects of these indole derivatives was tested by using the AhR-specific antagonist CH-223191 and the Nrf2-specific agonist CDDO-IM, respectively, as well as by analyzing ROS levels with CM-H<sub>2</sub>DCFDA to investigate the later possibility.

The third Specific Aim of our project to test the effect of IAld on disease severity by administering IAld (5 mg/kg) by oral gavage daily, starting on day 5 after immunization of Lewis rats with Mtb, a well-characterized model for the induction of autoimmune arthritis (12). The severity of disease in IAld-treated animals was compared to that of arthritic controls treated with vehicle.

Our findings provide evidence for the potential role of these indole derivatives in modulating inflammatory and stromal remodeling processes in health and disease. In addition, IAld exhibited a promising therapeutic potential that will require further testing for combination therapy with mainstream drugs.

## Chapter 2: General Introduction

### 2.1 Introduction to Autoimmune Diseases

Autoimmune diseases occur when the immune response to one's own tissues causes damage. At the turn of the 20<sup>th</sup> century, "*horror autotoxicus*" was coined by Dr. Paul Ehrlich to refer to autoantibodies (13). At the time though, Dr. Ehrlich considered their existence to be theoretically impossible; however, by the middle of the century several individuals including Drs. Henry Kunkel ("The Father of Immunopathology") (14), Noel Rose ("The Father of Autoimmunity") (15), Deborah Doniach and Ivan Roitt (16), showed that patients with certain disorders had autoantibodies. These disorders are now known as autoimmune diseases. It is now understood that in addition to autoantibodies, several immune and mesenchymal processes are aberrant in different autoimmune diseases (17, 18). In healthy individuals, a set of checks and balances ensures tolerance to one's own tissues by negatively selecting autoreactive T and B cells (19–21), tuning T cells to regulate T cell differentiation (22), and insuring that an innate immune response does not persist chronically (23, 24). Additionally, there is important cross-talk between cellular and stromal remodeling pathways with the immune system (25, 26). An aberrant state of one or more of these processes can contribute to over 80 autoimmune diseases. The most common autoimmune diseases include rheumatoid arthritis (RA), multiple sclerosis (MS), and Type 1 diabetes (T1D). Autoimmunity is ubiquitous, but for most, these autoreactive responses are highly regulated and do not manifest as a disease. Therefore, the rapid global increase in the prevalence of individuals having serum biomarkers of autoimmunity and presenting with one or more autoimmune diseases is concerning (27–30), but the reason(s)

why remains unknown. Indeed, the etiology of most autoimmune diseases is unknown. This lack of understanding has hampered the development of cures, although therapeutic progress has been substantial.

Indeed, over the last several decades the identification of novel disease pathways and introduction of modern non-steroidal anti-inflammatory drugs (NSAIDs) and biologic agents to the clinic has improved the life expectancy and living standards of those with autoimmune diseases. Even with these current drug options, treatment is inadequate for many. This is, in part, because of the development of drug resistance by patients over time and association of many therapeutics with severe side effects. These will be discussed below in more detail. Thus, better elucidation of disease factors and novel treatments are crucial to address current medical shortfalls.

## **2.2 The Prevalence of Autoimmune Diseases in the United States**

In 2002, autoimmunity was considered the third leading cause of disease in the United States of American (U.S.A.) according to the National Institutes of Health (NIH), it estimated that 14.7 – 23.5 million Americans had an autoimmune disease (31). Around the same time, American Autoimmune Related Diseases Association (AARDA) reported that at least 50 million Americans had an autoimmune disease (32). Now, over a decade later, it is likely that the number of individuals in the U.S.A with an autoimmune disease is much greater. Indeed, several reports have illustrated the unimpeded rise in autoimmune disease incidence in the U.S.A. and abroad (27–30). In April 2020, a concerning report came out that illustrated a drastic rise in prevalence of antinuclear antibodies (ANA), an indicator of autoimmune disease, in the U.S.A. population (27). Presence of ANA in the

serum serves as a biomarker of autoimmune diseases, especially in those diseases that affect the connective tissues, as does RA (33–38). This study reported an approximately 50% increase in the overall prevalence of ANA across all age groups from the year 2004 to 2012 and a staggering 300% increase in ANA prevalence in the adolescent age group. Genetic and environmental risk factors associated with autoimmune diseases, and particularly those of RA, that may, in part, explain this concerning trend are discussed below.

## **Chapter 3: Rheumatoid Arthritis (RA)**

### **3.1 The Epidemiology of RA**

It is estimated that 0.3 – 1% of the global population is afflicted by RA, making it one of the most common autoimmune diseases in the world (1–4). At the end of the 20<sup>th</sup> century, several reports concluded that the prevalence of RA in the U.S.A. and Europe were decreasing (39, 40); however, more recently, in a reversal of this trend, a rapid increase in RA prevalence was observed in these countries and globally (3, 4). Some factors that may account for this reversal include a higher average life expectancy, better diagnostic resources, and an adjustment to the American College of Rheumatology (ACR) criteria for diagnosing RA (41). Even so, the 2020 report on the rising prevalence of the autoimmune biomarker (including for RA) may be an indicator of a true increase in the prevalence of RA and other autoimmune diseases in the U.S.A (36–38).

The prevalence rates of RA vary greatly between ethnically and geographically distinct groups of peoples, illustrated in Figure 1, with higher rates of disease measured in industrialized countries of North America (3, 4, 42) and England (43) compared to areas of Africa (44, 45) and Asia (46, 47). Even within countries, there are significant differences in disease prevalence between different populations. For example, indigenous peoples of the U.S.A., Canada, Australia, and New Zealand have been found to have significantly higher rates of RA than the general population there (48).

For RA, as for many other autoimmune diseases, women are affected approximately 2 – 3 times more often than men (49–51). In addition, the peak age of disease onset at 70 – 74 years in women is lower than that for men at 75 – 79 years (4).

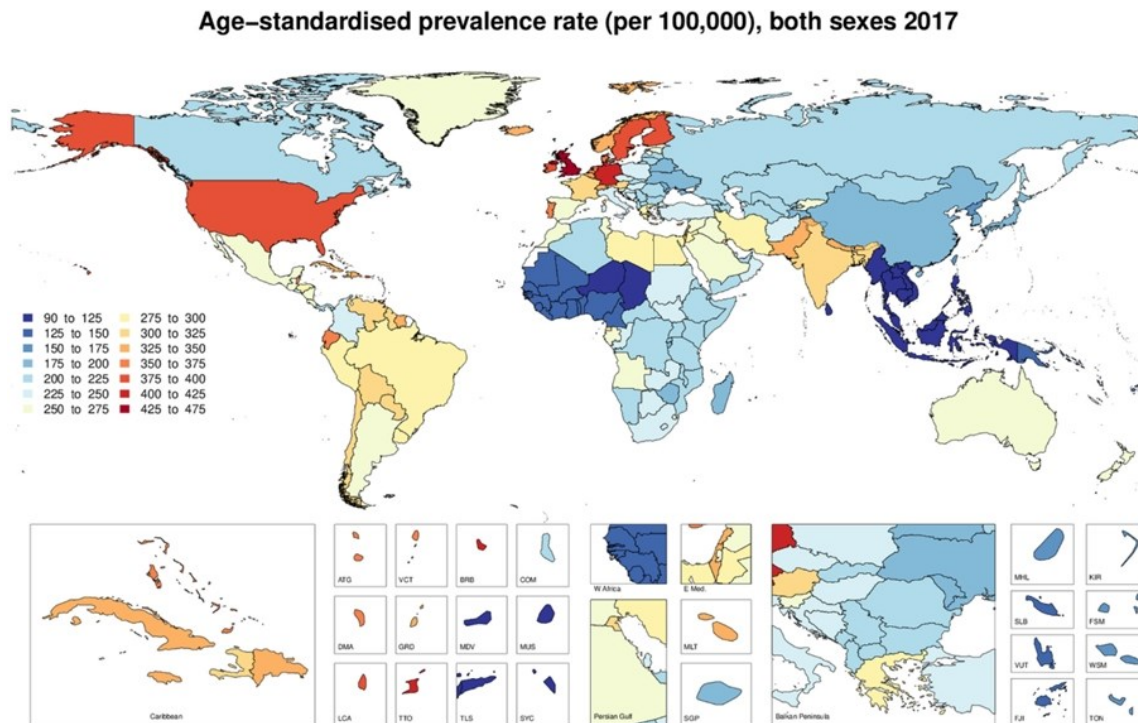


**Figure 1. Age-standardized prevalence rate (per 100,000), both sexes 2017.**  
 Age-standardized prevalence rate of RA per 100,000 population in 2017, by country. (Reprint from Safiri S, et al., *Annal Rheum Dis.* 2019; 78:1463–1471 with permission from BMJ Publishing Group Ltd) (4)

## 3.2 RA Risk Factors

RA involves both genetic and environmental risk factors, which makes it very difficult to pinpoint the precise etiology of RA. For any individual, the true cause of disease may be specific to that person and result from a summation of risk factors. Some of the risk factors described below were identified decades ago, whereas others were identified only recently and are more speculative in their relationship to the disease.

### 3.2.1 Genetic Risk Factors for RA

In the last several decades, genome-wide association studies have identified more than 117 RA-susceptibility loci (*e.g.*, protein tyrosine phosphatase, non-receptor type 22, C-C chemokine receptor type 2, interleukin-2 receptor alpha, Fc region receptor II-b, human leukocyte antigen (HLA)-DBR1, and others). Some of these risk loci are shared among common autoimmune diseases and have either defined or putative functional roles in disease (52–57).

The role of HLA-DBR1 haplotypes, arguably the best characterized genetic risk factors of RA, is now described as the ‘shared-epitope hypothesis’ (58). This hypothesis seeks to explain why having specific HLA class II haplotypes is associated with a greater prevalence of autoimmunity, namely RA, than that of the general population. It proposes that antigen presentation by major histocompatibility complex (MHC)-II molecules encoded by HLA-DBR1 haplotype risk alleles are more likely to cause an autoimmune response. These haplotypes encode the ‘shared-epitope’ (SE), a 5 amino acid sequence at position 70 – 74 (hypervariable region III) of the MHC-II. In 1976 and 1978, several groups

proposed a genetic predisposition to RA in association with HLA-DR4 (59–61). It was later determined that HLA-DR1, rather than HLA-DR4, was the predominant susceptibility loci for RA (62).

For siblings, sharing an MHC haplotype is estimated to account for 20% of their shared risk (63). In this meta-study, the shared risk of RA between siblings was significantly higher than that for 5 of 6 other prevalent autoimmune diseases for which this value was reported. Additionally, this analysis concluded a sibling of a person having RA has an 8-times higher probability of developing RA than that of an individual in the general population. Additionally, in several other studies, it was observed that monozygotic twins have a 4 or more times higher disease concordance rate of RA than do dizygotic twins (64–66). These reports clearly demonstrate that there is a genetic component to disease risk, but meta-analysis from twin concordance studies on RA and other common autoimmune diseases (*i.e.*, T1D, MS, Graves' disease, systemic lupus erythematosus (SLE)) also show that environmental factors may have a significant role to play in RA (65, 67). Indeed, in one study the monozygotic twin concordance rate for RA (14.5% pairwise; 25.4% probandwise) was the lowest among these diseases and, additionally, the familial and dizygotic association rate of RA was highly variable (1.6-15.5%) compared with other autoimmune diseases.

### *3.2.2 Environmental Risk Factors for RA*

There are several well-established environmental risk factors for RA. Smoking is a prominent one, especially for seropositive RA, which is defined by the presence of rheumatoid factor (RF) and/or anti-citrullinated protein antibodies (ACPAs) (68). The risks

afforded by smoking are also present for seronegative RA, although to a lesser degree (69). The dangers of cigarette and tobacco smoke were highlighted in the first Surgeon General's report, "Smoking and Health: Report of the Advisory Committee of the Surgeon General of the Public Health Service" in 1964 (70). This risk comes from the fact that cigarette smoke contains thousands of chemicals, many of which activate the aryl hydrocarbon receptor (AhR) (71). For example, it was shown that *ex vivo* exposure of synovial tissues from RA patients to 2,3,7,8-tetrachlorodibenzo-p-dioxin (TCDD), a classical AhR agonist found in smoke, induced the expression of key disease-causing inflammatory cytokines (*i.e.*, IL-1 $\beta$ , IL-6, and IL-8) (72). Another notable finding from this study was that the induction of these cytokines was significantly greater in RA than osteoarthritis (OA) synovial tissues. It was hypothesized that this discrepancy between RA and OA tissues was derived from the higher levels of TNF $\alpha$  in RA synovial cells which, in turn, induced higher expression of AhR in the RA tissues. The role of the AhR in mediating the deleterious effects of TCDD and smoke in animal models of RA is also described. Interestingly, SE-AhR cross-talk may underly a relationship between genetic factors the predispose an individual to developing RA and the compounded risk associated with smoking as a result of regulating osteoclastogenesis and T cell responses (73). Also, in the antigen-induced arthritis model of RA, exacerbation of disease by smoke was AhR-dependent (74).

Exposure to silicates and mercury may also increase susceptibility to autoimmune disease. Silicate exposure and chronic viral infection were shown to predispose low susceptibility and outbred mice to lupus-like autoimmunity (75, 76). Additionally, the induction of systemic autoimmunity in mice following xenobiotic exposure appears to require the Toll-like Receptor (TLR)-mediated innate immune response (77).

Antigenic mimicry between viral or microbial components and host components may result in cross-reactivity that causes autoimmunity. Examples of this include the glycoprotein-110 (gp110) of Epstein-Barr virus (78) and heat shock protein 65 (hsp65) of *Mycobacterium tuberculosis* (Mtb) (79). Also, it was recently shown that the Epstein–Barr virus nuclear antigen 2 may cluster host transcription factors at susceptibility loci of SLE and other autoimmune diseases (80). The Epstein–Barr virus genomic material has been detected in monocytes and neutrophils of a significant proportion of patients (81). However, exposure to microbes may not always increase disease risk.

In the 19<sup>th</sup> century, it was documented that in industrialized nations there was a rapid increase in atopic diseases, such as asthma and hay fever, especially in children without siblings. This led Strachan et al. to propose the ‘Hygiene hypothesis’ in 1989 (82). The idea that a hyperclean environment increases atopic disease risk is a concept that has been hotly debated and expanded to include other hyperinflammatory and autoimmune diseases (83–85). A more thorough encapsulation of this view is presented in one of our review articles (86). An illustration of the ‘Hygiene hypothesis’ is given in Figure 2.

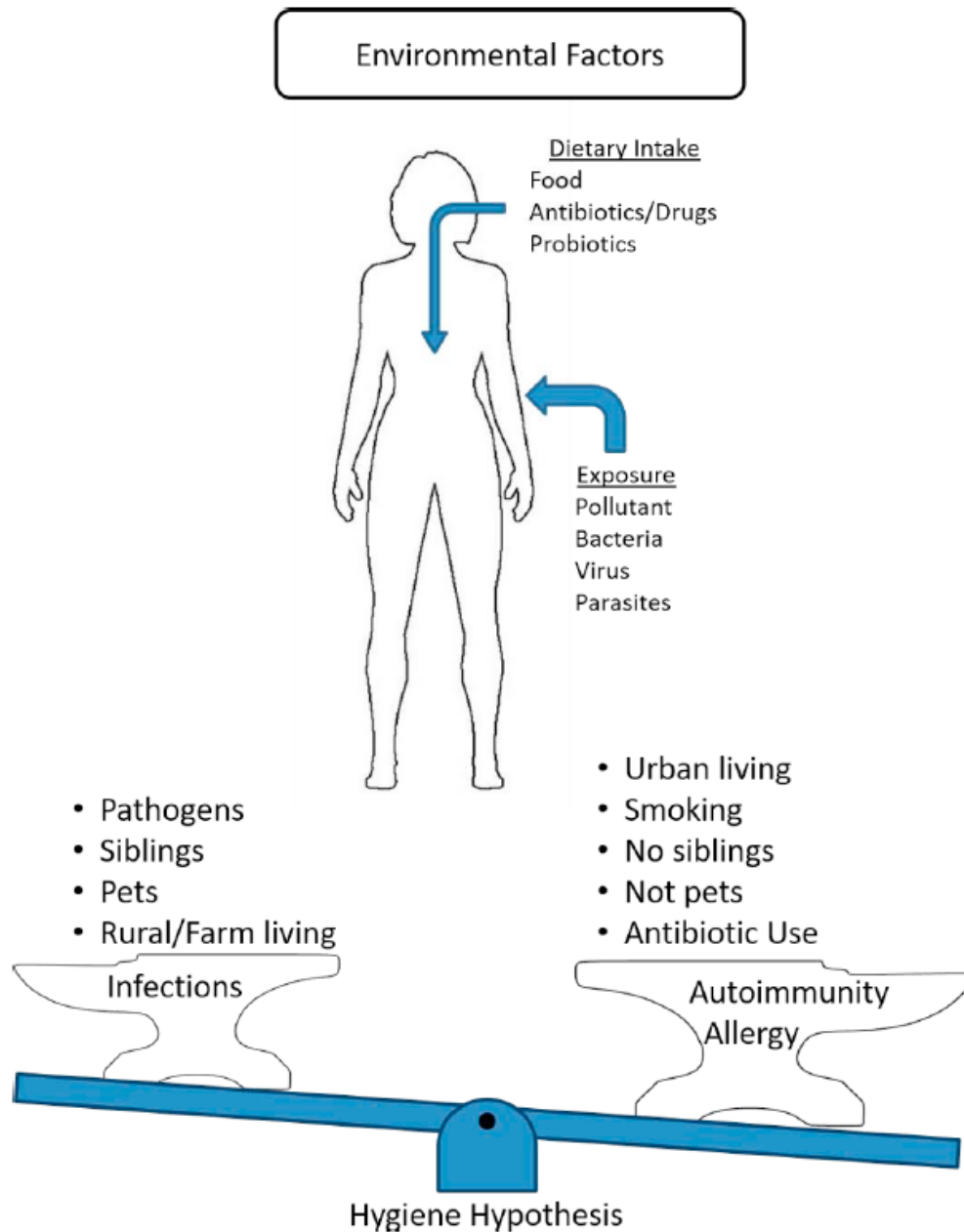


**Figure 2. The ‘Hygiene hypothesis’.**

The ‘Hygiene hypothesis’ proposes an imbalance in the host immune response (e.g., Th1 versus Th2; Th17:Treg ratio) to various environmental agents and pathogens such that the host is rendered more prone to allergies and autoimmunity, while retaining the ability to fight effectively against certain infectious pathogens. (Figure from Langan D, et al., *Cell Immunol.* 2019; 339:59–67) (86).

It is important not to overlook the influence of the diet and microbiome on host health when discussing the role of the environment in mediating chronic disease risk. This is still an emerging area of study, but the amount of evidence to suggest that these are important relationships is rapidly growing (87, 88). Recently, it was shown that a poor diet is associated with a perturbation of the microbiome and that in the elderly, this is linked to a steady health decline (89). The Arthritis Foundation and NIH recommend a Mediterranean-like diet that consists primarily of fish, spices like turmeric, and plant-based foods. A recent meta-analysis on the effect of curcumin and turmeric extracts on RA concluded that in 5 of 8 studies, these natural products resulted in relief from the pain. This pain relief was comparable to that from standard pain medications (90). Also, due to an increased consumption of certain fish, individuals on a Mediterranean diet have a high intake of omega-3 fatty acids, eicosapentaenoic acid and docosahexaenoic acid. These are eicosanoid precursors that are beneficial for health because they mitigate inflammation by competing with inflammatory eicosanoids, such as arachidonic acid (91). This involves the inhibition of prostaglandin (PG)E2 and leukotriene B4 (LTB4) synthesis, which is dependent on the cyclooxygenase (COX) and arachidonate 5-lipoxygenase (5-LOX) pathways, respectively (92). The clinical significance of these pathways is highlighted by the fact that glucocorticoids and NSAIDs to treat RA work by inhibiting COX-2 activity as well as PGE2 and LTB4 production. Those on a Mediterranean diet were recently shown to have specific functional and taxonomic components of the gut microbiome that are linked to lower cardiometabolic disease risk (88). This association was especially strong among individuals with low *Prevotella copri* (*P. copri*) levels. Interestingly,

cardiometabolic disease is a comorbidity of RA and elevated *P. copri* levels in the gut is linked to RA (93, 94).

Certain western-dietary practices are a detriment to our health, in part, because of the significant imbalance in the intake ratio of omega-3-fatty acids and omega-6-fatty acids (95). The most common omega-6-fatty acid, linolenic acid, when consumed in excess as a part of the western diet, is converted by the body into arachidonic acid and then by COX-1/2 and 5-LOX into the inflammatory eicosanoids, PGE2 and LTB4, respectively (96). These are serious inflammatory mediators that are implicated in RA progression. Salt (sodium chloride) is another component of the western diet that is commonly consumed in excess. Salt has been shown to enhance T helper 17 (Th17) cell activity (97) and inhibit Foxp3<sup>+</sup> T regulatory cell (Treg) function through a mechanism dependent on the serum/glucocorticoid regulated kinase 1 (98). An increase in the Th17:Treg ratio is associated with RA (99), and other autoimmune disorders.

In this light, sustaining good dietary practices is essential to mitigate systemic inflammation, autoimmune disease, and cancer. Importantly, the benefits of a good diet may, in part, involve the regulation of the gut microbiome and downstream mechanisms linked to specific microbiome metabolites.

### **3.3 Pathophysiology of RA**

In 2010, the ACR and European League Against Rheumatism (EULAR) collaborated to update the criteria for diagnosing RA (41). This disease is characterized by systemic inflammation of the synovial joints and gradual deformity of joints in the

extremities, especially of the hands and feet. Bone erosion and cartilage damage in parallel with synovial membrane thickening and synovitis lead to loss of joint mobility, ankylosis, and severe joint pain. Early diagnosis and aggressive treatment by 6 months of onset of symptoms can for some patients prevent the worst of these deformities (100). Even so, RA is not curable, and even when on drugs, the disease continues to progress in a significant portion of patients (100, 101). This is, in fact, also the case following treatment with modern biologics. According to the Mayo Clinic, approximately 40% of individuals with RA also experience non-joint related symptoms (102). These include pathologies of the skin, eyes, lungs, and the cardiovascular system. Other common symptoms of RA include tiredness, fatigue, and loss of appetite. Having RA is also linked to a higher risk of comorbidities, notably, including cardiovascular disease and premature death (103, 104).

Disease activity score-28 (DAS28) is a common method used for scoring the disease activity of an individual with RA by checking how many joints out of 28 are swollen or tender. The scoring of joints is combined with standard methods of measuring systemic inflammatory activity by taking blood and determining the erythrocyte sedimentation rate (ESR) or C-reactive protein (CRP) levels. Clinicians use this method to assess the effectiveness of a therapy by comparing a patient's DAS28 from before beginning treatment to their score after being placed on a treatment. The degree of improvement afforded by treatment is commonly graded on a clinical scale that is based on reaching a 20%, 50%, and 70% level of reduction in their DAS28.

### 3.4 The Role of the Immune System in RA

To ensure homeostasis, the innate and adaptive immune systems work in concert to protect the body from pathogens and cancer while preventing autoimmunity. Aberrant responses from either arm of the immune system can result in the development of chronic inflammation and autoimmune disease.

#### *3.4.1 Innate Immune Processes Involved in RA Pathogenesis*

Myeloid cells are recruited to the arthritic joint in high numbers along the chemokine gradient and in response to endothelial cell surface expression of integrins on highly vascularized synovial tissue (105).

Macrophages (M $\phi$ ) are a subset of myeloid cells that play a major role in RA. They contribute to the perturbation of the innate and adaptive immune responses, as well as to the aberrant stromal remodeling state (**Figure 3**). RA synovial-infiltrating M $\phi$  upregulate TLR2 and TLR4 (106). In the synovial fluid, high levels of TLR2 and TLR4 ligands (*e.g.*, high mobility group box 1 (HMGB1), fibrinogen and peptidoglycans) are present (107–109). These danger-associated molecular patterns (DAMPs) and pathogen-associated molecular patterns (PAMPs), in turn, induce an inflammatory response via Myeloid Differentiation Primary Response 88 (MyD88)-dependent signaling, which is responsible for activating downstream nuclear factor-kappa B (NF- $\kappa$ B) and mitogen-activated protein kinase (MAPK) transcriptional pathways. Expression of a dominant negative MyD88 in RA synovial tissue was shown to reduce the expression of M $\phi$ -derived pro-inflammatory cytokines that are elevated in RA, including TNF $\alpha$ , IL-6, and vascular endothelial growth

factor (VEGF) (110). These and other pro-inflammatory cytokines drive autoimmune arthritis (111). As such, they have been successfully targeted for therapeutic purposes in RA and are discussed in further detail in the therapeutic section of this thesis (112).

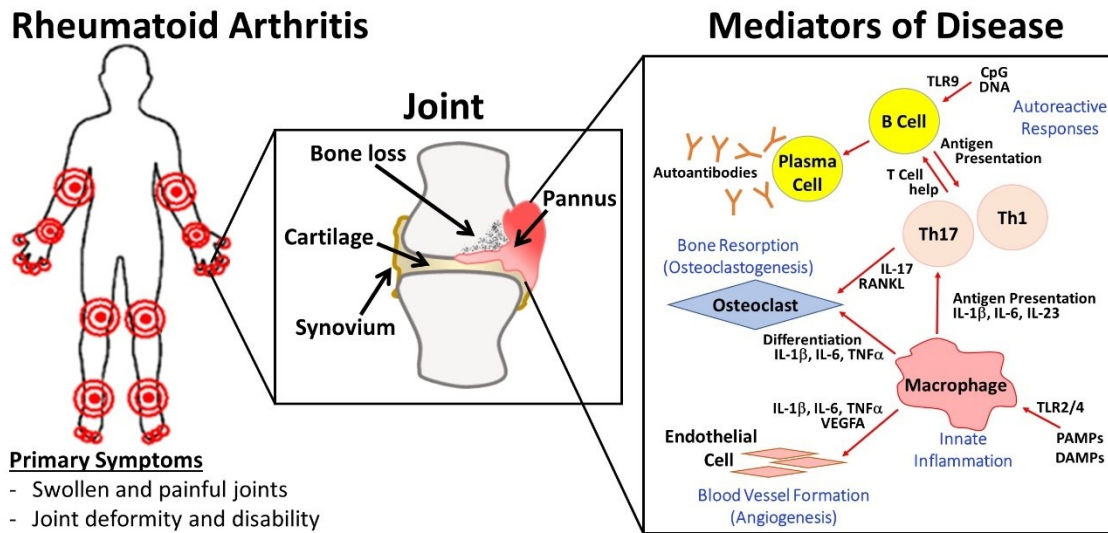


**Figure 3. Key mediators of RA pathogenesis.**

In RA, joint destruction is caused by the combined effects of aberrant immune and mesenchymal cell responses in the arthritic joint. M $\phi$  that respond to PAMPs and DAMPs through their TLRs produce pro-inflammatory cytokines and function as APCs to activate autoreactive T cells. M $\phi$  also serve as precursors to osteoclasts. Autoreactive T cells and B cells, which are vital components of the adaptive immune system, further propagate joint damage. The inflammatory mediators from immune cells also drive stromal remodeling events in the joint. These events include bone resorption (osteoclastogenesis) and blood vessel formation (angiogenesis). If left untreated, arthritic inflammation results in progressive and irreversible joint damage.

Epigenetic and metabolic changes dictate, in part, the progression of M $\phi$  to a classically activated (M1), inflammatory, or alternatively activated (M2), anti-inflammatory, phenotype (113). These main subsets were named to distinguished between subpopulations of M $\phi$  based on their polarization and cytokine profile following

stimulation with either IL-4 or IFN- $\gamma$  and/or LPS (114, 115). Studies on M $\phi$  have shown that the stimulatory condition *in vitro* and M $\phi$  *in vivo* have a range of phenotypes that fall between classical M1 and M2 cells (113), as such, it is now common to refer to M $\phi$  as being either M1- or M2-like. This fate is critical in determining if a M $\phi$  plays a protective or deleterious role in disease (116). In the blood and synovial fluid of RA patients, there is no clear distinction phase between M1 and M2 M $\phi$ , because of a range of intermediary phenotypes; however, there is a clear imbalance, with an overall reduction in the proportion of M $\phi$  that have a M2-like phenotype (117). There are several subtypes of M2-like M $\phi$ , generally identified by their ability to produce IL-4 and IL-10 and phagocytose dead cells, efferocytosis. Dead cells would otherwise contribute to elevated levels of DAMPs, such as free nuclear material and HMGB1, that stimulate TLRs to drive the innate inflammatory response. A subset of these M2-like M $\phi$  that are CD138<sup>+</sup> may specialize in clearing apoptotic cells (118). In the pristane-induced lupus model, high numbers of Ly6C<sup>hi</sup> peritoneal M $\phi$  and low numbers of CD138<sup>+</sup> small peritoneal M $\phi$  were associated with severe disease pathology (119). This highlights the differential contribution of various M $\phi$  subsets to inflammation. Interestingly, these CD138<sup>+</sup> M $\phi$  also express the scavenger receptor Marco and high levels of activated cyclic AMP-responsive element binding, a transcription factor involved in “alternative” or M2-like M $\phi$  differentiation (120).

A shift toward an M1-like inflammatory phenotype is associated with an increased glycolytic flux that enables rapid proliferation and production of pro-inflammatory cytokines. The M1 state also enables the expression of enzymes (*i.e.*, COX-2, inducible Nitric oxide synthases (iNos), and NADPH oxidase 1 (Nox1)) and mitochondrial activity that collectively result in the formation of large amounts of reactive oxygen species (ROS)

(*e.g.*, nitric oxide (NO), superoxide ( $O_2^{\cdot-}$ ), hydrogen peroxide ( $H_2O_2$ )), and inflammatory mediators such as prostaglandins. High levels of intracellular ROS then feed forward to activate NF- $\kappa$ B, MAPK, and HIF1 $\alpha$  pathways to further induce pro-inflammatory cytokine expression, enhance Th17 differentiation, drive angiogenesis, and increase osteoclastogenesis. Dendritic cells (DCs) are the classical APC, but M1-like cells express higher levels of MHC-II molecules and CD80/CD86 costimulatory factors that enable them to also function as APCs and activate CD4<sup>+</sup> T cells to propagate the autoreactive T cell response (121). Furthermore, human monocytes and M $\phi$  of the M1-like subtype express iNos and convert L-arginine into NO and L-citrulline. The expression of iNos and citrullination of proteins by M $\phi$  means that these cells may serve as a source of citrullinated autoantigens and subsequently contribute to the production of ACPAs by plasma cells that are associated with rheumatic diseases (122).

Additional evidence for the role of M $\phi$  in RA comes from a study based on the collagen antibody-induced arthritis model in which it was found that CXC chemokine receptor (CXCR)3: CXC chemokine ligand (CXCL)10 dysfunction inhibits M $\phi$  migration to the arthritic joint and causes disease resistance (123). Interestingly, CXCL10 may have several roles in autoimmune arthritis by regulating the deleterious M $\phi$  response. In response to CXCL10, there is a cross-talk between CXCR3 and TLR4 on CD4<sup>+</sup> T cells that causes an induction of pro-inflammatory cytokines (*i.e.*, RANKL, IL-6, and TNF $\alpha$ ) that drive osteoclast-differentiation of M $\phi$  (123). Also, murine bone marrow M $\phi$  (BMM) are more likely to become osteoclasts when concomitantly treated with CXCL10 during *ex vivo* differentiation (124). However, it is not yet clear if there is any TLR4: CXCR3 cross-talk that influences M $\phi$  differentiation into osteoclasts directly.

Other myeloid cells besides M $\phi$  have not been as intensely studied for their role in RA as M $\phi$ , include basophils, mast cells, and neutrophils. A study on juvenile RA showed elevated numbers of peripheral blood basophils (125). In contrast, a study on adults with RA showed fewer peripheral blood basophils compared to healthy controls; however, the activity of basophils from these adult RA patients was significantly higher and this level of activity positively correlated with the patient's DAS28 (126). Mast cells, on the other hand, may be a significant source of IL-17 (127). IL-17 blockade has proven successful in the treatment of inflammatory arthritis (128). Although interest for also using this approach to treat RA persists, achieving clinical success for RA with IL-17 blockade therapy has proven challenging (129). Neutrophils are found at high numbers in the joints of RA patients early after onset (130). In the autoantibody-induced K/BxN model of arthritis, neutrophil influx into the joint and subsequent joint damage is regulated by LTB<sub>4</sub> receptor 1 (BLT1) (131, 132). Preventing neutrophil influx into the arthritic joint may, in part, explain the therapeutic effect of NSAIDs that block LTB<sub>4</sub> synthesis. Specific targeting of neutrophils to ameliorate disease has proven difficult though because they make up approximately 20% of blood leukocytes and exhibit rapid turnover.

#### *3.4.2 Adaptive Immune Processes Involved in RA Pathogenesis*

Generally, autoreactive T cells are deleted during thymic selection on medullary thymic epithelial cells that express the transcription factor autoimmune regulator (20, 22). However, a subset of autoreactive T cells become Treg, a cell subset that is critical to preventing autoimmunity, unlike autoreactive Th cells of the Th1 or Th17 lineages (133). This is also true in relevant rodent models. Interestingly, the T cell repertoire of RA patients

is often less diverse than that of healthy individuals and those diagnosed with other autoimmune diseases, such as SLE (134–136). However, in RA, peripheral blood T cells often have shorter telomere lengths, a sign of having undergone more rounds of division, possibly from their chronic autoreactive response to self-antigens. It has also been suggested that this T cell phenotype may be associated with the HLA-DBR1 risk alleles (136).

Cytokines are critical in determining the differentiation of an activated naïve T cell into defined T cell subsets. For Th1 cells, IL-12-mediated activation (M1-like M $\phi$  are a significant source of IL-12) of signal transducer and activator of transcription(STAT)4 upregulates interferon gamma (IFN- $\gamma$ ) expression. Subsequent IFN- $\gamma$ -mediated activation of STAT1 upregulates T-box transcription factor (T-bet) expression which is required to stabilize the Th1 phenotype. IFN- $\gamma$  producing Th1 cells are abnormally high in RA synovial tissue and their numbers are positively associated with disease activity (137, 138). The Th17 subset was identified about 15 years ago (139). Its pathogenic role in RA, colitis, MS, and other diseases is increasingly being appreciated. In a study on the experimental autoimmune encephalomyelitis (EAE) model of human MS, that preceded the identification of Th17 cells, it was observed that IL-23 deficiency significantly attenuated disease (140). In that study, it was concluded that M $\phi$  and DCs were the predominant source of IL-23. IL-23 is involved in the maintenance of a cell's Th17 phenotype by enhancing RAR-related orphan receptor gamma (ROR $\gamma$ ) and IL-17 expression (141, 142). Although other cell types produce IL-23, M $\phi$  also secrete IL-1 $\beta$  and IL-6 which are also essential factors for human Th17 cell differentiation (143, 144). Another critical cytokine for Th17 differentiation is transforming growth factor beta (TGF $\beta$ ). Interestingly though,

TGF $\beta$  is also critical for Treg differentiation (145), but in the presence of high levels of IL-6, it can induce Th17 cell differentiation (146, 147). The AhR is another critical factor that dictates the Treg *versus* Th17 fate decision (148). In a ligand-specific manner, the AhR has been shown to either enhance (149) or prevent (150) EAE, in part, by regulating Treg and Th17 cell differentiation.

Intestinal-associated lymphoid tissues harbor a significant majority of the Th17 cells because these cells respond to bacterial infections and regulate the commensal microbiota (151). The diet and microbiome may be a significant source of AhR ligands that regulate Treg-Th17 balance (152, 153). Gut ‘dysbiosis’ in RA may directly contribute to the autoreactive T cell response in autoimmune arthritis. In one study that used the SKG mouse model of human RA, adoptive transfer of intestinal T cells from mice harboring fecal microbiota of RA patients with high numbers of *P. copri* caused recipient mice to develop more severe disease (154). Interestingly, other evidence of the link between T cells in the gut contributing to autoimmune arthritis comes from rat preclinical studies showing that therapies to inhibit intestinal trafficking of  $\alpha 4\beta 7^+$  T cells ameliorate not only gut-associated autoimmunity, namely Crohn’s disease, but also systemic disease in autoimmune arthritis (155). Also, most RA synovial T cells have been shown to be  $\alpha 4\beta 7^+$  (156).

B cells also participate in the pathogenesis of rheumatic diseases. Developing autoreactive B cells are usually removed from the repertoire either by being deleted in the bone marrow or by undergoing receptor rearrangement, but this process is imperfect (157). Autoreactive T cells may activate residual autoreactive B cells. Alternatively, in a T cell-

independent manner, TLR9 activation by free nuclear material and CpG-DNA may activate immature autoreactive B cells in RA patients (158). B cell zones and highly proliferative B cells surrounded by plasma cells are observed in follicular structures of pannus in arthritic joints of RA patients (159). In addition to producing autoantibodies including RF and ACPAs, which serve as predictive biomarkers of seropositive RA (160, 161), B cells may also contribute to the autoreactive T cell response in RA by expressing high levels of costimulatory molecules, like CD86, and functioning as APCs (158, 162).

### **3.5 Stromal Remodeling in Arthritis**

Bone and blood vessel remodeling processes are frequently coupled during health and disease, and both contribute to RA pathology. Proper bone integrity is maintained by a fine balance between bone formation by osteoblasts and bone resorption by osteoclasts. In health, for example, osteoclasts increase their bone-resorptive activity to keep pace with bone formation by osteoblasts to properly sculpt the developing bone tissue during adolescence, bone regeneration, and healing of fractures (163, 164). Likewise, proper tissue vascularization is necessary to bring oxygen and nutrients to healthy tissues and to the site of wound healing, but improper levels of vascularization can propagate pathological processes in certain diseases (165).

In inflammatory arthritis, excessive inflammation increases the generation of osteoclasts that express enzymes involved in bone resorption, namely cathepsin K (CatK) and tartrate-resistant acid phosphatase (TRAP) (166, 167). These cells form resorptive pits at sites where they associate with the bone. Receptor activator of NF- $\kappa$ B-ligand (RANKL) and macrophage-colony stimulatory factor (M-CSF) induce the expression of cFos and

NFATc1 in myeloid precursors or M $\phi$  to facilitate their differentiation into osteoclasts (168). Additionally, the induction of cFos and NFATc1 leads to the autoamplification of these master transcription factors, thereby increasing differentiation and the maturation of a cell with high bone-resorbing activity (169). M $\phi$  are not only osteoclast-precursors, they also are a major source of IL-1 $\beta$ , IL-6, and TNF $\alpha$ , key pro-osteoclastogenic cytokines that are upregulated following TLR2 and TLR4 signaling from DAMPs and PAMPs in the synovium. M $\phi$  are also a source of VEGF which activates VEGFR2 on endothelial cells and stimulates angiogenesis. More recently, it was shown that the binding of VEGF to VEGFR2 on M $\phi$  activates phosphoinositide 3-kinase and enhances osteoclast survival and bone-resorptive activity (170). As a source of matrix metalloproteinase-9 (MMP-9), mature osteoclasts are also capable of enhancing angiogenesis (171). MMP9 promotes endothelial cell recruitment and blood vessel branching.

In the inflamed synovial tissue, blood vessels branch toward areas of hypoxia and along the chemokine gradient of vascular growth factors (*e.g.*, VEGF and endothelial growth factor). Additionally, *in vivo*, the inflammatory response and angiogenesis are interdependent (172). This increase in synovial vascularization maintains the inflammatory and tissue-invasive environment of the RA joint and as such, inhibition of undesirable vascularization has been recognized as an approach for RA treatment for over two decades (173). Despite the excessive vascularization of the synovial tissue in RA, the tissue environment remains hypoxic (174, 175). In collagen-induced arthritis (CIA) mice, an animal model of autoimmune arthritis, it was shown that the expression and release of VEGF in the synovium coincides with the development of hypoxic tension (176). In the hypoxic environment of a tumor, it was shown that the loss of HIF1 $\alpha$  in endothelial cells

disrupts the VEGF autocrine loop that is necessary for tumorigenesis (177). A similar pathway may also contribute to excessive synovial vascularization in RA.

Synovial-infiltrating cells that are recruited to the inflamed tissue proliferate, consume oxygen to form a hypoxic environment, and produce ROS, pro-inflammatory lipids, and pro-inflammatory cytokines. In turn, these metabolic changes support the inflammatory environment that further drives bone resorption and angiogenesis. Interestingly, as with the innate immune response to TLR ligands, these stromal remodeling processes are also regulated by NF- $\kappa$ B and MAPK pathways that are activated downstream of factors that enhance angiogenesis and osteoclastogenesis. Thus, the cellular and molecular mediators of the above processes are potential therapeutic targets in RA and other diseases that share similar processes.

### **3.6 Adjuvant-Induced Arthritis (AA): An Animal Model of RA**

AA was the first among the commonly used animal models of RA (12). Many features of this model recapitulate the pathophysiology of human RA. AA is induced in rats by subcutaneous (s.c.) immunization with heat-killed *M. tuberculosis* H37Ra (Mtb) in mineral oil. As in RA, MHC-II haplotype influences disease susceptibility in rats. The Lewis rat (LEW) (RT.1<sup>l</sup>) has a high susceptibility to AA and therefore, this inbred rat strain is commonly used in AA studies. In AA, antigenic mimicry and cross-reactivity between hsp65 epitopes and mycobacterial hsp65 (Bhsp65) has been proposed as a major determinant of disease (178, 179). A few other antigens have also been identified as potential targets of the T and B cell response in AA rats.

Clinical manifestations of AA pathophysiology are principally characterized as occurring in 4 phases that correspond to incubation, onset, peak, and regression (**Figure 4**). First signs of joint inflammation in AA rats usually appear at 8-10 days (onset) post-immunization with Mtb. At 18-20 days post-immunization, the disease severity (recorded as arthritic score) reaches its peak, followed by a regression phase during which the disease score gradually decreases, but joint damage and deformity often persists. The disease presents in the synovial joints of the fore- and hind- paws, which mirrors that of the hands and feet in RA patients, respectively. In AA, joint histology shows a soft tissue growth, a pannus, invading the joint space which resembles a similar pathology in RA. This tissue is highly vascularized and laden with pathogenic synovial-infiltrating cells that contribute to synovitis (180). Subsequently, cartilage erosion and bone resorption lead to bone fusion that immobilizes the joints, known as ankylosis (181).

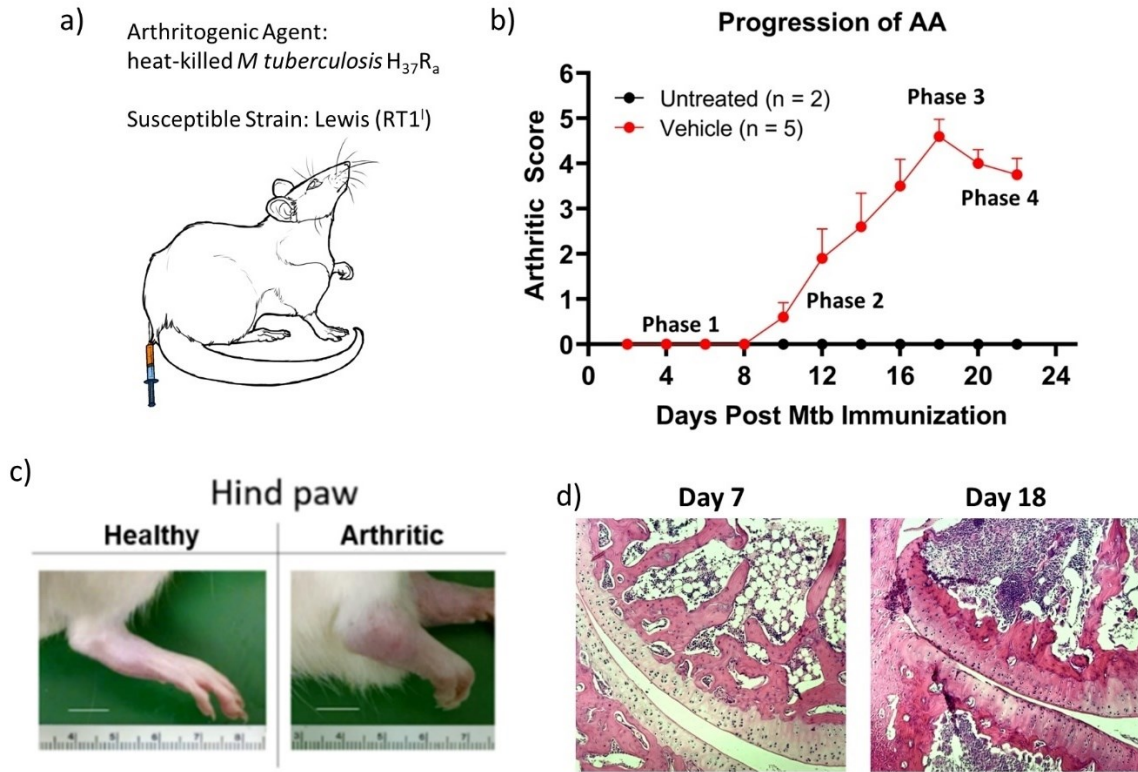


**Figure 4. Adjuvant-induced arthritis (AA): An animal model of RA.**

a) AA is induced in Lewis rats (RT1<sup>l</sup>) by s.c. immunization with heat-killed *M. tuberculosis* H37RA (Mtb) in mineral oil. b) Clinical manifestations of AA pathophysiology are principally characterized as occurring in 4 phases that correspond to incubation (phase 1), onset (phase 2), peak (phase 3), and regression (phase 4). c) Image of a hind paw taken of a rat without AA (left) and of the hind paw of a rat at the peak phase of AA (right). d) Images depicting the micromorphological characteristics of the joint in a rat with AA at 7- and 18-days post immunization.

### **3.7 Therapeutic Options for RA**

In 2010, the ACR and EULAR jointly updated the criteria for diagnosing RA and treatment standard for patients (41). It was recommended that strong therapeutic intervention be taken by 6 months of developing symptoms. Additionally, strong, and patient-tailored interventions should be taken in the event of an ineffective treatment (182). Guidelines now recommend first prescribing Methotrexate (MTX) alone or with corticosteroids, and if these do not work, to treat with modern biologics such as adalimumab and infliximab (100, 183). Following these guidelines, disease activity decreases by 50% in 75% of patients overtime. Unfortunately, that still leaves a significant number of individuals without an effective therapy. Additionally, with time, many individuals experience adverse effects, development of drug tolerance, or incur significant financial burden that requires treatment to be changed or stopped. USFDA-approved commonly prescribed drugs for RA are described in Table 1. Preventing, or even reversing, tissue damage while avoiding severe side effects is key for an effective treatment of RA.

**Table 1. USFDA-approved, commonly prescribed drugs for RA.**

<b>Agent Class</b>	<b>Drug (Example)</b>	<b>Drug Target</b>
Conventional DMARDs	Methotrexate	DHFR, inhibitor
	Leflunomide	DHODH, inhibitor
	Sulfasalazine	Under investigation
Biologics	Adalimumab Infliximab	TNF $\alpha$ , antagonist
	Tocilizumab	IL-6R, antagonist
	Anakinra	IL-1, antagonist
	Baricitinib Tofacitinib	JAK, inhibitor
	Rituximab	CD20, cytolytic antibody
	Abatacept	T cell co-stimulatory signal, inhibitor
NSAIDs	Aspirin Ibuprofen	COX-1 and COX-2, inhibitors
	Rofecoxib Celecoxib	COX-2, inhibitors
Corticosteroids	Dexamethasone Prednisone Triamcinolone Methylprednisolone	Glucocorticoid receptor, agonist

DMARDs: disease-modifying anti-rheumatic drugs, DHFR: Dihydrofolate reductase, DHODH: Dihydroorotate dehydrogenase, NSAIDs: non-steroidal anti-inflammatory drugs, JAK: Janus kinase, COX-2: cyclooxygenase-2.

### *3.7.1 Corticosteroids*

In the 1920's, the connection between hormonal steroids of the adrenal cortex and RA was made as a result of the observation that both jaundiced men and pregnant women experienced a dissipation of disease activity (184). By the 1950's, adrenal-derived steroid hormones, corticosteroids, were shown to have efficacy for treating RA and other rheumatic diseases (185). There are two groups of corticosteroids: glucocorticoids and mineralocorticoids. Glucocorticoids, namely dexamethasone, prednisone, and their derivatives, are approved by the FDA for the treatment of a range of diseases including RA. These compounds function by activating nuclear receptor subfamily 3 group C member 1 (NR3C1), which is ubiquitously expressed in almost all cell types of the body and regulates gene transcription and cellular metabolism.

### *3.7.2 Non-Steroidal Anti-inflammatory Drugs (NSAIDs)*

Traditional NSAIDs function by inhibiting COX-1 and COX-2, enzymes that lead to the production of prostaglandins (186), which influence inflammatory processes (92). COX-1 is expressed constitutively, whereas COX-2 is upregulated in cells following an innate immune response to DAMPS, PAMPs, and other endogenous inflammatory stimuli (187, 188). Inflamed articular tissue in RA often expresses high levels of COX-2 and harbors excessive levels of inflammatory prostaglandin lipid byproducts (187, 189). Aspirin and ibuprofen, which are approved for RA, are examples of traditional NSAIDs. PGE<sub>2</sub>, PGF<sub>2</sub>α, PGD<sub>2</sub>, and other lipid products from COX-1 and COX-2 action are derived from arachidonic acid and regulate both physiological and inflammatory pathways by binding several G-protein-coupled receptors that are nearly ubiquitously expressed in

the body (190, 191). As a result of inhibiting the ubiquitously expressed COX-1, traditional NSAIDs often cause serious side effects, namely ulcers and gastrointestinal bleeding (192, 193). Selective COX-2 inhibitors, like Etoricoxib and Celecoxib, were designed to provide relief from GI symptoms associated with traditional NSAIDs (192, 194). Even so, such drugs can cause myocardial infarction and cardiovascular disease that may be fatal (195, 196). Most of these drugs have been taken off the market because of these serious adverse effects.

### *3.7.3 Disease-modifying Anti-rheumatic Drugs (DMARDs)*

There are two major classes of DMARDs. They are named so because they ameliorate disease, but their mechanisms of action differ from that of corticosteroids and NSAIDs. Small molecule DMARDs include MTX, leflunomide, and sulfasalazine, which have different mechanisms of action that are described in Table 1. MTX is considered the “gold standard” drug for RA treatment and is highly prescribed in the U.S.A. Dr. Farber and colleagues at Harvard University first highlighted its clinical use for cancer in 1947 (197). Interestingly, MTX at high concentrations inhibits nucleic acid synthesis, especially in rapidly dividing cancer cells by inhibiting dihydrofolate reductase (DHFR). However, at low concentrations, MTX reduces cellular proliferation and inhibits inflammatory pathways by enhancing adenosine levels, which in turn, inhibits M $\phi$  activation and leukocyte trafficking (198). These low dose effects, which formed the basis for its use in RA, were first highlighted in 1951 (199). Second generation DMARDs have now been developed and are generally prescribed when conventional DMARDs, like MTX, fail to effectively manage the disease (100, 183).

### 3.7.4 *Biologics*

Our modern understanding of the pathophysiology of RA and technologies of protein engineering have enabled the development of biological inhibitors that target specific disease processes. These drugs first came to the market in the 1990s. Currently, FDA-approved biologics include those that target TNF $\alpha$  (anti-TNF $\alpha$ ), IL-6 (sIL-6R), and IL-1 (sIL-1Ra). These cytokines regulate various aspects of RA pathophysiology, including myeloid cell and fibroblast activation, bone resorption, angiogenesis, B cell proliferation, and Th17 differentiation (99). In the U.S.A., patients are often first started on MTX alone, but may be prescribed dual treatments using both MTX and anti-TNF $\alpha$  or anti-IL-6R when MTX alone is not sufficient to stop disease progression. Even with aggressive dual therapy, it is common for 20-40% of patients to fail to meet set DAS28 or ACR improvement standards, with some 30-60% of patients experiencing mild to serious side effects (200–202). Additionally, patients often develop anti-drug antibodies that lead to loss of drug efficacy over time and an additional 23–46% eventually become non-responsive (101).

## **Chapter 4: Microbiome and ‘Hygiene Hypothesis’: Implications for Autoimmunity, Including RA.**

The seminal work of Louis Pasteur, Robert Koch, and Joseph Lister in the 19<sup>th</sup> century provided the framework for the “Germ Theory,” “Koch Postulates,” and sterilization procedures. These were crucial to showing that single pathogens can cause specific diseases. Their work, along with others, fueled discussions on the legitimacy of sterilizing our whole environment to prevent disease. However, in the 20<sup>th</sup> century, with the development of germ-free animal systems and the technological age of high-throughput 16S ribosomal RNA sequencing, it became evident that many microbes are not pathogenic, but rather are important commensal microbes (88, 203, 204). Indeed, relationships between host and certain microbiota have developed over millennia, and symbiotic or commensal relationships have formed that are believed to be important for maintaining a ‘healthy microbiome.’ However, although progress has been made, we still have not truly elucidated what makes up a ‘healthy microbiome.’ Some of the animal studies illustrating the influence of the microbial environment on the pathogenesis of autoimmunity are shown in Table 2.

**Table 2. The impact of exposure to microbes or helminths on disease susceptibility and severity in animal models of autoimmunity.**

<b>Response</b>	<b>Diseases</b>	<b>Mechanisms</b>	<b>Ref</b>
Immune response to Hsps	RA	Spontaneous T cell response to carboxy-terminal determinants of Bhsp65 can protect against adjuvant-induced arthritis in conventionally housed F344 rats	(86)
	MS, T1D, and IBD	Oral treatment with Bhsp65-expressing <i>L. lactis</i> promotes Treg induction	(205–207)
Immune tolerance	Allergy and IBD	Germ-free environment increases invariant natural killer T cells which exacerbate oxazolone-induced colitis and ovalbumin-induced allergic Asthma	(205)
	T1D	TLR and MyD88 adaptor function is necessary for commensal bacteria-mediated resistance to T1D in Non-obese Diabetic Mice	(208)
	Allergy, IBD, T1D, RA, and MS	Healthy probiotic species has been used to protect against ovalbumin-induced asthma, spontaneous/dextran sodium sulfate-induced colitis, spontaneous T1D, CIA, and MOG-induced EAE. Typically, the mechanisms of immune-regulation involve decreasing proinflammatory cytokines such as TNF- $\alpha$ and IFN- $\gamma$ , but increasing IL-10 and TGF- $\beta$	(209–214)
	IBD and MS	Polysaccharide A from <i>Bacteroides fragilis</i> can protect against infectious colitis by increasing IL-10-producing CD4 <sup>+</sup> T cells, and against EAE by inducing IL-10-secreting FoxP3 <sup>+</sup> Tregs	(215, 216)
	Allergy, IBD, and Arthritis	<i>Bifidobacterium</i> and <i>Bacteroides</i> produce acetate and propionate that bind to G-protein receptor 43 expressed on granulocytes, and can suppress colitis, K/BxN arthritis, and ovalbumin-induced asthma	(217)
	Allergy	Endotoxin tolerance from exposure to farm dust can protect against dust mite-induced asthma by reducing IL-5 and IL-13, and it requires A20 (deubiquitylating enzyme) to be expressed in lung epithelial cells	(218)

**Table 2 continued.**

Allergy, T1D, RA, and MS	Nematodes, trematodes, and a protozoan parasite have been used to treat ovalbumin- and house dust mite-induced asthma, anaphylaxis, CIA, spontaneous arthritis in MRL/lpr mice, T1D, and EAE. While most typical mechanisms involve increasing FoxP3+ Tregs and elevating TGF- $\beta$ levels, some parasites can increase IL-10-producing T or B cells. Components of parasites such as egg antigen or excretory-secretory products can elicit Tregs, increase IL-5 and IL-33, or induce Th2 skewing	(219– 237)
-----------------------------------	---	---------------

---

Bhsp65: mycobacterial heat shock protein 65, IBD: irritable bowel disease, MOG: myelin-oligodendrocyte glycoprotein, MRL/lpr: MRL lymphoproliferation strain, T1D: Type 1 diabetes (Table from Langan D, et al., *Cell Immunol.* 2019; 339:59–67) (86).

#### **4.1 ‘Dysbiosis’ in RA and Microbiota Correlates of Disease**

A ‘dysbiotic’ gut microbiome may contribute to disease risk and progression in rheumatic diseases (238, 239) and cancer (240, 241). Oral *Porphyromonas gingivalis* (*P. gingivalis*) contributes to periodontal disease (PD), prevalent in new onset and chronic RA patients (242). In hyperlipidemic mice, *P. gingivalis* causes inflammatory oral bone loss by activating the TLR2 response and driving atherosclerosis (243); both hyperlipidemia and atherosclerosis are comorbidities of RA. In this study, an association between disease severity and the recruitment of M $\phi$ , as well as elevated IL-1 $\beta$ , IL-6, and TNF $\alpha$  in periodontal lesions, was found (243). Additionally, *P. gingivalis* may directly contribute to the host’s loss of tolerance to citrullinated proteins because this bacterium harbors a unique set of genes that encode peptidyl arginine deiminase (PAD) enzymes that convert arginine residues in proteins to citrulline (244, 245). In seropositive RA, ACPAs are prevalent. Also, PAD2 and PAD4 genes are highly expressed in circulating and synovial-infiltrating cells,

including M $\phi$ , that have been shown to citrullinate the RA candidate autoantigen vimentin (246). Interestingly, M $\phi$  incubated with *P. gingivalis* were shown to contain *P. gingivalis* PAD and, in these co-cultures, citrullinated protein levels were high (244). Interestingly, *P. histicola* that lacks PAD genes was shown to suppress inflammatory arthritis in humanized mice expressing HLA-DQ8, an RA risk allele (247). In another study using the collagen-induced arthritis (CIA) model, administration of a mutant W83 strain of *P. gingivalis* with a loss-of-function *P. gingivalis* PAD-deaminase (PPAD) gene did not exacerbate disease, unlike the wild-type W83 strain (245). These findings illustrate that *P. gingivalis* and periodontitis may predispose individuals to RA by facilitating breaks in immune tolerance.

*P. copri* is a Bacteroidia species found at elevated numbers in the gastrointestinal tract (GIT) of RA patients (93). When fecal samples from RA patients containing high numbers of *P. copri* were administered to SKG mice, a spontaneous mouse model of human RA that has a mutation in Zap70 (248), arthritis progressed rapidly and these animals had higher numbers of Th17 cells (154). The activation by *P. copri* of autoreactive T cells that recognize 60S ribosomal protein L23a (RPL23A) may have contributed to this outcome. In 2018, Lucas and colleagues showed that K/BxN mice administered several *Prevotella* spp. had lower short-chain fatty acid (SCFA) levels and significantly greater bone loss than control mice (249). SCFAs were shown to reduce osteoclast differentiation and their bone resorptive activity. However, it is not clear whether administration of SCFAs to *Prevotella*-recipient mice could prevent *Prevotella*-mediated exacerbation of arthritis and more severe bone loss. Another seminal finding came from Littman's group, which showed that segmented-filamentous bacteria (SFB) found in the GIT of certain mouse

strains can induce Th17 differentiation (250). Later, Mathis and colleagues showed that gnotobiotic K/BxN mice harboring SFB developed severe arthritis (251). The role of SFB in human disease is minimal and few studies, mostly of very few children of a young age, have identified SFB in the human GIT (252).

In a relatively recent study, it was found that some rare lineage species of Actinobacteria and Firmicutes, *Collinsella*, *Eggerthella*, and *Faecalibacteria*, were in higher numbers in the GIT of RA patients than that of healthy individuals and first-degree relatives (253). Further assessment of the possible contribution of *Collinsella* to disease risk was illustrated through *in vivo* studies showing that feeding *Collinsella* to humanized mice with CIA increased their severity of arthritis and gut permeability. It is possible that species which are present in the GIT of humans at a relatively low number and which have not yet been identified, may significantly influence disease outcome.

#### **4.2 Beneficial Commensals and Their Bioactive Metabolites**

There are commensal microbes that may also impart protection against disease. Arguably, the best demonstration of this beneficial potential of microbiota for managing disease is the success of fetal microbiota transplantations for *Clostridioides difficile* infection (254). In RA, ‘dysbiosis’ of the microbiome may be partially corrected by therapeutic intervention (255, 256), but it remains to be determined whether this partial correction in the microbiome contributed to any improved outcome from treatment. Evidence for the direct protection afforded by beneficial microbiota comes from pre-clinical studies using animal models of RA. Candidate probiotic strains of *Lactobacillus* spp. were shown to reduce arthritis severity in recipient AA rats and CIA mice as compared

to control animals (257, 258). However, strong evidence for the clinical benefit of probiotic spp. in human RA is less conclusive (259, 260). Much of the protection afforded by probiotics and commensal microbiota is derived from their bioactive metabolites (8–10). The production of beneficial or detrimental metabolites is influenced by the host’s diet and exposure to exogenous compounds (Figure 5). These confounding factors that influence the microbiome or probiotic behavior can be easily controlled for in animal studies; however, these factors may contribute to discrepancies in the efficacy of probiotic studies in human clinical trials because of a lack of control over what people consume or are exposed to during the course of treatment.

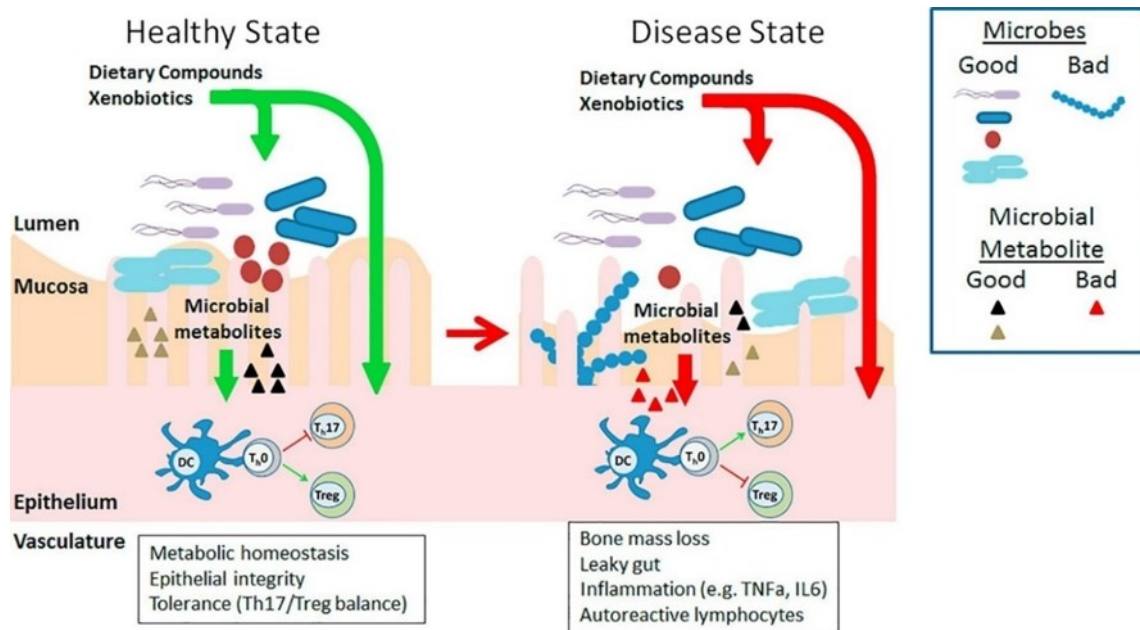


**Figure 5. The impact of diet and exposure to exogenous compounds through the gut has critical implication for health and disease.**

Good dietary habits and limited exposure to xenobiotics helps maintain a healthy microbiome that supports homeostasis and prevents disease risk. Perturbation of the microbiome because of poor dietary choices and elevated exposure to xenobiotics can increase numerous immunological factors associated with disease risk. (Figure from Langan D, et al., *Cell Immunol.* 2019; 339:59–67) (83)

#### 4.2.1 Short-chain Fatty Acid-metabolizers and SCFAs

Probiotic clinical studies for RA have focused primarily on utilizing a few classes of bacteria, chosen because they ferment SCFAs (*e.g.*, acetate, propionate, and butyrate) (259, 260). *Bifidobacterium* and *Lactobacillus* spp. produce SCFAs by fermenting carbohydrates, and for this reason they are the spp. from which most probiotics are derived. These metabolites activate G protein-coupled receptors (GPR43) on immune cells to varying degrees (261) and have been found to suppress diseases such as colitis (262) and CIA (263). Also, in the spontaneously developing arthritis K/BxN model, SCFAs were shown to be protective (249); however, in the similar arthritis model induced by serum transfer, SCFAs worsened disease (264). Interestingly, this dichotomy in the effect of SCFAs on autoimmune arthritis disease severity was also observed in the EAE model of MS (265). In this study, administration of SCFAs altered the course of EAE development by ameliorating central nervous system inflammation; however, when T cells were harvested from diseased mice and treated with acetate (SCFA) before adoptive transfer to naïve mice (passive transfer model of EAE), those receiving SCFA-treated T cells developed more severe disease than those receiving untreated T cells. This finding suggests that metabolites may have differential effects on disease outcome depending on the stage of disease. To expand on the scope of the influence of the microbial metabolome on health and disease, researchers have begun studying other microbiota-derived metabolites and elucidating their cross-talk with various immune pathways.

#### 4.2.2 Catabolites of Tryptophan (Indole Derivatives)

Dysregulated endogenous metabolism of tryptophan in RA has received attention for several decades now (266–268). The observation that indicators of tryptophan metabolism in conventionally-housed mice *versus* germ-free mice are considerably different (269), suggests that ‘dysbiosis’ may also contribute to dysregulated tryptophan metabolism in RA patients (270). Certain *Bifidobacterium* and *Lactobacillus* spp. that can produce SCFAs can also produce indole derivatives from tryptophan, and they have been used as probiotics in RA and animal models (257, 259, 260, 271). Specific indole derivatives are putative ligands of two host xenobiotic receptors, the AhR, which is highly expressed in many tissues, including hematopoietic cells, and the pristane X receptor (PXR), which is expressed largely in the GIT and liver mesenchymal cells (153). As discussed above, the AhR has been shown to regulate the effect of smoke and the smoke compound, TCDD, on RA synovial tissue explants and in animal models of RA; therefore, the AhR is a target molecule that is of interest in the treatment of RA.

Interestingly, SCFAs were shown to enhance the AhR responsiveness of human Caco-2 (colonic epithelial cells) and Young adult mouse colonic epithelium cells to tryptophan catabolites known to be derived from gut microbiota, namely indole, tryptamine, and 1,4-dihydroxy-2-naphthoic acid (DHNA) (272). This implies possible cross-talk between different host pathways that are activated by different microbiota metabolites. In this case, the histone deacetylase activity of SCFAs appeared to enhance the AhR-responsiveness of cells to these tryptophan catabolites. However, it has yet to be

shown whether similar cross-talk occurs *in vivo*. This begs the question of whether this mechanism may explain outcomes of SCFA treatment studies.

Several microbiota-derived indole derivatives have been shown to improve intestinal barrier function by both AhR and PXR-dependent mechanisms (11, 273, 274). Additionally, in murine EAE, it was shown that microbiota-derived tryptophan metabolites mediate disease in an AhR-dependent manner through induction of Type I IFN in astrocytes (275). Aromatic amino acid aminotransferase has been identified in some *Lactobacillus* spp. and as a result of expressing this enzyme they produce certain putative AhR ligands including indole-3-acetic acid (I3AA), indole-3-acetaldehyde, and indole-3-aldehyde (IAld) (11). *L. acidophilus*, *L. casei*, *L. rhamnus* and *L. reuteri* produce these indole derivatives and have shown some success as probiotics for RA (259, 260). Although microbial tryptophan metabolism may play a role in the development of RA and disease in animal models of RA, causation has yet to be established. There are several enzymatic pathways of indole derivatives that are expressed by gut microbiota (**Figure 6**). Harboring microbiota with different enzymes that metabolize tryptophan is likely to differentially influence the host health and immune state as a result of altering the bioavailability of specific indole derivatives.

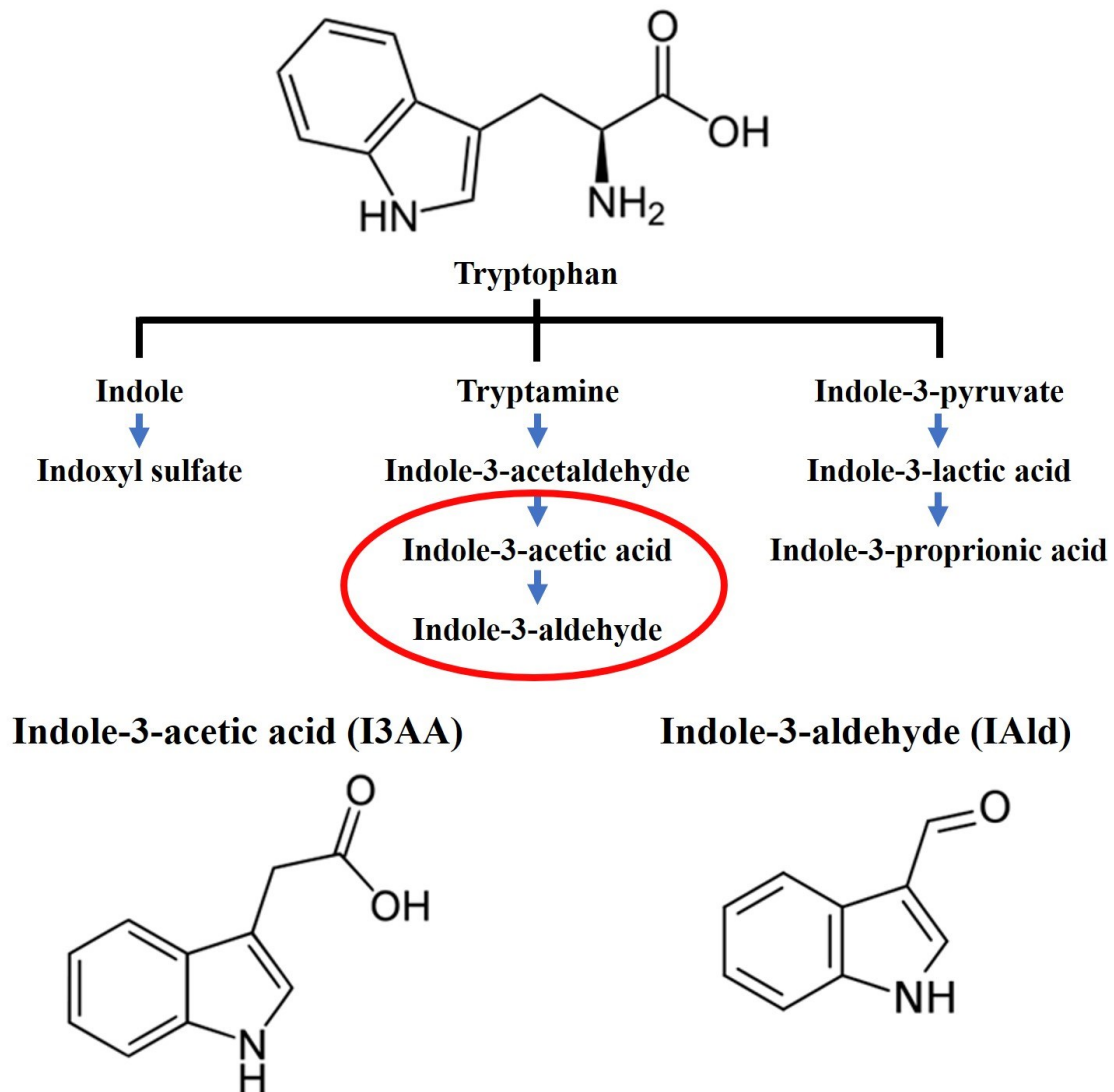


**Figure 6. Microbiota-derived catabolites of tryptophan (indole derivatives).**

The metabolism of tryptophan by microbiota involve several different pathways and lead to the production of specific indole derivatives with bioactivities that influence host health and disease. The indole derivatives IAld and I3AA, tested in this study, are circles in red.

#### 4.2.3 Other Microbiota-derived Immunoregulatory Metabolites that Influence Arthritis

The metabolite DHNA, produced by *Propionibacterium freudenreichii* and *Lactobacillus casei* LP1, is an AhR ligand (276, 277). *L. casei* has been investigated as a probiotic therapy for RA but is also known to produce SCFAs and indole derivatives. Another metabolite, vitamin K2, is a class of menaquinones (MK) that vary in chain length, of which MK5 to MK12 are produced by microbiota. Plant-derived MK4 has been tested in CIA as well as in clinical studies (278). Observations showing that vitamin K2 enhances bone mineralization of human osteoblasts as well as apoptosis of osteoclasts and RA synovial-infiltrating cells were used as the foundation to test MK4 and MK7 in RA clinical trials (279, 280). MK7, which unlike MK4 is produced by microbiota, showed greater efficacy by reducing general inflammatory markers, namely CRP and MMP-3, as well as the DAS28 of RA patients. The neurotransmitter  $\gamma$ -aminobutyric acid, another anti-arthritic metabolite that is produced by certain microbiota (281), has been shown in preclinical studies of T1D, MS, and RA to effectively reduce disease (282–284).

## Chapter 5: The Xenobiotic and Antioxidant Responses

The xenobiotic and antioxidant responses of a cell are controlled by two major cytosolic receptors, AhR and nuclear factor erythroid 2-related factor 2 (Nrf2), respectively. Chemical agents that are not expected to be present in an organism are termed xenobiotics. These chemicals are neither essential nor are they normally synthesized endogenously. Chemical agents from smoke, like TCDD, as well as mercury and silicates, which are discussed above in the section on environmental risk factors, are examples of xenobiotics. TCDD was the agent first used in the identification of the AhR (285). The AhR is activated by many xenobiotic agents, as well as by certain endogenous metabolites (152, 286). Upon activation, AhR translocates to the nucleus where it induces the expression of genes with the xenobiotic response element (XRE, also sometimes called a dioxin response element) in their promoter region, namely phase I enzymes (*e.g.*, Cytochrome P450 monooxygenase (CPY) enzymes CYP1A1 and CYP1B1). Phase I enzymes break down xenobiotic agents and metabolize endogenous compounds (286). They also produce ROS as a byproduct of their oxidative enzymatic activity. More recently, the AhR has been shown to regulate other transcription pathways by binding to factors such as RELB (287) and STAT1 (288).

ROS (*e.g.* NO,  $O_2^{\cdot-}$ ,  $H_2O_2$ ) are a byproduct of cell metabolism and can act as secondary messengers; however, intracellular ROS levels are normally low in quiescent cells. In a state of chronic activation and hyperproliferation, such as for synovial infiltrating cells and stromal cells in the arthritic joints of an individual with RA, intracellular ROS can accumulate to high levels. If left unchecked, this can contribute to tissue damage and

chronic inflammation. The gene encoding Nrf2 is constitutively expressed, but the level of Nrf2 in a non-stressed cell is normally low and the protein is excluded from the nucleus because it associated with Kelch-like ECH-associated protein 1 (Keap1) in the cytosol. This association leads to proteasomal degradation (289). In an activated cell, ROS can build up and upon cleavage of the disulfide bond between KEAP1 and Nrf2 by a ROS, Nrf2 translocates to the nucleus and upregulates genes with the antioxidant response element (ARE, also sometimes called an electrophile response element) in their promoter region, namely phase II enzymes (*e.g.*, HMOX1 (Heme oxygenase 1) and NQO1 (NADPH dehydrogenase [quinone] 1)) that metabolize ROS species into non-cytopathic products. In M $\phi$ , ROS can also act as anti-microbial agents (290), or as second messengers that activate NF- $\kappa$ B and MAPK pathways (291, 292). In osteoclasts, for example, ROS enhances NF- $\kappa$ B and AP-1 signaling as well as induces the expression of NFATc1, the osteoclast master transcription factor (293). Expression and auto-amplification of NFATC1 thereby increase osteoclastogenesis (169). Also, synthetic scavengers of ROS have shown promise for RA treatment by reducing ROS and subsequently driving inflammatory M $\phi$  to an anti-inflammatory differentiation state (294). These findings highlight the crucial role that the antioxidant response has in mitigating tissue damage in RA by keeping ROS levels low.

The AhR is now known to regulate a myriad of processes, including T cell differentiation (148), inflammatory responses of M $\phi$  (288, 295), angiogenesis (296), and osteoclastogenesis (297). Interestingly, Nrf2 has been shown to regulate these same processes, and in some cases, in a similar way as AhR (298–301). This activity makes both pathways a target for the treatment of RA. Some of the overlap in AhR- and Nrf2-dependent effects on cellular processes may be due to significant cross-talk between the

xenobiotic and antioxidant pathways. In fact, this interplay has made classifying AhR and Nrf2 ligands difficult. Such was the case for sulforaphane which was first thought to be an AhR ligand, but later determined to be a monofunctional Nrf2 agonist (302). Also, plant-derived phytochemicals have even been identified that regulate one (monofunctional) or both (bifunctional) AhR and Nrf2 responses in either specific agonistic or antagonistic manners (303).

Some of this cross-talk between pathways involves transcriptional upregulation of NRF2 by AhR, and vice versa. The AhR recognizes XREs in the NRF2 promoter to induce its expression (304). Also, the phase I enzymes expressed upon AhR activation produce ROS byproducts that, in turn, activate Nrf2. Likewise, Nrf2 recognizes AREs in the AHR promoter and induced its expression (305). The consequences of this cross-talk in cancer progression and treatment success are already recognized (303). It is also likely that the cross-talk between these pathways is important to consider in RA progression and treatment. However, the effects of AhR or Nrf2 activation on cellular processes appears to be highly ligand-specific. More work is needed to understand how the AhR and Nrf2 pathways specifically contribute to RA and, in turn, what environmental factors might contribute to disease risk by differentially regulating the AhR and Nrf2 responses. Some of the main points discussed above in this section are illustrated below (**Figure 7**).

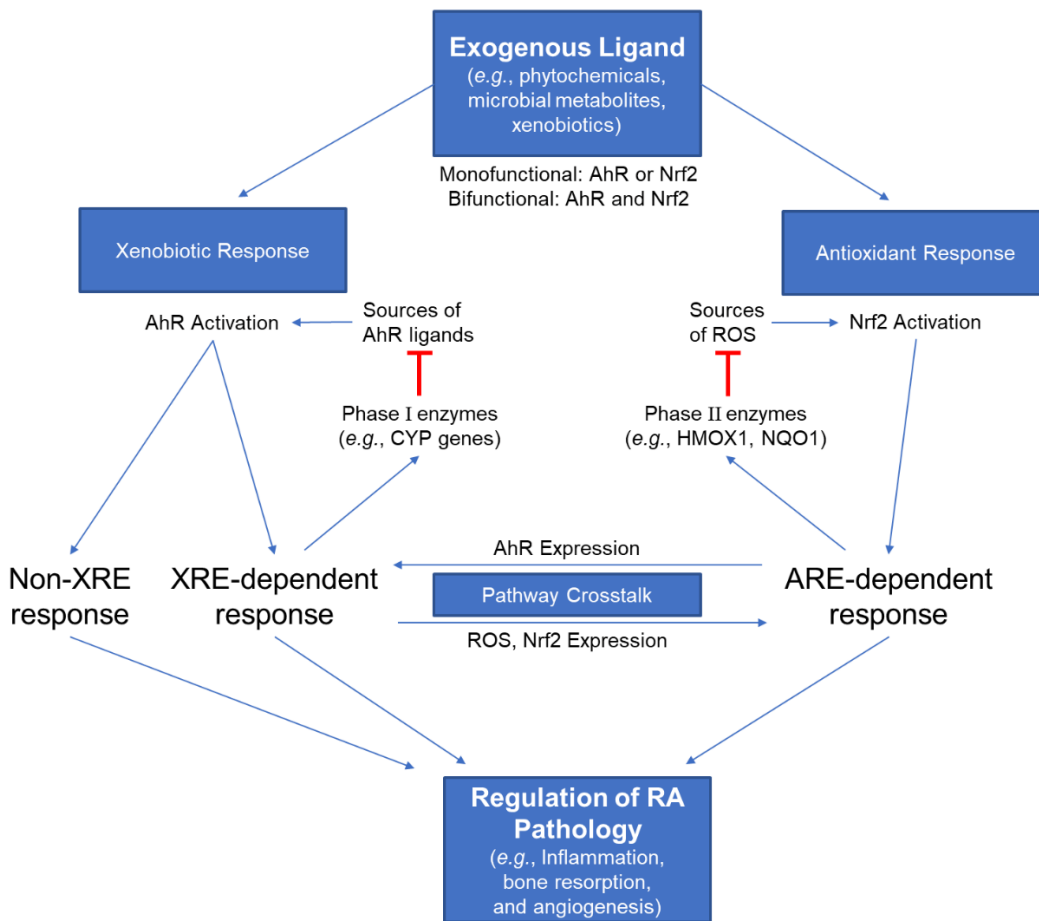


**Figure 7. The environment is a source of exogenous AhR and Nrf2 ligands that regulate RA pathology.**

Specific environmental ligands regulate the xenobiotic response, which is controlled by AhR, and the antioxidant response, which is controlled by Nrf2, in specific agonistic and antagonistic manners that involve their activity as either monofunctional or bifunctional agents. These two pathways exhibit significant cross-talk. In addition to regulating the expression of enzymes (phase I enzymes by AhR and phase II enzymes by Nrf2, respectively) that convert agonists of these receptors into inert products to be removed from the body, these two pathways are critical regulators of numerous cellular processes involved in RA pathogenesis. Exogenous ligands that regulate the xenobiotic and/or antioxidant response can therefore have a significant impact on RA pathology.

## Chapter 6: Materials and Methods

### 6.1 Cell Culture

RAW 264.7 (RAW) cells (ATCC, Manassas, VA) were maintained in Quality Biological Dulbecco's Modified Eagles Media XL (DMEM XL) (Gaithersburg, MD). Human Umbilical Vein Endothelial Cells (HUVEC) (ATCC) were maintained in Cell Applications Endothelial Cell Growth Media (cat#211-500, San Diego, CA). Media for culturing all cell lines contained 10% heat-inactivated fetal bovine serum (FBS), Penicillin (100 units/mL), Streptomycin (100 µg/mL), and L-Glutamine (2 mM) (Gibco, Gaithersburg, MD).

### 6.2 Chemicals and Reagents

Indole-3-acetic acid (I3AA), indole-3-aldehyde (IAld), and CH-223191 (CH22) were all from MilliporeSigma (Billerica, MA). The 1-(2-Cyano-3,12,28-trioxooleana-1,9(11)-dien-28-yl)-1H-imidazole (CDDO-IM) was from Tocris (Minneapolis, MN), and CM-H<sub>2</sub>DCFDA was from Invitrogen (Carlsbad, CA). All above-mentioned compounds were solubilized in dimethyl sulfoxide (DMSO) (MilliporeSigma). The 3-(4,5-dimethylthiazol-2-yl)-2,5-diphenyltetrazolium bromide (MTT) and the Leukocyte Acid Phosphatase Kit for TRAP staining were purchased from MilliporeSigma. Heat-killed *M. tuberculosis* HR37a (Mtb) was purchased from Becton, Dickinson and Company (Sparks, MD). This Mtb was used in the preparation of sonicate supernatant with minor modifications of a previously described procedure (306). Protein-free *E. coli* LPS was prepared as described previously (307), and was a kind gift of Dr. Stefanie Vogel, UMB.

Recombinant human vascular endothelial growth factor peptide (VEGF<sub>165</sub>) and murine soluble receptor activated NF-κB ligand (RANKL) were both supplied by Peprotech (Rockhill, NJ). Matrigel growth factor reduced basement membrane matrix was from Corning (Corning, NY). Primary antibodies (anti-IκBα (44D4), anti-phosphorylated ERK1/2 (197G2), anti-phosphorylated p38 (D3F9), anti-phosphorylated p65 (D3H1), and anti-total p38 (9212) were all obtained from Cell Signaling (Beverly, MA).

### **6.3 Cytotoxicity Assessment by MTT Assay**

In a 96-well plate, RAW or HUVEC were seeded at either  $8.0 \times 10^4$  or  $7.5 \times 10^3$  cells/well, respectively, one day before treatment with I3AA or IAld. After 24 h, MTT was then added to cells as directed by the kit protocol for the MTT Assay for Cell Viability and Proliferation. Absorbance (595 nm) was measured on a Bio-Rad iMark plate reader. Relative absorbance (Mean  $\pm$  SEM) was calculated by normalizing to DMSO-treated cells after subtracting background, and results were presented as relative cell viability (308). MTT is a colorimetric assay that works to measure relative cell viability because in live cells MTT is converted into a crystalline form by NAD(P)H-dependent cellular oxidoreductase enzymes. The amount of MTT conversion in a culture is positively correlated to the absorbance of light (595 nm); therefore, a change in the absorbance of light from cell cultures treated with an agent as compared to control cell cultures will indicate the effect of said agent on cell viability and/or growth rate.

## 6.4 Quantitative Real-time Polymerase Chain Reaction

Total mRNA from cells was isolated using TRIzol (Invitrogen) according to the manufacturer's instructions. The cDNA was then prepared using the qScript cDNA Synthesis kit (Quantabio, Beverly, MA) and tested in qRT-PCR using Power SYBR Green PCR Master Mix (Applied Biosystems, Forster City, CA). Primers were either obtained from a commercial source (Integrated DNA Technologies (IDT) or MilliporeSigma) or designed in-house. The latter were designed using the Primer Express 2.0 Program (Applied Biosystems) or were based on sequences in the Harvard primer bank and are listed in Table 3. Steady-state mRNA levels were normalized to the housekeeping gene hypoxanthine-guanine phosphoribosyl transferase (HPRT) and results expressed as fold change in expression relative to the untreated controls (fold induction) using the  $2^{-\Delta\Delta CT}$  method (309).

**Table 3. Sequences of in-house designed primers**

<b>Target</b>	<b>Sequence Fwd</b>	<b>Sequence Rev</b>
<b>HPRT</b>	5' – TTGCTGACCTGCTGGATTAC – 3'	5' – ACTTTTATGTCCCCCGTTGACTGAT – 3'
<b>IL-1<math>\beta</math></b>	5' – GGTCAAAGGTTTGGGAAGCAG – 3'	5' – TGTGAAATGCCACCTTTTGA – 3'
<b>IL-6</b>	5' – GATGGATGCTACCAAAGTGA – 3'	5' – TCTGAAGGACTCTGGCTTTG – 3'
<b>TNF<math>\alpha</math></b>	5' – GACCCTCACACTCAGATCATCTTC – 3'	5' – CCACTTGGTGGTTTGCTACGA – 3'
<b>COX-2</b>	5' – TGCCTGGTCTGATGATGTATG – 3'	5' – GGGGTGCCAGTGATAGAGTG – 3'
<b>CatK</b>	5' – CTCCAATACGTGCAGCAGA – 3'	5' – GCCGTGGCGTTATACATACA – 3'
<b>TRAP</b>	5' – ACGGCTACTTGCGGTTTCACTA – 3'	5' – GTGTGGGCATACTTCTTTCCTGT – 3'

## **6.5 Determination of the Immunomodulatory Effect of Indole Derivatives on the Response of RAW Cells to Mtb-sonicate or LPS**

RAW cells were seeded in 96-well plates at  $8.0 \times 10^4$  cells/well one day prior to treatment. Then, Mtb (10  $\mu\text{g}/\text{mL}$ ) or LPS (20  $\text{ng}/\text{mL}$ ) was added to cells and total RNA isolated after another 16 h or 2 h, respectively. RNA from 6-8 identically treated wells was pooled for analysis of mRNA by qRT-PCR. The role of AhR in mediating the effect of I3AA and IAld on Mtb-induced gene expression was assessed using CH-223191, which was added concomitantly with vehicle (Veh), I3AA, or IAld. Agents were added to cells 1 h prior to the addition of Mtb. For immunoblot analysis, RAW cells were seeded in 12-well plates at a final concentration of  $1.5 \times 10^6$  /well one day prior to treatment with LPS (100  $\text{ng}/\text{mL}$ ). Pretreatment of cells with Veh, I3AA (0.5 mM), or IAld (0.5 mM) began 1 h before the addition of LPS. Lysates were collected from cells treated as described above and from cells left untreated and then subject to immunoblot analysis.

## **6.6 Analysis of Cell Signaling by Immunoblot Analysis**

Cells lysates were processed and immunoblots run as previously described (310). Cells were lysed in a buffer (1% Triton x100, 25 mM HEPES, 100 mM NaCl, 0.1% SDS) on ice before freezing at  $-80^\circ\text{C}$  until further use. Lysates were separated by electrophoresis on a tris-glycine gel (Biorad, Hercules, CA). Subsequently, the proteins thus separated were transferred on to a Polyvinylidene difluoride (PVDF) membrane. The blots were then blocked with 5% non-fat dry milk in tris-buffered saline containing Tween 20 Detergent (TBST) (0.3% Tween), washed three times with TBST while shaking over the course of 1 h, and incubated overnight with the primary antibodies at  $4^\circ\text{C}$  in either TBST containing

5% non-fat dry milk or 5% BSA. The following day, membranes were washed with TBST three times and then incubated with the anti-rabbit HRP-conjugated secondary antibody (Jackson Immunochemicals, West Grove, PA) in TBST containing 5% milk. Blots were developed using the ECL Plus Western Blotting Detection Reagent (Amersham Biosciences, Piscataway, NJ). Before subsequent re-probing, the blots were stripped with Bio-Rad western stripping reagent. Total MAPK p38 protein served as the loading control for normalization of densitometry analysis using ImageJ software (NIH). The ratio of the signaling intensity relative to total p38 was then calculated.

### **6.7 Osteoclast Generation and Subsequent Testing of the Effect of IAld and I3AA**

To generate osteoclasts, RAW cells were treated with RANKL for 5 d and the resulting osteoclasts were counted as described (**Figure 8**) (311). At  $1.4 \times 10^4$  cells/cm<sup>2</sup> in a 48 well dish, RAW cells were seeded one day prior to adding RANKL (100 ng/mL) in addition to either Veh, I3AA, or IAld (0.0125 – 0.2 mM). On d 3, the media and reagents were refreshed. On d 5, cells were stained to detect TRAP expression in accordance with the manufacturer's instructions. After differentiation and staining of cells for TRAP expression, images were taken of several regions in each well with a BZ-X710 Microscope (Keyence, Osaka, Japan). The number of osteoclasts (*i.e.*, TRAP<sup>+</sup> and multinucleated (3+ nuclei) cells) were enumerated using ImageJ software. The role of AhR in mediating the effect of either I3AA or IAld on osteoclast formation was assessed with the addition of CH-223191 added concomitantly with Veh, I3AA, or IAld, as indicated. In parallel with staining, cells were treated identically as for imaging, but the expression of genes involved in bone resorption was assessed by qRT-PCR.

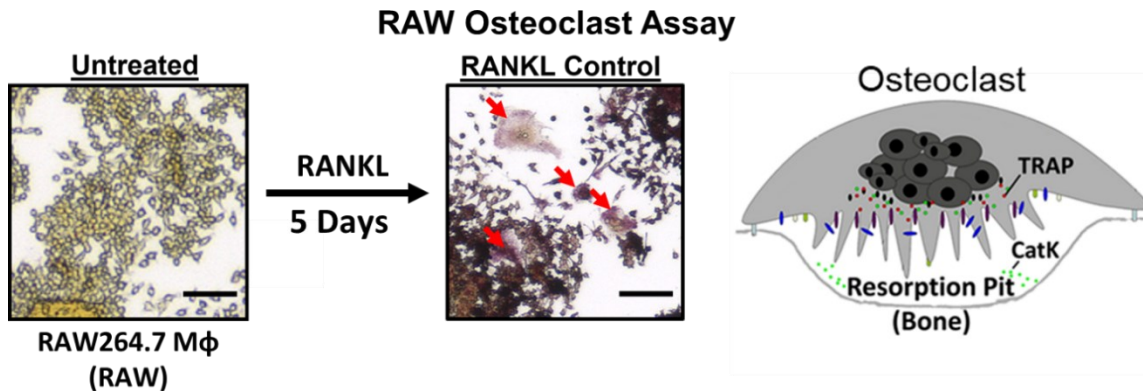


**Figure 8. The generation of osteoclasts from RAW cells.**

RAW cells are seeded the day prior to treatment with RANKL (100 ng/mL). On d 3, the media and reagents are refreshed. On d 5, these cells are stained for TRAP expression. In parallel, total RNA is prepared from cells for qRT-PCR analysis of the expression of osteoclast genes. Osteoclasts are indicated with a red arrow. Osteoclasts form resorptive pits, where they associate with the bone and secrete bone-resorbing enzymes.

### 6.8 Analysis of a Role for Nrf2 in Mediating the Effect of IAld on Mφ

First, we tested whether IAld could inhibit the expression of antioxidant genes in response to an Nrf2-specific agonist, CDDO-IM. RAW cells were plated and treated with either Veh, IAld (0.05 – 0.2 mM), or I3AA (0.2 mM) for 1 h before the addition of CDDO-IM (0.1 μM). Steady-state mRNA levels in untreated cells were used to calculate fold induction of antioxidant genes HMOX1 and NQO1 by qRT-PCR. To assess the potential consequence of this interplay in osteoclast formation, osteoclasts were generated as described above, with the addition of CDDO-IM (0.004 – 0.1 μM). A similar, experiment with the addition of CDDO-IM (0.1 μM), was performed on RAW cells treated with Mtb as previously described.

## 6.9 Intracellular ROS in RANKL-treated RAW Cells and Impact of IAld

Relative intracellular ROS levels were measured in untreated RAW cells and compared to that of cells treated with RANKL alone or concomitantly with RANKL and IAld (0.02 – 0.2 mM). At varying time points after starting treatment, media was removed, cells were washed with Hank's Balanced Salt Solution (HBSS), and CM-H<sub>2</sub>DCFDA (5 μM) in HBSS was added. CM-H<sub>2</sub>DCFDA is a cell permeable dye that is cleaved by intracellular esterases and then links to thiol groups of intracellular proteins, thereby becoming locked inside the cell. Upon exposure to ROS, the dye gets cleaved into a fluorescein isothiocyanate-derivative. Cells were incubated (30 min at 37 °C) before washing and suspending them in fresh HBSS. Equivalent viability of cells was ensured by quantification by trypan blue exclusion on an aliquot of cells from each condition. Next,  $8.0 \times 10^4$  cells were taken from each suspension and added to four wells of a 96-well plate to assess fluorescence (Ex: 495 nm; Em: 525 nm) using a Gemini XPS microplate reader (Molecular Devices, San Jose, CA). Fluorescence intensity was normalized by subtracting out background using the mean fluorescence value from cells that were not loaded with the CM-H<sub>2</sub>DCFDA. Then, the percentage of intracellular ROS was calculated relative to cells not treated with RANKL (untreated), but that were loaded with CM-H<sub>2</sub>DCFDA. This was done by dividing the normalized fluorescence of cells within each set of wells by the mean normalized fluorescence of the untreated set. After analyzing on the plate reader, cells were allowed to settle for analysis by fluorescence microscopy on a BZ-X710 microscope (Keyence). Representative images were taken. The basic workflow used to test the role of the AhR and Nrf2 pathways on mediating the effect of these indole derivatives is shown below (**Figure 9**).

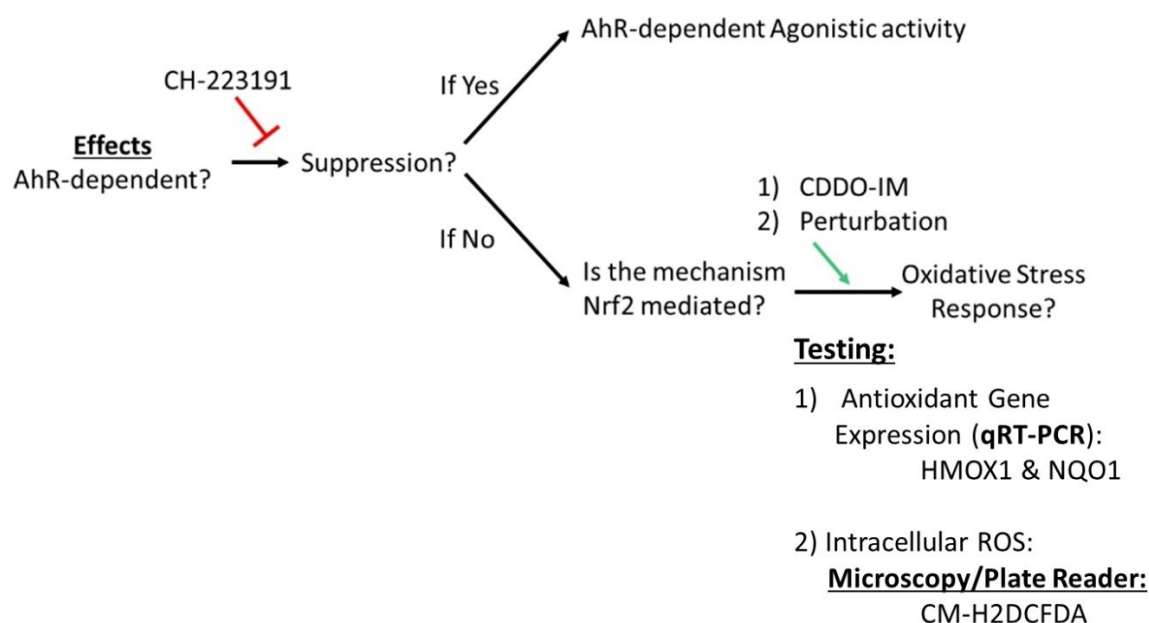


**Figure 9. Experimental design of how a potential role for the AhR and Nrf2 pathways in mediating the observed effects of the indole derivatives were tested.**

It was first tested whether the observed effect of an indole derivative on any of the cell types was AhR-dependent. This was done by antagonizing the AhR with CH-223191. If AhR antagonism did not suppress the effect of an indole derivative, then it was tested whether the indole derivative could regulate the Nrf2-dependent antioxidant response and alter the level of oxidative stress in cells perturbed with RANKL. To test this, the effect of the indole derivative on Nrf2-dependent induction of antioxidant genes was assessed by qRT-PCR and by using the Nrf2 agonist, CDDO-IM. Next, the effect of the indole derivative on intracellular ROS levels following perturbation was tested using the CM-H<sub>2</sub>DCFDA dye.

### 6.10 2D-Matrigel Tube Formation Assay with HUVEC and Subsequent Assessment of the Effect of Indole Derivatives

The 2D-Matrigel tube formation assay with HUVEC was performed as described previously, with minimal modifications (**Figure 10**) (312). Cells were serum-starved overnight with Endothelial Cell Basal Media (ECBM) 210-500 (Cell Applications, San Diego, CA) supplemented with 1% FBS. The cells were then trypsinized to suspend them, next washed and resuspended in fresh ECBM media with 1% FBS. Afterwards, HUVEC

were added to a 96-well plate at  $2.5 \times 10^4$  cells/well containing 30  $\mu$ L of solidified Matrigel in media containing VEGF<sub>165</sub> (25 ng/mL). To ensure equal seeding density, wells were checked 30 min after seeding cells. At 1 h after seeding, Veh, I3AA (0.25 – 1.0 mM), or IAld (0.125 – 1.0 mM) was added to the cells. The role of the AhR pathway in mediating the effect of I3AA and IAld on angiogenesis was assessed by adding CH-223191 (3  $\mu$ M) at the time of cell seeding along with VEGF, followed by I3AA or IAld 1 h later. Phase contrast images were taken with a BZ-X710 fluorescent microscope (Keyence). Images were taken from 4 regions of each well either 8 or 16 h after cells were seeded. The morphology of capillary-like structures was analyzed and the number of completed loops in each image enumerated using ImageJ Software.

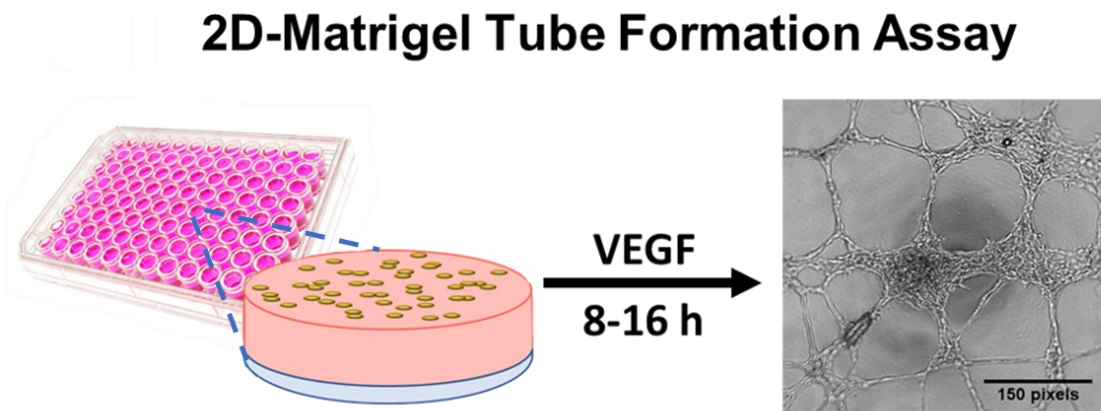


**Figure 10. The 2D-Matrigel tube formation assay using HUVEC.**

HUVEC are seeded in a 96-well plate containing solidified growth factor reduced Matrigel with media containing VEGF (25 ng/mL). Tubes form over 8-16 h before phase contrast imaging.

## 6.11 Induction of AA, Disease Evaluation, and IAld Treatment

Animal work was conducted in accordance with guidelines of the Institutional Animal Care and Use Committee (IACUC) of the University of Maryland School of Medicine, Baltimore (UMB) and the SRS Committee of Veterans Affairs (VA) Medical Center, Baltimore. Male Lewis rats (LEW/SsNHsd (RT.1<sup>h</sup>)) (Envigo, Madison, WI, USA) at 5-6 weeks of age were injected s.c. with heat-killed *M. tuberculosis* H37Ra (Mtb) (Becton, Dickinson and Company, Sparks, MD) (1.5 mg/rat) suspended in mineral oil (MilliporeSigma) at the base of the tail to induce AA as previously described (306). A group of these rats (treated) received IAld (5 mg/kg) daily by oral gavage starting on d 5 post-Mtb immunization whereas the other rats received the vehicle only. Another group of these rats was left untreated as a naïve control. Following immunization, the paws were examined daily or on alternate days for the signs of arthritis. Arthritic score, an indicator of disease severity, was determined for each paw on a scale from 0 to 4 based on redness and swelling, and the total arthritic score determined by summing of the scores of all 4 paws as described previously (313).

## 6.12 Extraction of Indole Derivatives and Standard Spike Analysis by HPLC-UV

Blood was collected from anesthetized rats by cardiac puncture. Blood samples were placed on ice until some samples were spiked with indole derivatives (0.01 – 50  $\mu$ M). Then, the blood was allowed to clot at 37 °C for 15 min before centrifuging it at 3,000 RCF for 7 min at 4 °C. Thereafter, the serum fraction was collected into a new tube and frozen at -80 °C until needed for chloroform-methanol extraction. For extraction, an ice-cold methanol-chloroform mixture (1:1 v/v) was prepared. The plasma was thawed, and the

methanol-chloroform mixture was added to it at (1:2 v/v). This mixture was vortexed for 2 min, followed by centrifugation at 15,000 RCF, 5 min, 4 °C to obtain phase separation. The polar (upper) phase was collected and passed through a 70- $\mu$ m filter. The samples were then allowed to evaporate to dryness using a SpeedVac. The final solution was reconstituted in methanol and stored at -80 °C until being analyzed by HPLC-UV. Then, samples were run through a 00G-4144-B0 spherclone 5  $\mu$ m ODS(2) C18 column, 250 mm  $\times$  2.00 mm, at a constant flow rate, and at 40 °C. Mobile phase consisted of 0.1% acetic acid:80% acetonitrile (37:63).

### **6.13 Statistical Analysis**

Statistical analysis was performed using GraphPad Prism (v8.4.3) statistical software. Ordinary one-way analysis of variance (ANOVA) or two-way ANOVA with the subsequent recommended post-hoc test for multiple comparisons of more than two groups was run. Either paired or standard Student's *t* test (two-tailed) was used to compare the results from two groups when data was collected and combined from multiple independent experiments, or when replicates of a single representative experiment were used, respectively. A p-value of less than 0.05 was considered to be statistically significant.

## Chapter 7: Results

### 7.1 Assessment of Cytotoxicity of IAld and I3AA on RAW Cells and HUVEC.

RAW cells or HUVEC were treated with either Vehicle (DMSO), Resveratrol (Res), IAld (0.1 – 1.0 mM), or I3AA (0.1 – 1.0 mM) for 24 h followed by the addition of MTT to measure relative cellular viability (**Figure 11**). Results from analysis of cells treated with Res, an agent known to exhibit cytotoxic effects, clearly show reduction of cell viability. In comparison, cells treated with either IAld or I3AA showed minimal differences in cell viability compared to the control cells treated with vehicle. These findings suggest that the immunomodulatory and stromal-regulatory effects of IAld and I3AA in our study (described below) are not the result of cytotoxicity.

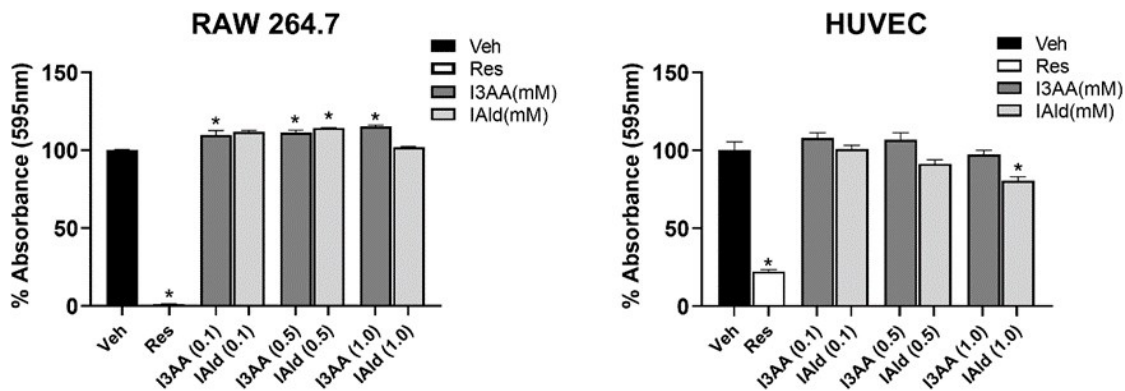


**Figure 11. Assessment of cellular cytotoxicity of I3AA and IAld by MTT assay.**

RAW cells or HUVEC were treated for 24 h with either vehicle (Veh), indole-3-acetic acid (I3AA), or indole-3-aldehyde (IAld), at the indicated concentrations (mM), followed by addition of MTT. Results of a representative experiment ( $n = 3-4$ ) are reported as percent absorbance (595 nm) (Mean  $\pm$  SEM) relative to the Veh control. Resveratrol (Res) was used as a positive control for the cytotoxic effect. Even at 1 mM, both IAld and I3AA showed minimal effects. Statistical differences were assessed using ordinary one-way ANOVA with Dunnett's correction for multiple comparisons. Asterisk (\*) indicates the conditions with  $p < 0.05$ . (Figure from Langan D, et al., *Int J Mol Sci.* 2021; 22(4):2017) (314).

## 7.2 IAld, but not I3AA, Inhibits Expression of Several Pro-inflammatory Cytokines by M $\phi$ in Response to Mtb

The steady-state level of mRNA for genes encoding several myeloid-derived mediators of inflammation was measured by qRT-PCR in RAW cells (murine M $\phi$ ) stimulated with Mtb (an arthritogenic agent for AA in rats) that activates both TLR2 and TLR4 (315). The induction of genes encoding various mediators of inflammation (*e.g.*, cytokines and COX-2) and angiogenesis (*e.g.*, VEGF) in response to Mtb was compared between Mtb-treated cells (controls) and cells concomitantly treated with Mtb and IAld or I3AA. The level of expression of inflammatory mediator genes were upregulated by Mtb (**Figure 12**), but the addition of IAld (0.25 mM) altered the induction of a subset of these genes. Inhibited cytokine gene expression was observed for IL-1 $\beta$  ( $p = 0.0013$ ) and IL-6 ( $p = 0.0195$ ) (**Figure 12a**). A trend toward inhibition of COX-2 expression by IAld was also observed, but statistical significance was not reached ( $p = 0.085$ ). In contrast, expression of TNF- $\alpha$  was unaffected by the addition of IAld. Additionally, there was a significant increase ( $p = 0.0183$ ) in the expression of VEGFA, a critical pro-angiogenic factor.

I3AA failed to have a significant effect on the expression of any of the genes tested (**Figure 12b**). Even high concentrations of I3AA (up to 1.0 mM) failed to elicit any effect (data not shown). Importantly, IAld and I3AA had no cytotoxic effect at the concentration (0.25 mM) used in the above experiments (**Figure 11**).

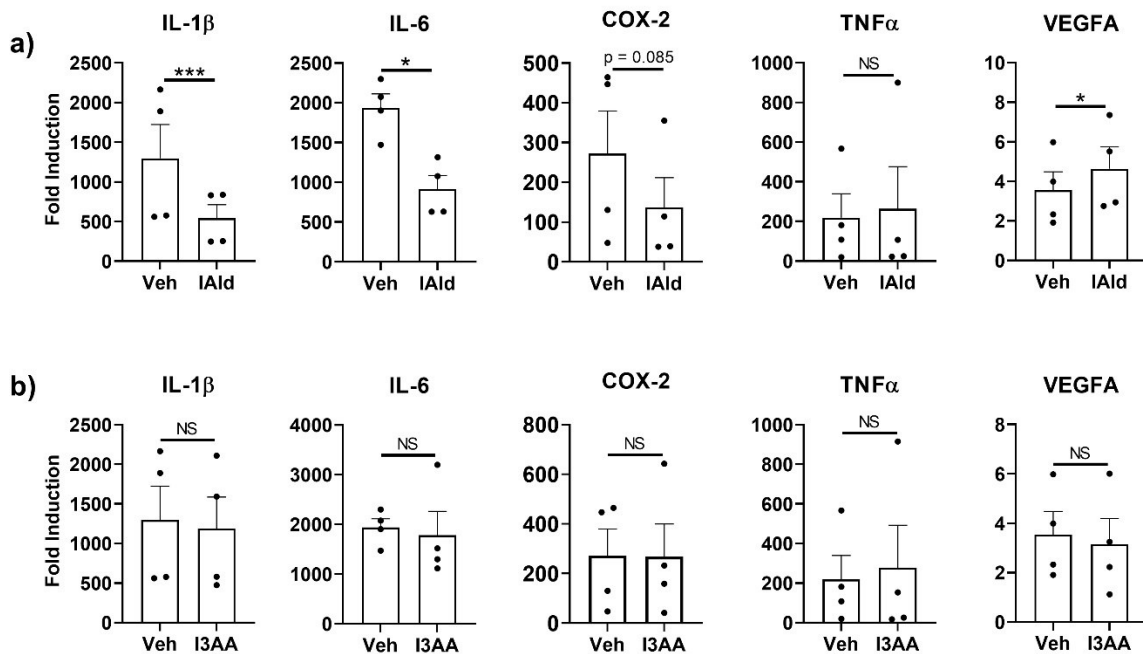


**Figure 12. IAld inhibits the production of subsets of pro-inflammatory cytokines and other mediators by RAW cells in response to Mtb.**

RAW cells were treated with vehicle (Veh) or IAld (0.25 mM) (a), or with Veh or I3AA (0.25 mM) (b), 1 h before the addition of Mtb sonicate (10  $\mu$ g/mL), followed by a 16 h incubation. Gene expression relative to the untreated vehicle control (Fold Induction) is reported. Data shown are from the combined results (Mean  $\pm$  SEM) of 4 independent experiments (n = 4). Statistical difference between two groups in each panel was determined by a paired Student's t test. Two-tailed p-value: NS = Not significant, \* p  $\leq$  0.05, and \*\*\* p  $\leq$  0.001. (Figure from Langan D, et al., *Int J Mol Sci.* 2021; 22(4):2017) (314).

### 7.3 Inhibition of Mtb-induced IL-1 $\beta$ and IL-6 Expression by IAld was Only Partially Reversed by AhR Antagonist CH-223191

It has been reported that several microbiota-derived indole derivatives may activate the AhR pathway (153). The potential role of AhR in mediating the observed inhibitory effect of IAld on the induction of IL-1 $\beta$  and IL-6 mRNA by Mtb in M $\phi$  was elucidated by treating with CH-223191, an AhR inhibitor that is commonly used to identify AhR-

dependent mechanisms. RAW cells treated concomitantly with Mtb and CH-223191 had a significantly higher expression of IL-1 $\beta$  mRNA ( $p = 0.0012$ ) (**Figure 13a**), but unaltered expression of IL-6 mRNA (**Figure 13b**) compared to Mtb-treated control cells. Addition of CH-223191 with IAld partially reversed the suppression by IAld of Mtb-induced IL-1 $\beta$  expression. In contrast to this, CH-223191 failed to reverse to any extent the suppression by IAld of Mtb-induced IL-6 expression. Therefore, AhR antagonism with CH-223191 partially reversed the immunomodulatory activity of IAld on M $\phi$  treated with Mtb.

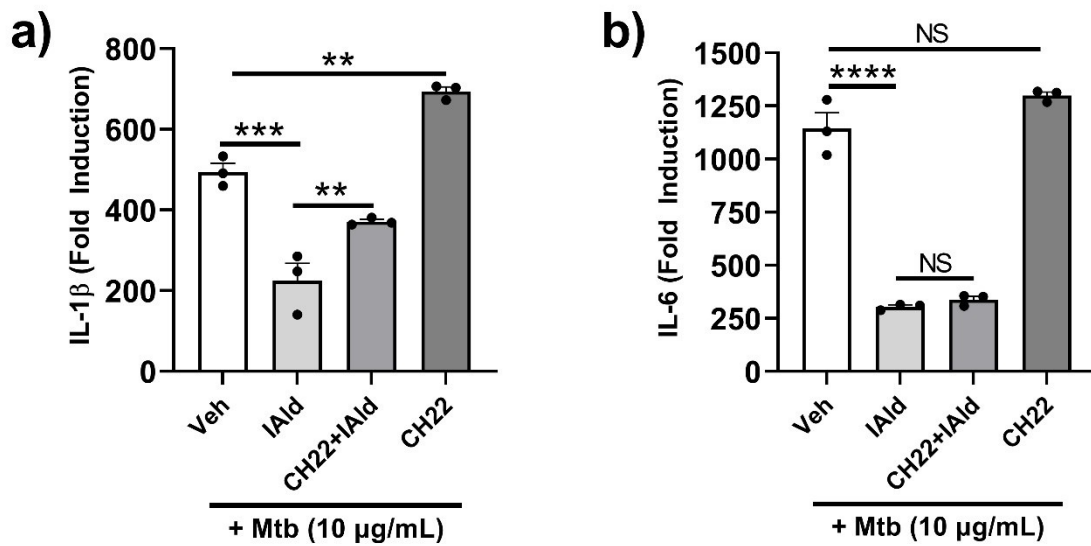


**Figure 13. AhR antagonist CH-223191 partially reversed IAld-induced inhibition of the IL-1 $\beta$ , but not IL-6 response of Mtb-treated M $\phi$ .**

Cells were treated with vehicle (Veh), IAld (0.25 mM), and/or CH-223191 (CH22) (10  $\mu$ M), as indicated, 1 h before the addition of Mtb sonicate (10  $\mu$ g/mL) followed by 16 h incubation. The expression of IL-1 $\beta$  (a) and IL-6 (b) mRNA relative to the untreated control (Fold Induction) is shown ( $n = 3$ ). Data reported is derived from a representative experiment (Mean  $\pm$  SEM) whose results are consistent with those of at least 3 independent experiments. Statistical difference was determined by an ordinary one-way ANOVA with Šidák correction for multiple comparisons. Two-tailed  $p$ -value: NS = Not significant, \*\*= $p \leq 0.01$ , \*\*\*= $p \leq 0.001$ , and \*\*\*\*= $p \leq 0.0001$ . (Figure from Langan D, et al., *Int J Mol Sci.* 2021; 22(4):2017) (314).

#### **7.4 IAld-mediated Inhibition of Pro-inflammatory Cytokine Production by RAW Cells Was Not Associated with MyD88-dependent Activation of Canonical NF- $\kappa$ B or MAPK Pathways**

MyD88-dependent pathways mediate numerous pathophysiological processes in RA, cancer, and numerous other diseases. TLR2 and TLR4 activate MyD88 upon binding to their respective ligands, and in turn, also activate downstream NF- $\kappa$ B and MAPK pathways. To gain insights into the mechanistic activity of IAld and I3AA in M $\phi$ , we used a classical inducer of MyD88-dependent signaling, the TLR4 agonist LPS. This allowed us to assess whether these indole derivatives might differentially regulate MyD88-dependent signaling pathways downstream not only of TLR4, but also of other potential receptors contributing to RA pathogenesis. Interestingly, IAld suppressed the induction by LPS of not only IL-1 $\beta$  (0.5 mM;  $p < 0.0001$ ) and IL-6 (0.5 mM;  $p = 0.0004$ ) mRNA, but also of TNF $\alpha$  mRNA (0.5 mM,  $p = < 0.0001$ ) (**Figure 14a**). In contrast to IAld, I3AA (0.5 mM) did not alter, and had only a minor suppressive effect, on IL-6 and TNF $\alpha$  mRNA induction in response to LPS, respectively. I3AA did, however, significantly reduced IL-1 $\beta$  mRNA induction ( $p = 0.0005$ ), although to a much lesser extent than did IAld. This provides further evidence for the potential relevance that the bioavailability of IAld and I3AA has on mediators of inflammation-associated diseases.

As expected, the NF- $\kappa$ B pathway was rapidly activated by 15 min after treatment of M $\phi$  with LPS. This was evident from immunoblot analysis showing more cytoplasmic p65 phosphorylated at the Ser536 residue and a parallel reduction in I $\kappa$ B $\alpha$  levels compared to untreated M $\phi$  (**Figure 14b**). Analysis of lysates from M $\phi$  treated concomitantly with

LPS and IAld or I3AA (each at 0.5 mM) showed that phosphorylation of p65 and degradation of I $\kappa$ B $\alpha$  was the same as in Mtb-treated control cells. Although, in some experiments the amount of I $\kappa$ B $\alpha$  protein in cells treated concomitantly with LPS and IAld (or I3AA) showed small differences compared to that in LPS-treated controls, there was no consistent difference ascertained from the results of multiple independent analyses.

As expected, the activation of MAPK pathways was evident from the phosphorylation of both ERK1/2 (Thr202/Thy204) and p38 (Thr180/Thy182) by 15 min after treatment of RAW cells with LPS. Cells treated concomitantly with LPS and either IAld or I3AA showed comparable levels of phosphorylated ERK1/2 and p38 to that of LPS-treated control cells.

Importantly, the concentration (0.5 mM) at which IAld and I3AA were tested did not elicit cytotoxic effects and had significant inhibitory properties on a subset of LPS-induced inflammatory cytokines. Thus, based on these results we ruled out that IAld or I3AA inhibits LPS-induced expression of inflammatory cytokines by altering MyD88-dependent activation of these three canonical inflammatory pathways.

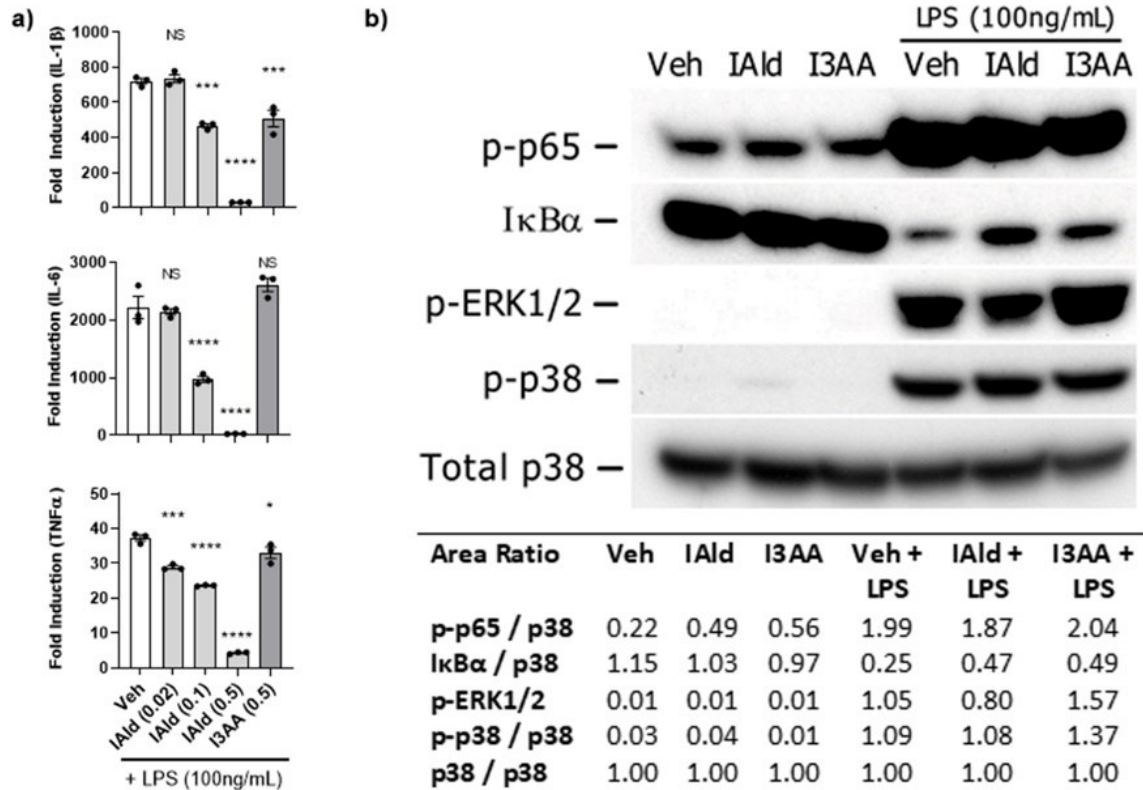


**Figure 14. IAld-mediated inhibition of pro-inflammatory cytokines apparently was not induced via the MyD88-dependent signaling pathway.**

The effect of IAld and I3AA on the inflammatory response of RAW cells stimulated with LPS (100 ng/mL) was assessed. **a)** The steady-state levels of pro-inflammatory cytokine mRNA was measured by qRT-PCR at 2 h after stimulation. Statistical differences were measured by ordinary ANOVA with Dunnett's multiple comparisons test. Statistical differences between the respective controls (Veh) and the treatment groups are indicated by a mark above each bar on the graph. Two tailed p-value is shown; NS = not significant, \*  $p \leq 0.05$ , \*\*\*  $p \leq 0.001$ , \*\*\*\*  $p \leq 0.0001$ . Data shown are from one experiment representative of three separate experiments. **b)** Activation of canonical inflammatory pathways was assessed by western blot analysis of cell lysates collected after stimulation of cells with LPS (100 ng/mL) alone or with LPS in the presence of either IAld or I3AA (each at 0.5 mM). The lysates were collected from cells after 1 h of treatment of cells with Veh, IAld, or I3AA alone and from cells treated in parallel with an additional 15 min exposure to LPS. The densitometry ratio of each band to the loading control (total p38) is shown for cells stimulated with medium only or LPS. Blots are from a single representative experiment. (Figure from Langan D, et al., *Int J Mol Sci.* 2021; 22(4):2017) (314).

## 7.5 Modulation of RANKL-induced Differentiation of RAW Cells into Osteoclasts by IAld, but Not I3AA

We further tested whether IAld or I3AA directly regulates the differentiation of M $\phi$  into osteoclasts in response to RANKL, and thereby influence stromal remodeling of bone independent of mitigating the upstream innate inflammatory response (*e.g.*, pro-inflammatory cytokines). *In vitro* osteoclastogenesis of RAW cells is a well-established model to study the bone resorption aspect of bone remodeling (311, 316). In this assay, after treatment with RANKL, cells that express TRAP and have undergone fusion with several other M $\phi$  to form cell bodies with 3 or more nuclei are considered osteoclasts. Cells that were treated with RANKL and Veh served as the control.

At d 5 of treatment with RANKL, numerous osteoclasts had formed in the control cultures. The addition of IAld resulted in the generation of significantly more and, also, larger osteoclasts than in the controls. In contrast, no difference in the formation of osteoclasts, both in number and morphology, were noted from the addition of I3AA compared to the controls (**Figure 15**).

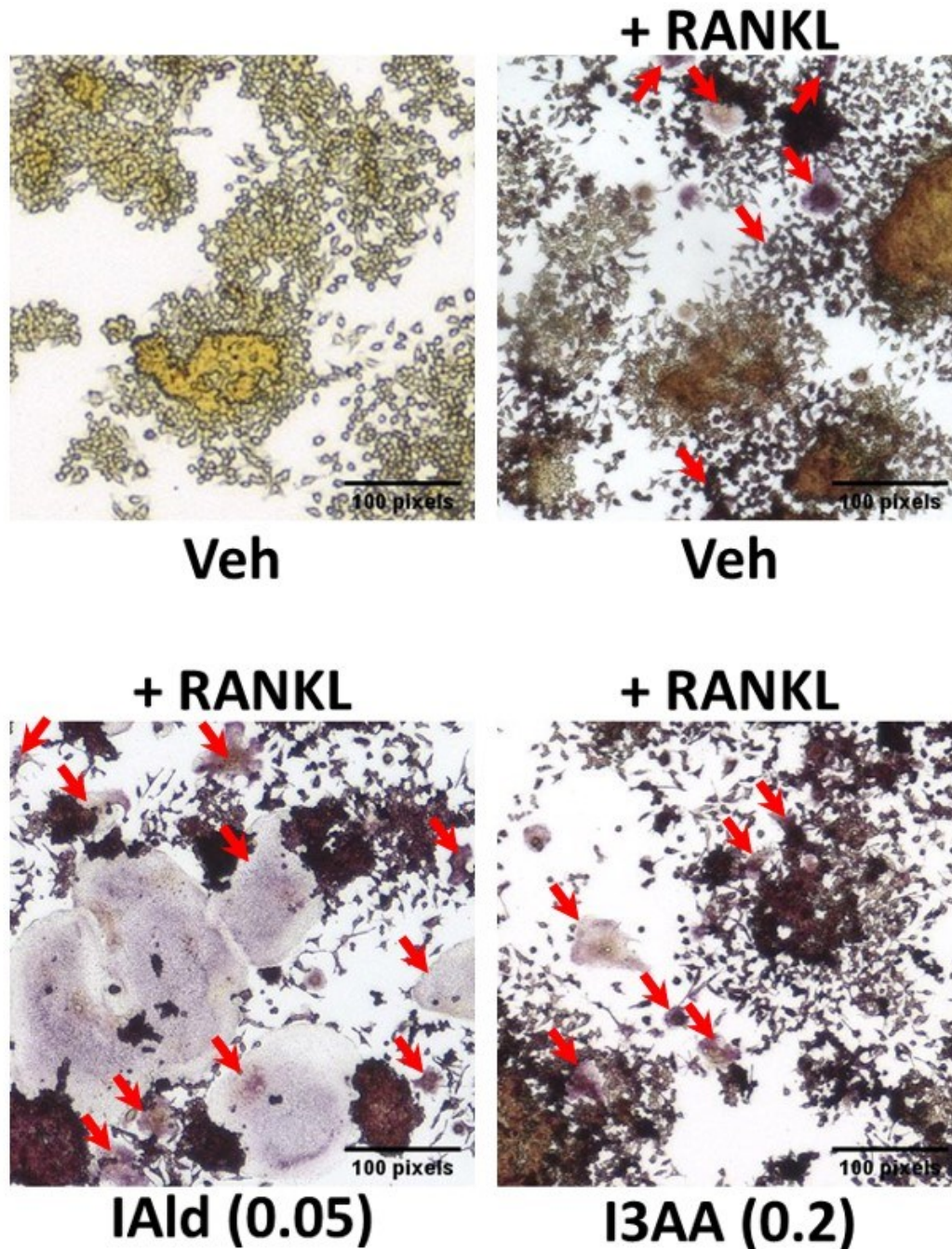


**Figure 15. Osteoclast numbers and cell morphology are altered in the presence of IAld.**

Osteoclasts were generated from RAW cells treated with RANKL (100 ng/mL) as described under methods. Images were taken of TRAP-stained untreated, Veh, IAld (0.05 mM), and I3AA (0.2 mM) treated cells on d 5. A representative image of each condition is shown at 20X magnification. Osteoclasts are indicated by a red arrow. The results depict consistent trends observed in multiple independent experiments. (Figure modified from Langan D, et al., *Int J Mol Sci.* 2021; 22(4):2017) (314).

The pro-osteoclastogenic effect of IAld described above was dose-dependent. At 0.2 mM of IAld, about 16 times ( $p < 0.0001$ ) more osteoclasts were formed, whereas at 0.0125 mM, about 5 times ( $p < 0.0001$ ) more osteoclasts were formed compared to controls (**Figure 16a**). At 0.003 mM of IAld, there was no difference in the number of osteoclasts formed compared to control cells ( $p = 0.3676$ , data not shown). In addition, by d 5, when cells were treated with 0.8 mM of IAld, the number of cells on the plate were far fewer than in the control condition (data not shown). We propose that this may be the result of an effect of IAld on cell proliferation and/or cell viability at high concentrations. In addition, IAld-treated (0.05 – 0.2 mM) cells expressed elevated levels of key enzymes involved in the bone resorption activities of osteoclasts, namely TRAP ( $p = 0.007$ ) and CatK ( $p = 0.030$ ), compared to control cells (**Figure 16c**). In contrast, cells treated with I3AA (0.2 mM) formed an equivalent number of osteoclasts ( $p = 0.175$ ) expressing similar levels of TRAP and CatK as control cells (**Figure 16b, d**).

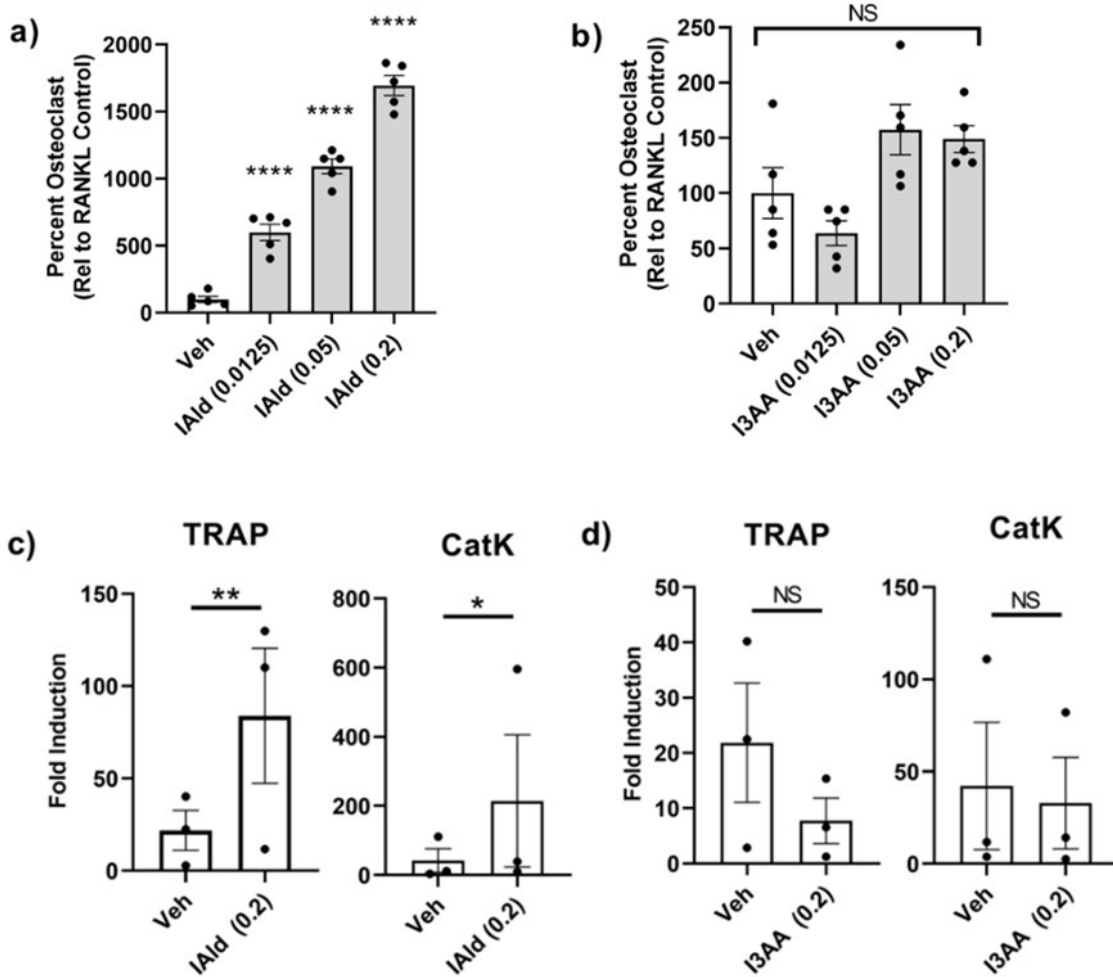


**Figure 16. IAld enhances the bone remodeling process of osteoclastogenesis.** Osteoclasts were generated from RAW cells treated with RANKL alone or with RANKL in the presence of either IAld or I3AA (0.0125 – 0.2 mM) as described under methods. **a, b)** Cells were fixed and then stained for TRAP expression on d 5 and the number of osteoclasts were enumerated from multiple regions of each well (n = 5). Data are reported as the percentage of osteoclasts relative to the RANKL-treated controls (Mean ± SEM) from a representative experiment. Statistical difference relative to RANKL-treated control cells was determined by ordinary one-way ANOVA with Šidák correction for multiple comparisons. **c, d)** The transcription of osteoclast genes TRAP and CatK on d 5 is reported from the combined results (Fold induction) of 3 independent experiments (n = 3). Statistical difference was determined by paired Student's *t* test. Indicators of statistical difference are as follows: Two-tailed p-value: NS = Not significant, \**p* ≤ 0.05, \*\**p* ≤ 0.01, \*\*\*\**p* ≤ 0.0001. All results depict consistent trends observed in multiple independent experiments. (Figure modified from Langan D, et al., *Int J Mol Sci.* 2021; 22(4):2017) (314).

## 7.6 Differential Regulation of Endothelial Cell Tube Formation by IAld and I3AA

Excessive blood vessel formation, angiogenesis, often occurs in parallel with bone loss in the arthritic joint (317). We examined the impact of indole derivatives IAld and I3AA on angiogenesis using a well-established model system, the *in vitro* endothelial cell (HUVEC) 2D-Matrigel tube formation assay. HUVEC seeded on Matrigel form distinct capillary-like tubes. Complete looping structures form by 8 h on Matrigel and these structures remain stable even at 16 h. By 24 h after seeding, the integrity of these structures begins to deteriorate, as expected; therefore, quantification of tubes after 16 h of seeding cells was avoided in the experiments whose results are shown below.

The effect of these indole derivatives on angiogenesis was compared to control cells (cells treated with VEGF and Veh) at 16 h after seeding cells on to Matrigel (**Figure 17**). At this time point, the addition of IAld caused formation of more numbers, but smaller loops, than those formed by control cells. This was attributed to significantly more branching by IAld-treated cells. In contrast to the pro-angiogenic activity of IAld, cells treated additionally with I3AA appeared to form similar structures as controls, and by 16 h after seeding, many loops had dissociated in contrast to that seen for control-treated cells. Evidence of blebbing along areas where tubes had initially formed and then disassembled is marked by black arrows (**Figure 17b**).

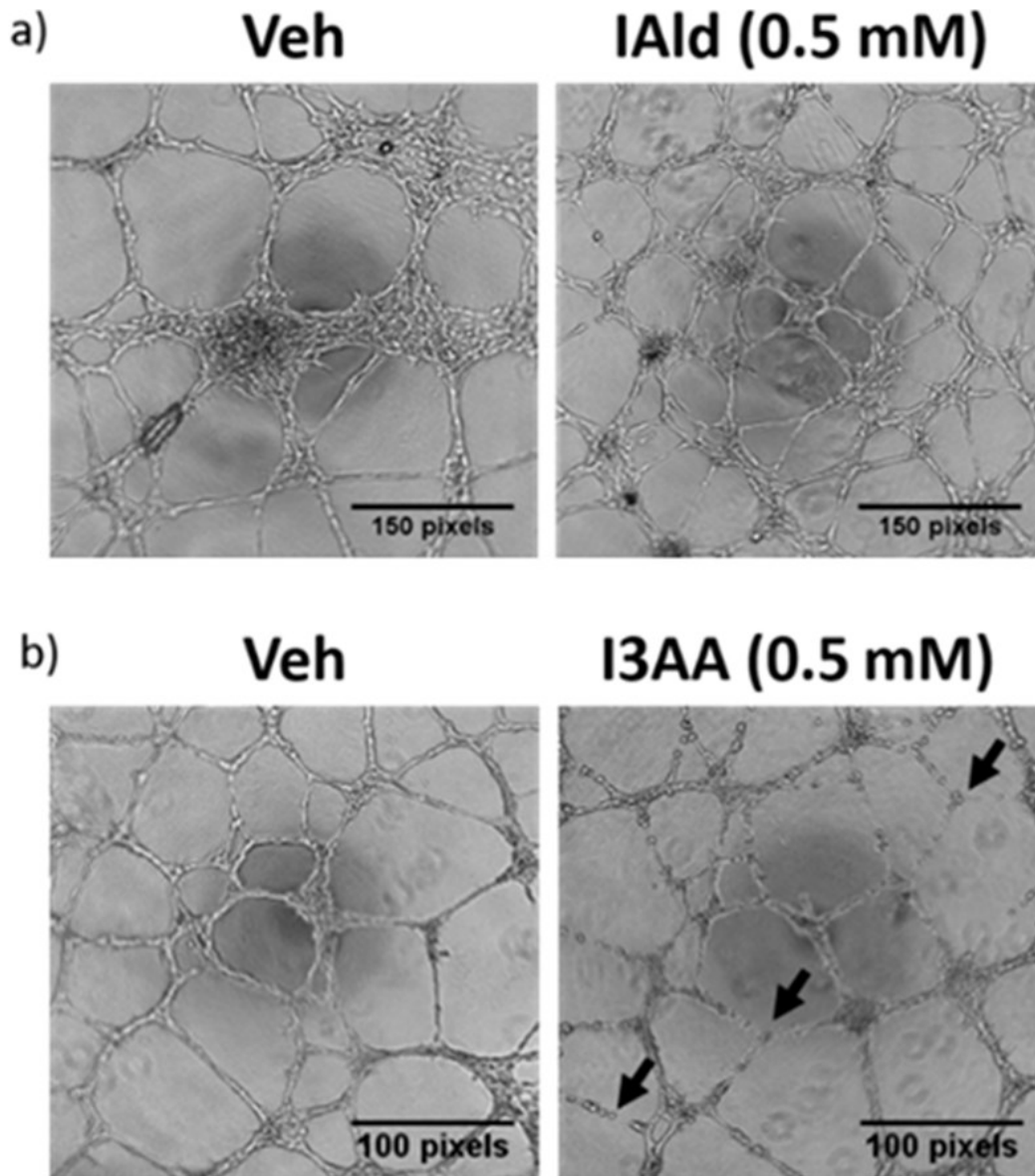


**Figure 17. HUVEC tube morphology in the presence of IAld and I3AA in a 2D-Matrigel tube formation assay.**

HUVEC were seeded on to Matrigel with VEGF (20 ng/mL). Either IAld (0.5 mM) (a) or I3AA (0.5 mM) (b) was added to cells 1 h after seeding. Vehicle (Veh) was added to some cells as a control. Shown are phase contrast images (4X) of each condition taken with a Keyence microscope at 16 h following HUVEC seeding. The formation of loops and capillary-like tube structure was compared. Tube dissociation is indicated by a black arrow. (Figure modified Langan D, et al., *Int J Mol Sci.* 2021; 22(4):2017) (314).

The differential effects of IAld and I3AA on angiogenesis were further characterized with respect to the concentration of indole derivatives and the duration of observed effects. IAld-treated cells formed significantly more loops than control cells at 16 h after seeding in a dose-dependent manner and at a concentration as low as 0.25 mM ( $p = 0.007$ ) (**Figure 18a**). Additionally, the percent increase in loops formed by the addition of IAld (0.5 mM) at 8 h was equivalent to the percent increase at 16 h after seeding ( $p = 0.244$ ) compared to controls at corresponding time points (**Figure 18b**). Therefore, the time of exposure to IAld was not a significant factor in its effect. In contrast to the pro-angiogenic effect of IAld, a dose-dependent anti-angiogenic effect of I3AA was observed. The addition of I3AA disrupted tube formation even at the lowest concentration tested (0.25 mM,  $p = 0.010$ ). (**Figure 18c**). Additionally, this effect of I3AA was highly time-dependent, whereby at 8 h after seeding, cells treated with I3AA and VEGF formed an equivalent number of tubes as did the control cells, but a profound inhibitory effect of I3AA on the stability of tubes was marked by their dissociation at 16 h after seeding of cells (**Figure 18d**). Importantly, even at 1 mM of I3AA and 24 h after exposure, no cytotoxic effect of I3AA on HUVEC was detectable by the MTT assay (**Figure 11**). This suggests that the dissociation of tubes caused by I3AA at 16 h was likely not a result of cell death.

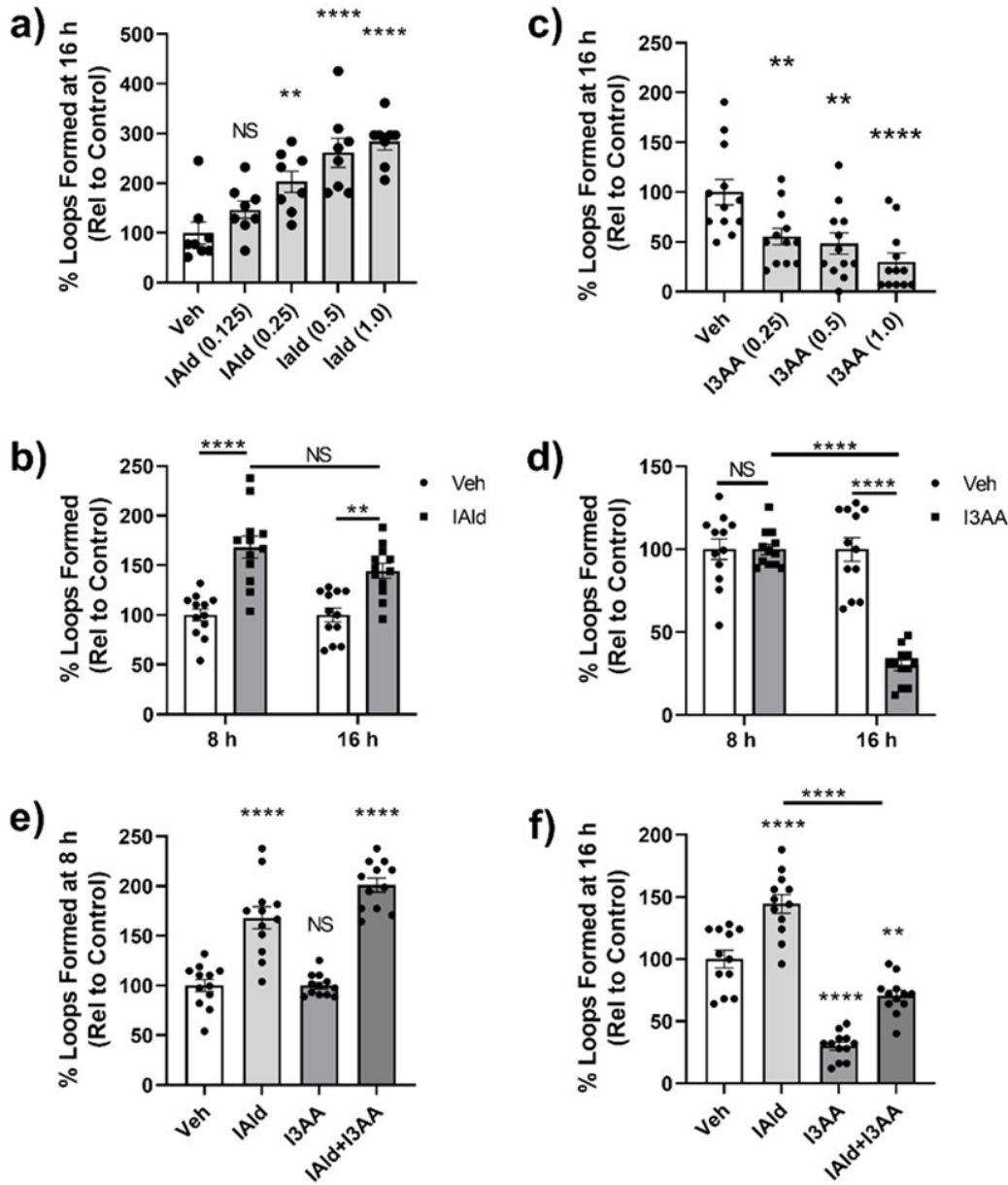


**Figure 18. IAld and I3AA differentially influence angiogenesis.**

A 2D-Matrigel tube formation assay with HUVEC treated with VEGF (20 ng/mL) was performed. Vehicle (Veh), I3AA, and/or IAld were added 1 h after seeding cells. The dose effect (mM) of IAld (a) or I3AA (c) at 16 h following treatment is shown. Also shown is the effect of IAld (b) and I3AA (d) (both at 0.5 mM) at both 8 h and 16 h. The effect when treated additionally with I3AA, IAld, or both (both at 0.5 mM) at 8 h (e) and 16 h (f) are shown. Data are reported as the percent of loops formed relative to VEGF-treated controls (Mean  $\pm$  SEM) in which multiple regions of each well were examined (n = 8-12). Statistical differences were determined on unnormalized data by ordinary one-way ANOVA (a, c, e, f), and by two-way ANOVA (b, d) with Šidák correction for multiple comparisons. NS= Not significant, \* $p \leq 0.05$ , \*\* $p \leq 0.01$ , \*\*\*\* $p \leq 0.0001$ . (Figure modified from Langan D, et al., *Int J Mol Sci.* 2021; 22(4):2017) (314).

Given that IAld and I3AA are generated by gut microbiota via a common pathway, we anticipate that tissues will be exposed concurrently to these two indole derivatives. Therefore, we tested the formation of tubes by HUVEC when both IAld and I3AA were added concurrently with VEGF. An interesting interplay between IAld and I3AA was observed. At the early time point (8 h) after seeding cells, cells treated with both IAld and I3AA formed a comparable number of loops with similar morphology as IAld-treated cells (without I3AA) (**Figure 18e**). The temporal effect of I3AA on HUVEC tube formation that was mentioned above was further evident upon treating HUVEC with a mixture of IAld and I3AA. As was observed for cells treated with I3AA, dissociation of tubes and loss of loops at ~16 h occurred in cells treated with a mixture of IAld and I3AA (**Figure 18f**). Although treatment with both I3AA and IAld resulted in more loops formed at 16 h than cells treated with I3AA (without IAld), it was evident that a similar degree of loop dissociation had occurred between the 8 h and 16 h time points because both had approximately 60% less loops than the corresponding cells not treated with I3AA.

### **7.7 AhR Antagonist Inhibited the Anti-angiogenic Effect of I3AA, but Not the Stromal Remodeling Effects of IAld on Endothelial Cells and Osteoclasts**

We again used CH-223191, but this time to test for AhR-dependence in mediating the effects of IAld and I3AA on the stromal remodeling events tested above. No measurable effect was observed of CH-223191 alone on the formation of loops by HUVEC in the 2D-Matrigel tube formation assay (**Figure 19a, b**). Addition of CH-223191 with IAld showed that loop formation was comparable to that of cells treated with IAld alone ( $p = 0.999$ ) (**Figure 19a**). Therefore, CH-223191 did not change the pro-angiogenic effect of IAld.

However, CH-223191 prevented I3AA-mediated tube dissociation (**Figure 19b**). At 16 h, treatment with both CH-223191 and I3AA resulted in an equivalent number of loops formed as controls, whereas I3AA alone had about a third of the loops compared to controls at that time point.

Regarding osteoclastogenesis, addition of CH-223191 slightly increased the number of osteoclasts relative to controls ( $p = 0.046$ ). Addition of CH-223191 with IAld resulted in a comparable number of osteoclasts formed to that of cells treated with IAld alone (**Figure 19c**). Taken together, these results indicate that AhR antagonism did not alter the osteoclastogenic effect of IAld. As mentioned above, I3AA did not appear to have any effect on osteoclast generation; however, further evidence that I3AA regulates the AhR pathway came from the results of adding both CH-223191 and I3AA together when generating osteoclasts. Addition of CH-223191 revealed that the number of osteoclasts formed was more than that of the controls ( $p = 0.0321$ ), but the number of osteoclasts formed when treated with both CH-223191 and I3AA was not statistically different from that of controls (**Figure 19d**).

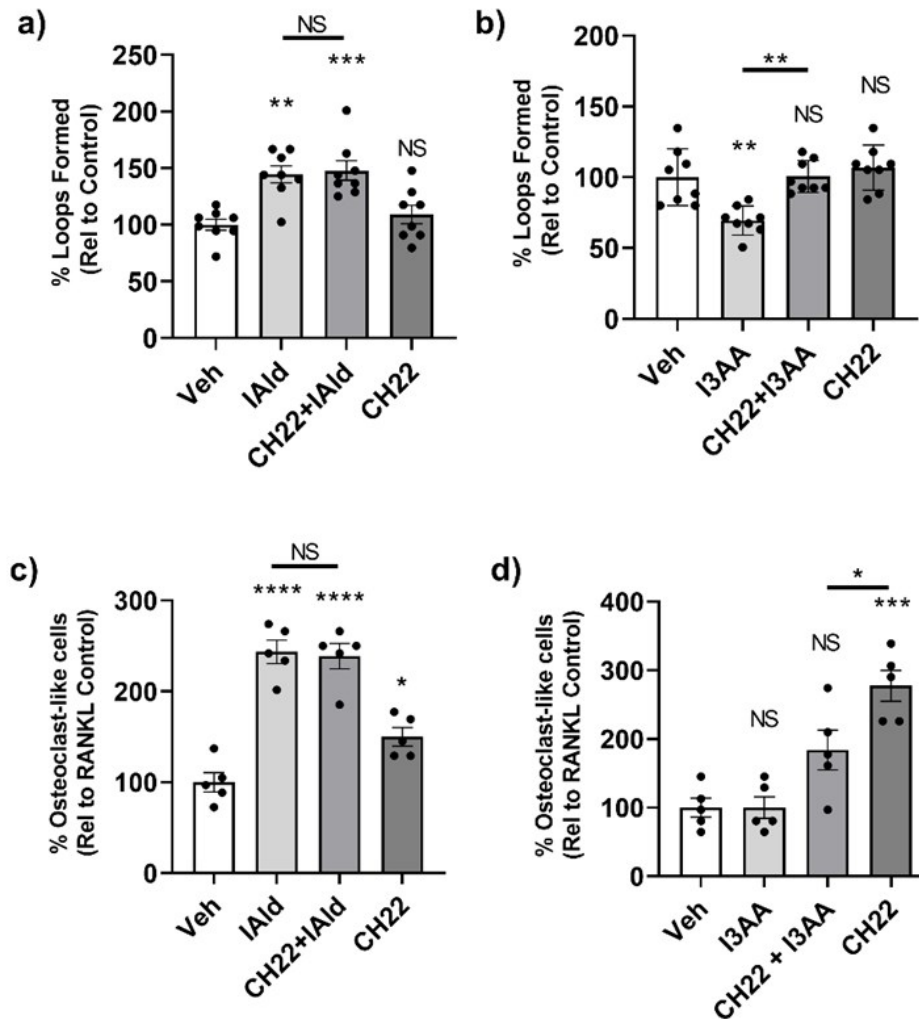


**Figure 19. AhR antagonist CH-223191 inhibits the disruption of angiogenesis by I3AA but fails to alter the effect of IAld on angiogenesis and osteoclastogenesis.**

a, b) HUVEC were treated with VEGF in a 2-D Matrigel tube formation assay as described under methods. c, d) Osteoclasts were generated from RAW cells treated with RANKL as described under methods. In some wells, HUVEC or RAW cells were treated additionally with IAld, I3AA, CH-223191, or a combination as indicated. (a-b) The percentage of loops relative to control cells treated with Veh is reported (n = 8). (c-d) The percentage of osteoclasts relative to control cells treated with Veh was shown (n = 5). Statistical difference was determined on unnormalized data of either the number of loops formed (a, b) or from the number of osteoclasts (c, d) by ordinary one-way ANOVA with Šidák correction for multiple comparisons. Statistical difference was determined between differentially treated cells and the control cells, except where there is a bar to indicate which two are being compared. The Mean  $\pm$  SD is reported along with points for individual values. NS = not significant, \*  $p \leq 0.05$ , \*\*  $p \leq 0.01$ , \*\*\*  $p \leq 0.001$ , \*\*\*\*  $p \leq 0.0001$ . Data are from one experiment representative of several separate experiments. (Figure from Langan D, et al., *Int J Mol Sci.* 2021; 22(4):2017) (314).

## 7.8 Nrf2 Agonism Reverses the Effect of IAld on Osteoclastogenesis.

Our findings showing that the AhR antagonist, CH-223191, failed to reverse IAld-enhanced osteoclastogenesis (**Figure 19**) suggest that the observed effects of IAld are AhR-independent. Nrf2 activation upregulates the expression of antioxidant enzymes (*i.e.*, HMOX1 and NQO1), that in turn, lead to ROS reduction. Since an increase in ROS facilitates osteoclastogenesis (293), it is expected that inhibition of the Nrf2-antioxidant response would potentiate osteoclastogenesis (298, 299). We hypothesized that the increase in osteoclastogenesis induced by IAld is caused by the increase in ROS levels resulting from Nrf2 inhibition. To test this hypothesis, we tested i) the effect of IAld on Nrf2 agonist, CDDO-IM, induced expression of HMOX1 and NQO1; ii) the effect of CDDO-IM on IAld-mediated potentiation of osteoclastogenesis; and lastly, iii) the effect of IAld on intracellular ROS levels following treatment of RAW cells with RANKL.

In response to the Nrf2 agonist, CDDO-IM (0.1  $\mu$ M), RAW cells upregulated the expression of the Nrf2-dependent antioxidant enzymes HMOX1 and NQO1 by 2 h, with an increase continuing at 7 h, and then returning to baseline by 24 h (**Figure 20a, b**). Addition of IAld (0.25 mM) to cells at 1 h prior to CDDO-IM suppressed the CDDO-IM-mediated induction of both HMOX1 and NQO1 genes by approximately 2-fold. In contrast to the inhibitory effect of IAld on Nrf2-dependent antioxidant gene expression, I3AA (0.25 mM) showed no effect on the induction of NQO1 or HMOX1 gene expression. These findings were consistent with our hypothesis, that IAld can inhibit the Nrf2-dependent antioxidant response. In this case, even in the absence of RANKL-induced osteoclastogenesis.

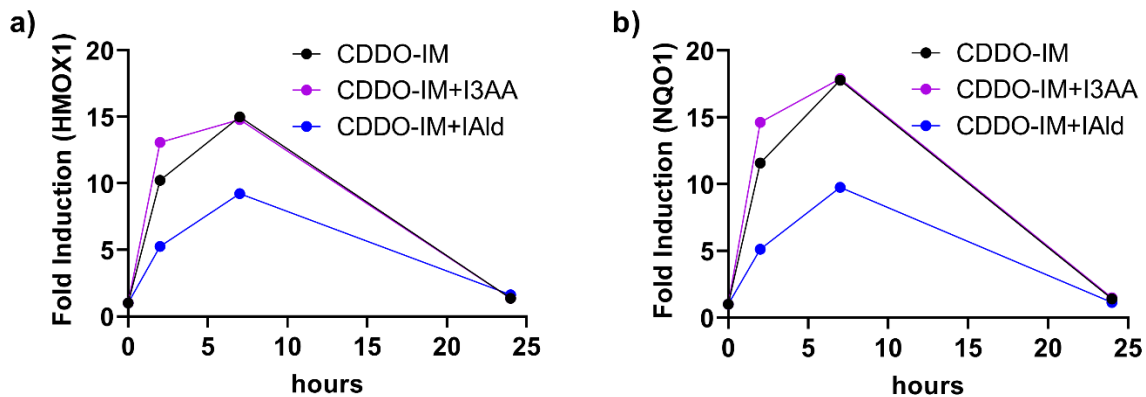


**Figure 20. IAld inhibits the induction of antioxidant gene expression by the Nrf2 agonist CDDO-IM.**

RAW cells were treated with either IAld (0.25 mM), I3AA (0.25 mM), or Veh, 1 h before the addition of CDDO-IM (0.1  $\mu$ M). Data are reported as the steady-state mRNA levels of Nrf2-dependent antioxidant genes HMOX1 (**a**) and NQO1 (**b**) at the indicated time points up to 24 h after treating the cells with CDDO-IM.

Next, we tested the effect of Nrf2 activation by CDDO-IM on IAld-mediated potentiation of osteoclastogenesis. CDDO-IM alone significantly suppressed osteoclast formation at concentrations  $\geq 0.004$   $\mu$ M (**Figure 21a**). CDDO-IM at concentrations  $\geq 0.1$   $\mu$ M were significantly cytotoxic; therefore, 0.1  $\mu$ M was the highest concentrations tested. Inhibition of osteoclastogenesis by CDDO-IM is Nrf2-dependent and is associated with the increased expression of HMOX1 and NQO1 leading to reduced intracellular ROS levels (318). CDDO-IM (0.004  $\mu$ M) partially reversed IAld-mediated potentiation of osteoclastogenesis ( $p = 0.0149$ ) (**Figure 21b**), and importantly, at this concentration CDDO-IM alone did not alter osteoclast numbers. **Figure 21c** shows that the potentiation of osteoclastogenesis by IAld was dose-dependently reduced by increasing concentrations of CDDO-IM (0.004-0.1  $\mu$ M).

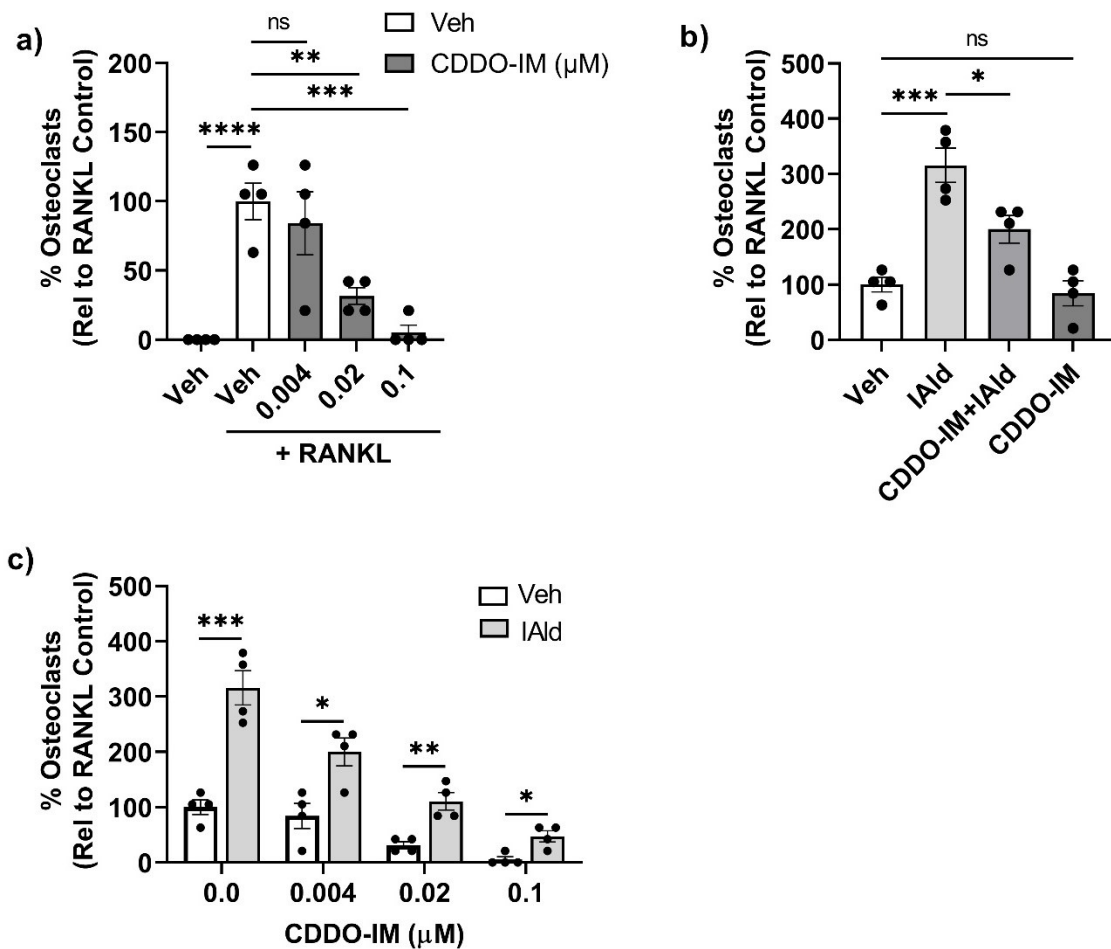


**Figure 21. Nrf2 agonist CDDO-IM partially reverses IAlD-mediated potentiation of osteoclastogenesis.**

Osteoclasts were generated from RAW cells. The methods used were similar to those described above, but with the addition of CDDO-IM (0.004 – 0.1 μM). Data are reported as the percentage of osteoclasts relative to control cells that were only treated with RANKL (Mean ± SEM) from a representative experiment (n = 4) in which cells were treated with CDDO-IM (0.004 – 0.1 μM) (a) and/or IAlD (0.05 mM) (b, c). Statistical differences were determined on unnormalized data by ordinary one-way ANOVA with Šidák correction for multiple comparisons (a, b), or Student's *t* test (c). NS = not significant, \*  $p \leq 0.05$ , \*\*  $p \leq 0.01$ , \*\*\*  $p \leq 0.001$ , \*\*\*\*  $p \leq 0.0001$ . Data are from one experiment representative of several separate experiments.

To further assess the potential that an inhibition of the Nrf2 response leading to an increase in oxidative stress is associated with the potentiation of osteoclastogenesis by IAld, the CM-H<sub>2</sub>DCFDA fluorescent indicator method was used to measure the intracellular ROS response of RAW cells following treatment with RANKL. As expected, RAW cells treated with RANKL had a higher level of intracellular ROS than untreated cells (**Figure 22**). We hypothesized that the addition of IAld would further increase the levels of ROS in cells; however, the addition of IAld resulted in cells having significantly lower fluorescent intensity, indicative of lower levels of ROS, than control cells. In fact, at the lowest concentration of IAld tested (0.02 mM), the fluorescent intensity at 24 h after addition of RANKL was found to be equivalent to untreated cells. Similar measurements of ROS levels with CM-H<sub>2</sub>DCFDA at 48 h and 72 h after treatment of cells with RANKL, also indicated significantly lower levels of intracellular ROS in cells treated with IAld than controls (data not shown). Importantly, there was no cytotoxic effect of IAld on RAW cells treated for 24 h with IAld at concentrations up to 1.0 mM (5-20 times greater than the concentrations tested in the ROS studies) (**Figure 11**). Therefore, the reduction in intracellular ROS was not the result of a loss of cell viability.

As supplementary work, we also tested whether IAld-mediated inhibition of Mtb-induced IL-1 $\beta$  or IL-6 gene expression is altered by Nrf2 activation with CDDO-IM (0.1  $\mu$ M). CDDO-IM did not alter Mtb-induced IL-1 $\beta$  or IL-6 gene expression (**Figure 23a**). Also, CDDO-IM had no measurable effect on the degree of IAld-mediated inhibition of Mtb-induced IL-1 $\beta$  and IL-6 gene expression (**Figure 23b**).

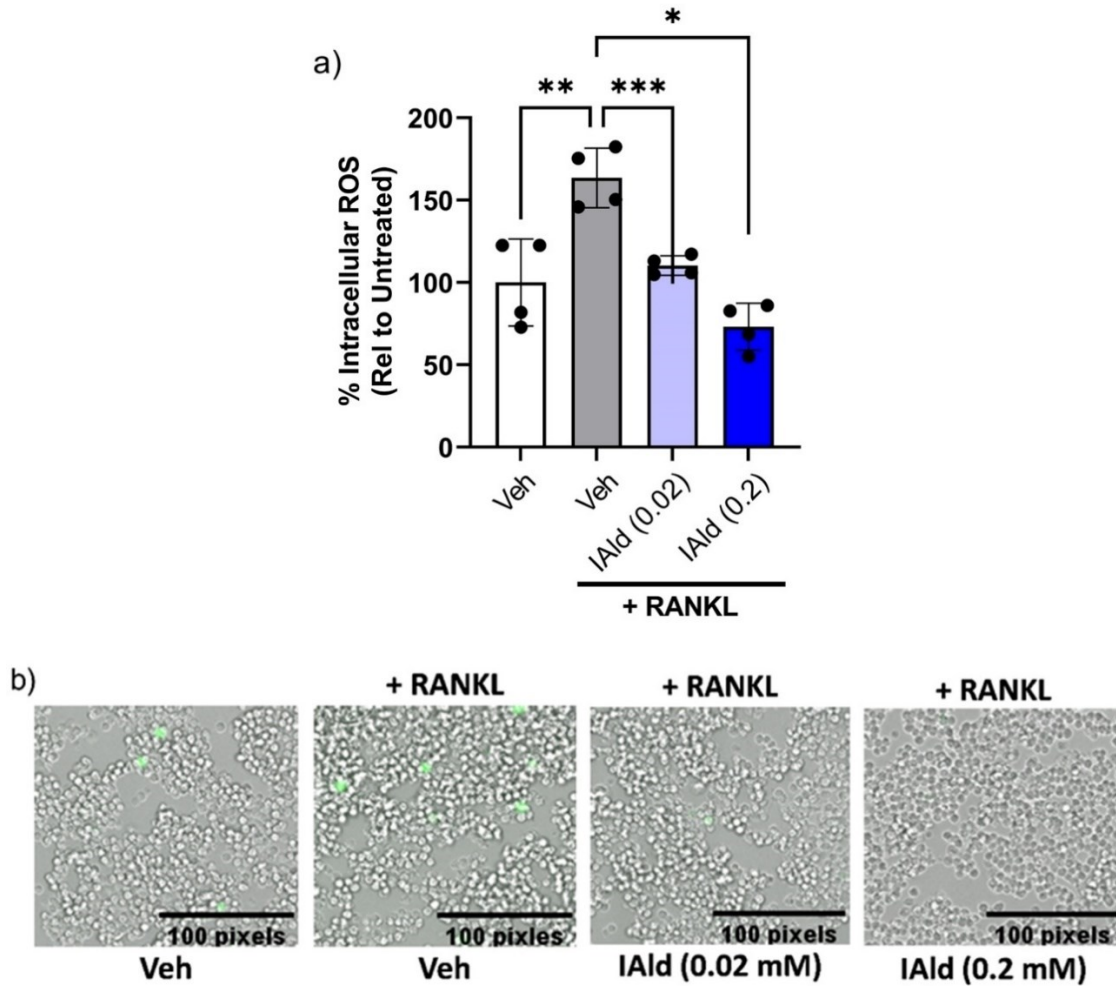


**Figure 22. IAld reduces intracellular ROS levels in RAW cells treated with RANKL.** RAW cells were treated with RANKL (100 ng/mL) alone or concomitantly with IAld (0.02 – 0.2 mM). At 24 h after the addition of RANKL, cells were loaded with CM-H<sub>2</sub>DCFDA (5  $\mu$ M) and processed for subsequent measurement of fluorescence intensity as described under Methods. a) Data are reported as the percentage of intracellular ROS (Mean  $\pm$  SEM; n = 4) determined by comparing the normalized fluorescent intensities of each condition to that of the untreated controls (Veh). Statistical difference tested by ordinary one-way ANOVA with Šidák correction for multiple comparisons, b) Representative image of the overlay of brightfield and fluorescence (FITC filter) images from a Keyence microscope. NS = Not significant, \*  $p \leq 0.05$ , \*\*  $p \leq 0.01$ , \*\*\*  $p \leq 0.001$ .

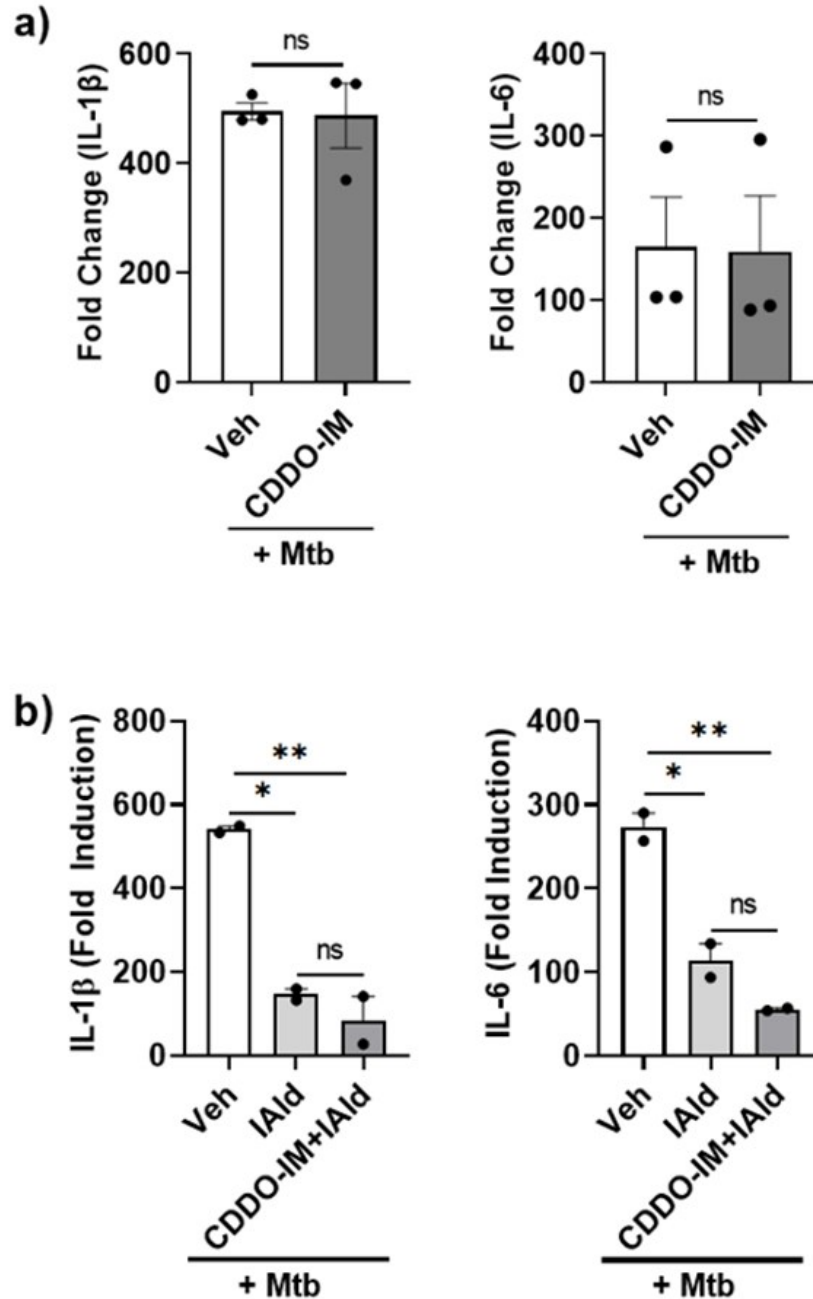


**Figure 23. Nrf2 agonist CDDO-IM does not alter IAld-mediated inhibition of Mtb-induced proinflammatory cytokine genes.**

RAW cells were treated with Mtb. The methods used were similar to those described above, but with the addition of CDDO-IM (0.1  $\mu$ M). **a)** Cells were treated with Mtb alone or 1 h prior with CDDO-IM (n = 3). **b)** Cells were treated with Mtb alone or 1 h prior with either IAld (0.25 mM), or CDDO-IM and IAld (0.25 mM) (n = 2). Data are reported as the fold induction of steady-state mRNA relative to untreated cells and are derived from independent experiments. Statistical difference tested by paired Student's *t* test (**a**) and by one-way ANOVA with Šidák correction for multiple comparisons (**b**). NS = not significant, \*  $p \leq 0.05$ , \*\*  $p \leq 0.01$ .

## 7.9 Treatment of AA with IAld.

To test a potential effect of IAld on autoimmune arthritis progression, two pilot experiments were conducted. A group of Lewis rats was immunized with heat-killed Mtb by s.c. injection at the base of the tail for the purpose of arthritis induction as described under Methods. Thereafter, IAld (5 mg/kg) was administered to the experimental rats by oral gavage once daily, starting 5 days after Mtb immunization, whereas the control rats received vehicle only. The progression of arthritis severity was monitored and graded as arthritic score (**Figure 24**). The disease onset in the IAld-treated animals occurred 2-3 days later than that in the arthritic controls. This is considered to be one of the signs of disease-protective effects of a test agent. In addition, the severity of arthritis in rats treated with IAld was significantly less than in arthritic controls ( $p = 0.0319$ ) (**Figure 24b**). In the latter control group that received vehicle, all 5 (100%) animals developed arthritis, but in the IAld-treated group, only 3 of the 5 (60%) animals developed arthritis (**Figure 24c**).

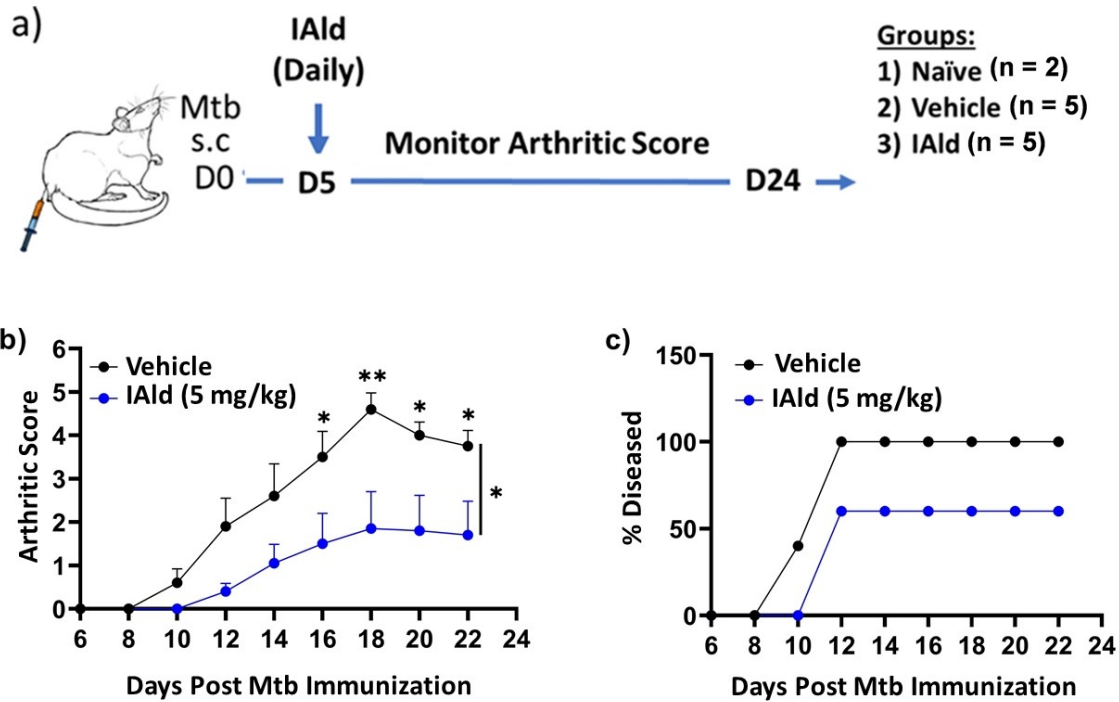


**Figure 24. Pilot experiment to assess the effect of oral treatment with IAld on arthritis progression.**

a) Design of experiments testing the effect of IAld on AA. **b)** Rats were immunized with heat-killed Mtb as described for the AA model under Methods. Experimental rats received IAld (5 mg/kg) daily by oral gavage starting on d 5 post-Mtb immunization whereas controls received the vehicle only (n = 5). Data are reported as arthritic score. Both the statistically significant difference between the two groups as well as statistically significant differences at specific days are indicated. Statistical difference tested by two-way ANOVA with Holm-Šidák multiple comparisons test. \*  $p \leq 0.05$ , \*\*  $p \leq 0.01$  (c). Data are reported as percent diseased (percentage of Mtb-immunized rats that developed signs of arthritis in each group). Data are taken from the combined results of two-independent experiments.

## Chapter 8. Discussion

Increasing evidence suggests a role for the gut microbiota in maintaining homeostasis (88, 203, 204), in part, by ensuring a healthy immune state. There also is evidence pointing towards the detrimental role of a ‘dysbiotic’ microbiome in contributing to autoimmune diseases (238, 239, 319–321), cancer (240, 241), and overall health decline with age (89). With the efforts of the Metagenomics of the Human Intestinal Tract consortium (MetaHIT) and Human Microbiome Project (HMP), immense progress has been made in characterizing the human microbiome (203, 322). Administering probiotics aimed at re-setting a proper balance of gut microbiota species is being explored as a prophylactic approach for maintaining health, as well as a treatment approach for autoimmunity, including RA (259, 260, 323, 324) and other diseases. However, this effort has been fraught with difficulties because gut microbiota are highly dynamic, and their metabolic state is significantly influenced by specific host factors. As such, use of alternative approaches (*i.e.*, pre-biotics, post-biotics, and synbiotics) are being investigated as potential strategies for harnessing the beneficial aspects of healthy-microbiota to prevent disease and/or treat disease states.

Evidence suggesting that the links between the microbiome and host health or disease are driven by microbiota-derived metabolites is rapidly expanding (8, 325). Of these metabolites, SCFAs have been rigorously characterized in a variety of disease contexts including bone loss and metabolic syndrome, which is disproportionately prevalent in patients with RA and some other rheumatic diseases (249, 326). In contrast, the study described herein focused on comparing two metabolites of tryptophan that belong

to the class of indole derivatives, IAld and I3AA. Specially, we investigated the potential of these metabolites to regulate innate inflammatory cytokines and stromal remodeling processes (osteoclastogenesis and angiogenesis) that cause joint damage in RA. Certain indole derivatives produced by the microbiota have received attention in RA, as it has been shown that I3AA and indole-3-acetaldehyde were reduced in RA compared to OA synovial fluid (327); however, the impact of this observation on arthritis-related processes remained to be defined. Also, there are other indole derivatives that may play a pivotal role in disease. Our findings highlight novel results depicting differential bioactivities of IAld *versus* I3AA against the innate inflammatory response, stromal remodeling, and oxidative stress, as well as the disparate roles of AhR in contributing to these outcomes.

Pro-inflammatory cytokines such as IL-1 $\beta$ , IL-6, and TNF $\alpha$  are upregulated upon activation of TLRs on M $\phi$  and other synovial-infiltrating cells and as such, are major mediators of arthritic inflammation in RA (106, 328, 329). TLR2 and TLR4 were shown to regulate the cytokine milieu in human RA synovial explants in a MyD88- and Mal/TIRAP-dependent manner (110). These TLRs can be activated by specific ligands including LPS and peptidoglycans, like those from Mtb; both LPS and Mtb were used in this study. We observed that IAld, but not I3AA, reduced the expression of proinflammatory cytokines IL-1 $\beta$  and IL-6 by RAW cells (murine M $\phi$ ) stimulated by Mtb or LPS. Interestingly, the expression of TNF $\alpha$  mRNA induced by LPS was significantly reduced by IAld. LPS activates TLR4, whereas Mtb can activate both TLR2 and TLR4. TLR2 and TLR4 have been shown to play differential roles in the mycobacterium-induced response of M $\phi$  (315). We speculate that this might partly explain the observed differences in the effect of IAld and I3AA on cytokine induction by Mtb *versus* LPS; however, this

idea remains to be tested experimentally. The cytokines tested here (IL-1 $\beta$ , IL-6, TNF $\alpha$ ) not only promote inflammation, but also drive pathological stromal remodeling by serving as upstream mediators of osteoclastogenesis (330) and angiogenesis (317). Therefore, by inhibiting these innate inflammatory responses, IAld and I3AA may prevent deleterious stromal remodeling of the bone and vasculature in the arthritic joint.

Not all the cytokines tested were suppressed by IAld. The expression of VEGF following treatment with Mtb was found to be further induced in the presence of IAld. Although this factor has pro-angiogenic activity, there is also mounting evidence in cancer studies that VEGF can promote Treg proliferation and the immunosuppressive activity of these cells (331). Also, VEGFR2 activation by VEGF was shown to inhibit T cell receptor (TCR) signaling and T cell proliferation in the Jurkat T cell line (332). In addition, VEGF was shown to suppress the TNF $\alpha$ -induced upregulation of Jurkat cell adhesion to endothelial cells *in vitro* and primary human endothelial cell expression of the inflammatory T cell chemoattractant ligands CXCL10, which also promotes osteoclastogenesis (124), and CXCL11 (333). In this study, using the B16 tumor mouse model, treating animals with sunitinib, a VEGFR inhibitor, resulted in increased expression of CXCL10 and CXCL11 in the tumor vessels and also increased T cell tumor infiltration. In the context of RA, VEGF might also suppress disease in certain circumstances by increasing Treg activities and reducing the recruitment of pathogenic cells to the arthritic joint. However, the potential anti-arthritic activities of VEGF may be outweighed by its pro-arthritic properties. Indeed, use of VEGFR2 blocking antibodies (*i.e.*, Ramucirumab) showed good protection alone and in combination therapy with MTX in the AA experimental model of human RA (334). These findings illustrate that a better

understanding of the role of VEGF in RA may be needed. In summary, novel approaches of targeting these cytokines, including by administration of microbial-derived metabolites as post-biotics, may prove beneficial in developing complementary approaches for disease management.

Microbial indole derivatives have been shown to ameliorate disease in animal models of EAE (275), colitis (11, 335), and atopic dermatitis (336) in an AhR-dependent manner. We observed that antagonism of the AhR with CH-223191 failed to reverse IAld-mediated suppression of IL-6 mRNA in Mtb-treated M $\phi$ . Furthermore, we speculate that the partial reversal of IAld-mediated IL-1 $\beta$  suppression by CH-223191 was possibly the result of CH-223191 directly increasing IL-1 $\beta$  expression. This speculation is in keeping with the findings from a study on LPS-induced septic shock, where AhR-deficiency in mouse peritoneal M $\phi$  caused increased IL-1 $\beta$  expression (295). From studies on the therapeutic effect of IAld on graft-versus-host disease (GVHD), paradoxical findings have suggested that AhR may or may not be involved in IAld-mediated protection against disease (337, 338). In one of these studies, evidence for the role of AhR in IAld-mediated protection was found to be inconclusive (337). In EAE, amelioration of disease by microbial-derived metabolite of tryptophan appeared to be AhR-dependent, but it is difficult to extrapolate, specially, which metabolites, namely indole derivatives, were AhR ligands (275). Additionally, recent studies directly analyzing IAld in mouse colonocytes and human primary hepatocytes showed potentially weak or ineffective AhR agonistic activity (339, 340). These findings suggest that IAld may have additional non-AhR dependent activities that, in part, facilitate its potential to regulate human health and disease.

As highlighted earlier, MyD88-dependent pathways are critical in regulating the TLR2- and TLR4-driven pathogenic responses of M $\phi$  in RA (110), including induction of pro-inflammatory cytokine expression and the subsequent response of cells to some of these pro-inflammatory cytokines (*e.g.* IL-1 $\beta$ ). In our study, we used a prototypic TLR4 agonist, LPS, to activate RAW cells to assess if these indole derivatives alter NF- $\kappa$ B and MAPK pathways downstream of TLR4-MyD88 activation. However, no indication of regulation of these pathways by IAld or I3AA was observed. Nevertheless, these findings do not rule out that the MyD88-mediated response might be regulated further downstream of these signaling events. For example, IAld altered binding of MyD88-dependent transcription factors to DNA or epigenetic changes that alter gene transcription might be involved in controlling these outcomes. These possibilities require further investigation.

Aberrant stromal remodeling of bone and blood vessels are frequently coupled in a disease state, and in addition to inflammation, also play a critical role in RA pathogenesis (167, 328). Secondary osteoporosis in RA, due to excessive inflammation, is the predominant factor in loss of mobility, ankylosis, and chronic joint pain. We showed that IAld enhanced osteoclast formation and related gene transcription of *CatK* and *TRAP* at concentrations of 10 – 20  $\mu$ M. To our knowledge, this is the first report describing a direct effect of IAld at this concentration range; previous reports have used IAld at 10- to 100-times higher concentrations to investigate its effects on biological processes (335). As with the anti-inflammatory response of IAld on M $\phi$ , the pro-osteoclastogenic effect of IAld was not affected by AhR antagonism. The implications of this pro-osteoclastogenic effect deserves further attention in the context of RA and other diseases involving bone resorption.

As mentioned above, aberrant bone and blood vessel remodeling are intimately coupled in RA. To our surprise, IAld and I3AA had opposing effects on endothelial cells tube formation, an indicator of angiogenic activity. Additionally, an interesting time-dependent interplay between IAld and I3AA on tube formation was observed. IAld significantly upregulated tube formation, which in theory, could have detrimental effects on arthritis progression by acting on the blood vessels that invade the pannus and synovial lining (317). The potential pro-angiogenic activity of IAld is further supported by our findings that IAld increased VEGF expression by Mtb-treated M $\phi$ . In contrast to IAld, our results lend further support for I3AA as an anti-angiogenic agent, as reported previously from a study showing I3AA inhibited VEGF signaling in HUVEC (341). This supports the potential detrimental impact of low I3AA levels in RA, as has been previously observed (327). Additionally, we found that CH-223191 failed to suppress the pro-angiogenic effect of IAld, but did reverse the anti-angiogenic effect of I3AA. This observed effect of I3AA tapered off at 0.25 mM, which corresponds with the lowest concentration at which I3AA was previously shown to have AhR agonistic activity in mouse colonic cells (339). Our findings on the anti-angiogenic activity of I3AA being AhR-dependent is also supported by the conclusion from a previous study showing that I3AA has AhR agonistic activity in human cells that tapers off at 0.25 mM (340).

These findings illustrate the differential activities of IAld and I3AA on stromal remodeling processes that are relevant not only for RA, but also for other diseases. For example, we speculate that the pro-angiogenic and pro-osteoclastic effects of IAld might promote tumor growth and bone-resorptive metastasis, while I3AA might reduce tumor growth by inhibiting angiogenesis. Also, because of the possibility that IAld may directly

potentiate stromal modeling but inhibit aberrant inflammatory responses upstream of pathological stromal remodeling, IAld may differentially regulate inflammatory arthritis (*e.g.*, RA) and non-inflammatory arthritis (*e.g.*, OA). However, these speculations will need to be tested experimentally. It is possible that ‘dysbiosis’ or perturbation in the bioavailability of these microbiota-derived metabolites may affect other aspects of health besides chronic disease, for example, by regulating proper sculpting of developing bone tissue during adolescence, bone regeneration, and healing of fractures (163, 164). Likewise, proper tissue vascularization is necessary to bring oxygen and nutrients to healthy tissues and to the site of wound healing, but improper levels of vascularization can propagate pathological processes in certain diseases (165). For these reasons, there is also precedence to characterize these microbial indole derivatives in non-disease states.

It is apparent that there is significant cross-talk between the AhR and Nrf2 pathways, and that this cross-talk is important to consider in cancer treatment (303, 304). There is also evidence that both pathways can similarly impact the above-studied processes which makes it important to understand how this cross-talk might contribute to autoimmune arthritis and other diseases. Although AhR-Nrf2 cross-talk was not directly investigated herein, it is plausible that this cross-talk could account for the discrepancy between the dependency upon AhR for mediating previously described *in vivo* effects of some indole derivatives, like has been suggested for IAld, but mounting evidence from *in vitro* studies suggesting IAld has ineffective AhR agonistic activity (339, 340). Specifically, if IAld or another indole derivative alters Nrf2 activity, there may also be a downstream AhR-dependent response. This phenomenon was recently shown as the mechanism-of-action by which the Nrf2 agonist, CDDO-IM, induces IL-22 in CD4<sup>+</sup> T cells

(342), and how Nrf2 modulation of AhR signaling influences adipogenesis (305). IAld has also been shown to increase IL-22 expression in cells within the mucosal tissue of *C. albican*-infected mice (11). This effect of IAld on IL-22 expression was absent in AhR-deficient animals, but a role for Nrf2 was not investigated.

We hypothesized that IAld may be a regulator of the Nrf2 pathway and, if so, that this would explain how IAld potentiates osteoclastogenesis. This was based on both the studies described above, in addition to other previous studies showing that potentiation of RANKL-dependent osteoclastogenesis by inhibition of the Nrf2 pathway is associated with a reduction in the expression of antioxidant genes and increased intracellular ROS levels (298, 299). By extrapolation, the activation of Nrf2, *e.g.* by CDDO-IM, is expected to inhibit osteoclast differentiation by reducing ROS levels. Much of the downstream effect of altering the Nrf2-antioxidant response during osteoclast differentiation involves regulation of intracellular ROS levels because ROS act as second messengers that facilitate osteoclast maturation and function (293). Therefore, we set out to test whether IAld could regulate the Nrf2-antioxidant response of M $\phi$ , and if this activity distinguishes it from I3AA.

IAld, but not I3AA, inhibited the expression of antioxidant enzyme genes, HMOX1 and NQO1, in response to Nrf2 activation by CDDO-IM. Expression of these enzymes was previously shown to be associated with the anti-osteoclastogenic activity of Nrf2 in M $\phi$  (318). Furthermore, we observed that CDDO-IM and IAld had antagonistic effects on osteoclast generation when added concomitantly. However, the pattern of antagonistic interplay that was observed between CDDO-IM and IAld on osteoclast generation suggests

that IAld did not potentiate osteoclastogenesis by inhibiting Nrf2 signaling and increasing oxidative stress. Further analysis of the impact of IAld on RANKL-mediated oxidative stress suggested this to be the case. IAld drastically reduced the increase in fluorescence intensity from the ROS indicator (CM-H<sub>2</sub>DCFDA) in M $\phi$  treated with RANKL compared to control cells. These findings introduce a confounding characteristic of IAld. IAld is able to suppress the cellular antioxidant response to a synthetic oleanane triterpenoid, CDDO-IM, that activates Nrf2, which is difficult to reconcile with the fact that this category of compounds is being investigated for cancer and inflammatory disease treatment (343). Nevertheless, IAld appeared to reduce ROS levels in a cell which, presumably, would be highly beneficial in reducing oxidative stress. DNA damage and excessive inflammation, as a result of oxidative stress, often contributes to cancer and inflammatory disease progression.

The *in vitro* findings described herein provided substantial evidence for the possibility that IAld and I3AA bioavailability could impact the underlying pathophysiology of RA by regulating these cellular processes. We suggest that the relative abundance of IAld and I3AA derived from the gut microbiota may dictate the beneficial vs. harmful outcome on RA. In this context, administration of IAld or I3AA as a post-biotic treatment to rectify any ‘dysbiosis’-associated imbalance that contributes to RA, might complement other approaches to prevent and/or treat this disease. We tested the effect of direct oral administration of IAld in the AA animal model of RA. Administration of IAld (5 mg/kg) daily to animals a few days before initial onset of clinical signs of arthritis significantly reduced the severity of disease compared to the controls. This dose of IAld that was administered was lower than the doses used in animal studies, previously

conducted, on animal models of EAE (20 mg/kg), GVHD (150 mg/kg), and intestinal homeostasis (150 mg/kg) (275, 337, 344). In addition to ameliorating the severity of arthritis, the percentage of animals that developed disease in the IAld-treated group was only 60% whereas 100% of animals developed disease in the control group. These results provide early indications of the potentially beneficial impact that a higher bioavailability of IAld may have on autoimmune arthritis.

## Chapter 9: Summary and Concluding Remarks

Our findings are the first to implicate the microbial indole derivatives, IAld and I3AA, as potential modulators of arthritis-related processes, to unravel the differential effects of the two metabolites (**Table 4**), and to elaborate mechanisms underlying these disparate effects (**Table 5**). In addition, we showed the therapeutic potential of IAld as a post-biotic using an animal model of RA (**Table 6**). In trying to understand fully the significance of these findings, it is imperative to consider that these processes not only contribute to the disease, namely RA, but also that they are involved in maintaining homeostasis in a healthy individual. For example, IAld may contribute to control of inflammation caused by a subclinical infection or injury. Similarly, the end plate of a growing bone needs blood supply, as provided by angiogenesis (345), and requires osteoclastic activity for proper bone sculpting as osteoblasts rapidly form bone (163). In a diseased individual, the suppressive effect of IAld on cytokine gene expression would help protect against arthritic inflammation. However, excessive availability of IAld may aggravate arthritis pathology by contributing to aberrant angiogenic and osteoclastogenic components. Also, in non-inflammatory arthritis IAld may differentially impact arthritis pathology because the inflammatory response is less of a contributing factor in these diseases than in inflammatory and autoimmune arthritis. Nevertheless, the anti-angiogenic effect of I3AA may help to counter the pro-angiogenic effect of IAld in a disease situation. Depending on the particular microbiota present in an individual's GIT, it may be possible that fluctuations in the metabolism of tryptophan by these microbiota could differentially impact the relative bioavailability of specific indole derivatives, such that some metabolites of the indole derivative class increase in concentrations whereas other metabolites

decrease. In this context, correcting the ‘dysbiosis, or metabolite deficiency/excess might help control the physiological/pathological outcomes of RA and possibly other diseases.

Identification of the immuno- and stromal-regulatory capabilities of IAld and I3AA are promising results from the work presented here in (**Figure 25**). These findings suggest potential physiological relevance of these potent bioactive microbial metabolites, which represent cause-and-effect agents and may explain the association between the microbiome and RA. Additionally, these indoles may have potential as biomarkers of microbiome ‘dysbiosis’, and also as potential therapeutic agents for clinical use in managing RA. The relative bioavailability of these metabolites may additionally be relevant for other diseases such as cancer that share with RA the mediators of inflammation, angiogenesis, and osteoclastogenesis.

**Table 4. Summary of results from the completion of Aim 1.**

<b>Disease Process</b>	<b>Observed (Effect)</b>	<b>Observed (Effect)</b>
<b>Innate Inflammation</b>	Partial Inhibition	Insignificant
<b>Osteoclastogenesis (Bone Resorption)</b>	Potentialiation	Insignificant
<b>Angiogenesis (Blood Vessel)</b>	Potentialiation	Inhibition

**Table 5. Summary of results from the completion of Aim 2.**

<b>Pathway Tested</b>	<b>Process for which assessed</b>	<b>Dependence of IAld</b>	<b>Dependence of I3AA</b>
<b>AhR Pathway (CH-223191, Antagonist)</b>	All 3	Failed to inhibit	Inhibition
<b>TLR-mediated MyD88-response</b>	Innate Inflammation	No indication of altered signaling	No indication of altered signaling
<b>Nrf2 Pathway (CDDO-IM, Agonist)</b>	Osteoclastogenesis	Inhibition	Not tested
<b>Nrf2 Pathway (CM-H<sub>2</sub>DCFDA)</b>	Osteoclastogenesis	Less ROS indicator fluorescence	Not tested

**Table 6. Summary of results from the completion of Aim 3.**

<b>Disease Model</b>	<b>Observed Effect (IAld)</b>	<b>Observed Effect (I3AA)</b>
<b>Rat adjuvant-induced arthritis</b>	Disease amelioration	Not tested

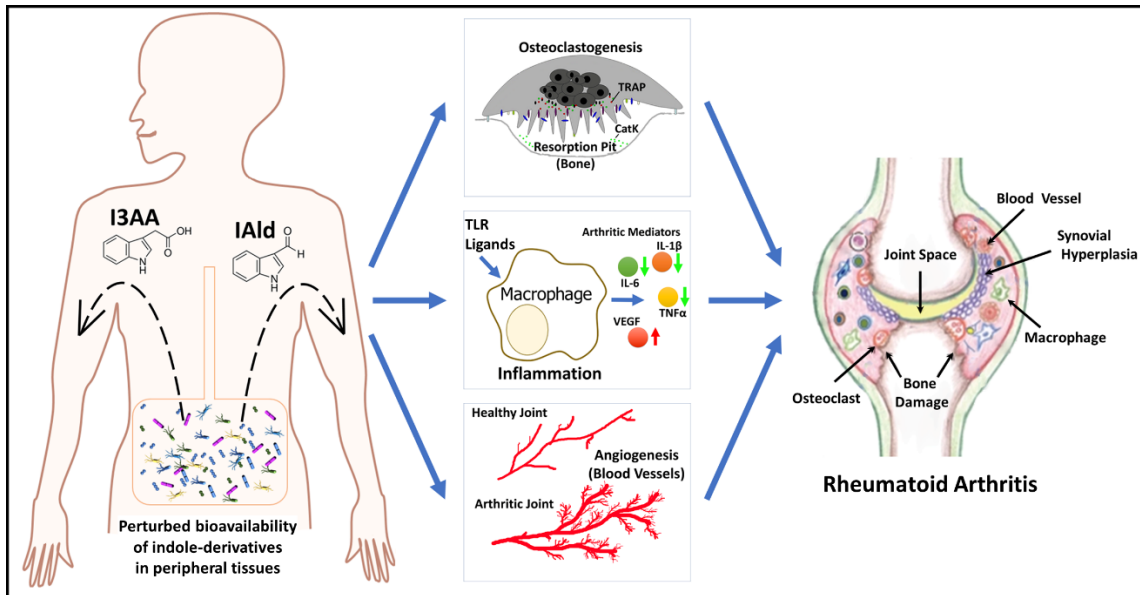


**Figure 25. The bioavailability of IAld and I3AA may impact pathophysiological processes that occur in the arthritic joint during RA.**

‘Dysbiosis’ of gut microbiota can change the bioavailability of IAld and I3AA in the host. In turn, changes in the concentration of these indole derivatives in peripheral tissues may contribute to the disease by impacting the innate inflammatory response of M $\phi$  to TLR ligands (*i.e.*, PAMPs and DAMPs), the formation of blood vessels (angiogenesis), and the bone-resorbing activity of osteoclasts. (Figure from Langan D, et al., *Int J Mol Sci.* 2021; 22(4):2017) (314).

## Chapter 10: Future Directions

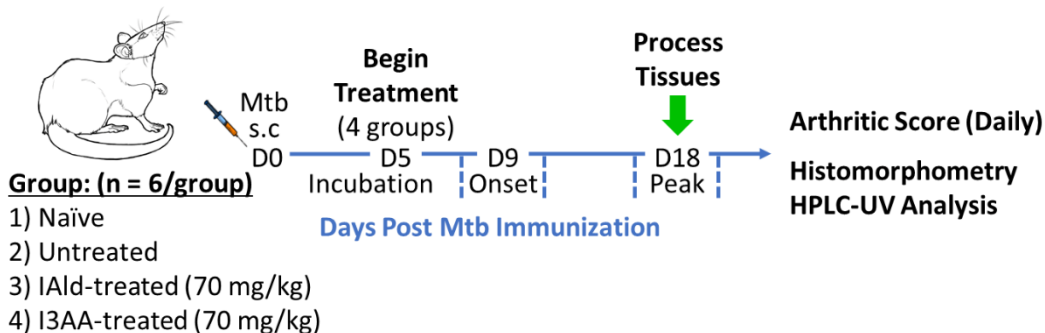
In subsequent detailed experiments on a larger number of animals, additional measurements on histomorphometry and on plasma and synovial fluid levels of IAld and I3AA in arthritic vs. healthy (control) rats will be performed (**Appendix I**) (346). In addition, the solubility and administration protocol for treatment of animals by oral gavage has been optimized so that IAld and I3AA can now be administered at a significantly higher concentration (70 mg/kg). We expect that administering IAld at this higher concentration will lead to a greater amelioration of disease than the lower concentration (5 mg/kg) tested herein. In anticipation of conducting a more thorough analysis of how oral feeding of IAld and I3AA altered their concentrations in the blood and the synovial tissue (joints), we optimized methanol-chloroform extraction, based on the Folch extraction method (347), and HPLC-UV analysis protocol for these indoles (**Appendix II**). This work sets the foundation for a later study to determine whether there is an association between the bioavailability of these indole derivatives and severity of arthritis. We anticipate that this will provide evidence for an *in vivo* mechanism of action that may corroborate our *in vitro* findings.

Given the current gaps in our understanding of the role of the AhR in mediating the effects of I3AA and IAld directly on M $\phi$ , a more direct assessment of how and whether AhR impacts their bioactivity, respectively, should be undertaken. Both AhR knockdown and AhR overexpressing RAW cells lines can be generated by transduction of a lentivirus harboring a relevant shRNAi or a gene expression cassette, respectively. This is important because during an inflammatory response, cells can greatly increase AhR expression levels,

which can affect how weak AhR ligands modulate the cellular response. Furthermore, the implications of the regulation of the antioxidant response by IAld and how this might facilitate an interplay with Nrf2 activity need to be reconciled. Our findings suggest that the bioavailability of IAld could impact Nrf2 agonist efficacy, which is relevant to the treatment of diseases like cancer, and this aspect of IAld needs further investigation. Additionally, although the results obtained from utilizing CM-H<sub>2</sub>DCFDA as an indicator of intracellular ROS levels suggested that IAld-mediated inhibition of the Nrf2 antioxidant response was not responsible for its potentiation of osteoclastogenesis, it is possible that there were convoluting factors associated with the results of these experiments and we would like to further address any potential role of Nrf2 in mediating the observed effect of IAld.

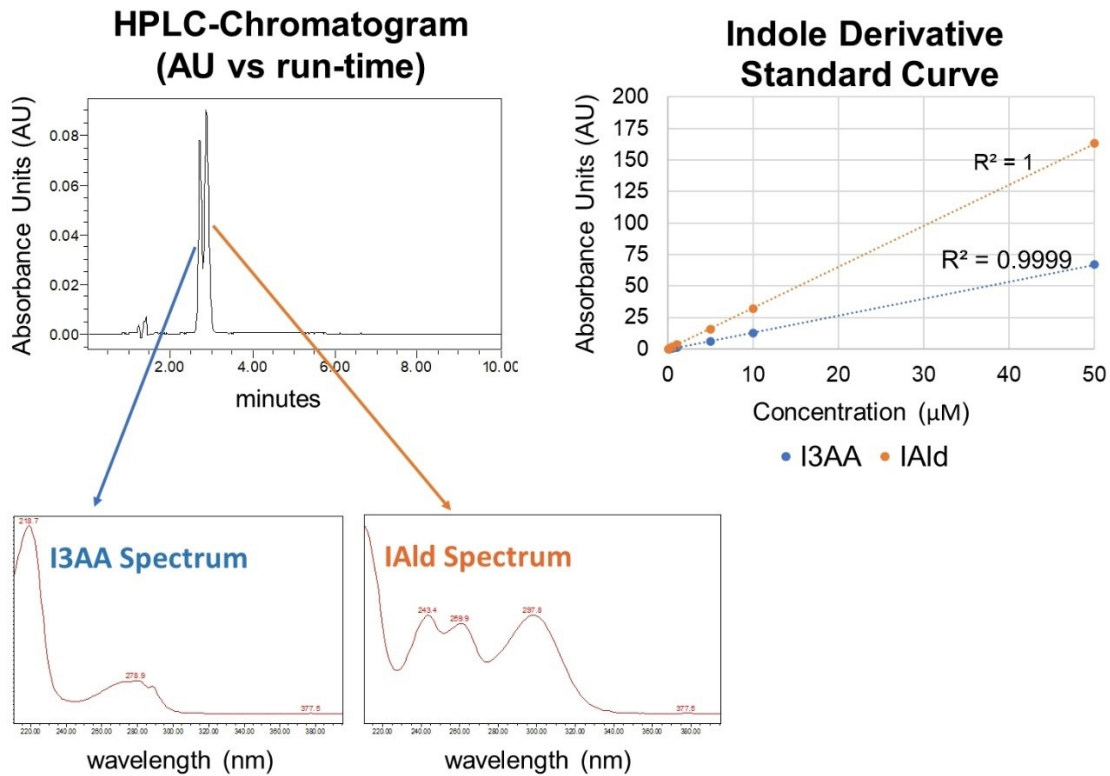
In summary, the results of above experiments are expected to advance our understanding of the prophylactic and/or therapeutic effects of IAld and I3AA on autoimmune arthritis and help define the precise role of non-AhR mechanisms in the observed activities of IAld.

## Appendices



### Appendix I. Experimental design illustrating how the therapeutic potential of indole derivatives for autoimmune arthritis will be assessed using the AA rat.

Male Lewis rats will be randomly assigned to 4 groups (n = 6/group): Naïve, untreated, IAld-treated, I3AA-treated. In all but the naïve group, rats will receive a s.c. injection with Mtb for the induction of AA. Rats receiving indole derivative (70 mg/kg) will begin daily treatment via oral gavage starting on d 5 after Mtb immunization. The untreated control will receive Veh only starting on d 5 after Mtb immunization. The arthritic score will be measured in rats over the course of disease. At the time corresponding to disease peak in AA rat (d 18), tissues (*i.e.*, joint, blood, synovial fluid) will be collected from animals in each group. Histomorphometry of joint sections will be run to assess bone damage in the joints. Plasma and synovial fluid will be processed for HPLC-UV analysis to assess the relative levels on IAld and I3AA in these tissues. A similar experiment will be performed in female Lewis rats to examine sex as a biological variable in regard to the bioactivity of IAld and I3AA.



## Appendix II. Optimization of indole derivative extraction from serum.

Blood was collected from rats. This blood was spiked with both IAId and I3AA before isolating serum. Next a methanol-chloroform extraction was performed on this serum as described in Methods. Extracted samples were run on a 5  $\mu\text{m}$  ODS(2) spherclone 250 mm  $\times$  2.00 mm C18 column at 40  $^{\circ}\text{C}$  and analyzed by UV. Results show peaks corresponding to I3AA and IAId as well as the standard curve from running samples spiked with both indole derivatives (0.01 – 50  $\mu\text{M}$ ).

## References

1. WHO. WHO | Chronic rheumatic conditions. *World Health Organization*. [cited 02/25/2021]; Available from: <https://www.who.int/chp/topics/rheumatic/en/>
2. Alamanos, Y., and A. A. Drosos. 2005. Epidemiology of adult rheumatoid arthritis. *Autoimmun Rev* 4: 130–136.
3. Helmick, C. G., et al., 2008. Estimates of the prevalence of arthritis and other rheumatic conditions in the United States: Part I. *Arthritis Rheum* 58: 15–25.
4. Safiri, S., et al., 2019. Global, regional and national burden of rheumatoid arthritis 1990-2017: a systematic analysis of the Global Burden of Disease study 2017. *Ann Rheum Dis* 78: 1463–1471.
5. Andersen, N. N., and T. Jess. 2014. Risk of infections associated with biological treatment in inflammatory bowel disease. *World J Gastroenterol* 20: 16014–16019.
6. Conway, R., and J. J. Carey. 2017. Risk of liver disease in methotrexate treated patients. *World J Hepatol* 9: 1092–1100.
7. Crofford, L. J. 2013. Use of NSAIDs in treating patients with arthritis. *Arthritis Res Ther* 15: S2.
8. McCarville, J. L., et al., 2020. Microbiota Metabolites in Health and Disease. *Annu Rev Immunol* 38: 147–170.
9. Wang, Z., and Y. Zhao. 2018. Gut microbiota derived metabolites in cardiovascular health and disease. *Protein Cell* 9: 416–431.
10. Mishima, Y., and S. Ishihara. 2020. Molecular mechanisms of microbiota-mediated pathology in irritable bowel syndrome. *Int J Mol Sci* 21: 1–25.
11. Zelante, T., et al., 2013. Tryptophan catabolites from microbiota engage aryl hydrocarbon receptor and balance mucosal reactivity via interleukin-22. *Immunity* 39: 372–385.
12. Pearson, C. M. 1956. Development of arthritis, peri-arthritis and periostitis in rats given adjuvants. *Proc Soc Exp Biol Med* 91: 95–101.
13. Fruton, J. S. 1957. The collected papers of Paul Ehrlich. *Yale J Biol Med* 29: 628.
14. Franklin, E. C., et al., 1957. An unusual protein component of high molecular weight in the serum of certain patients with rheumatoid arthritis. *J Exp Med* 105: 425–438.

15. Witebsky, E., et al., 1957. Chronic thyroiditis and autoimmunization. *J Am Med Assoc* 164: 1439–1447.
16. Doniach, D., and I. M. Roitt. 1957. Auto-immunity in Hashimoto’s disease and its implications. *J Clin Endocrinol Metab* 17: 1293–1304.
17. Langan, D., N. R. Rose, and K. D. Moudgil. 2020. Common innate pathways to autoimmune disease. *Clin Immunol* 212: 108361.
18. Theofilopoulos, A. N., D. H. Kono, and R. Baccala. 2017. The multiple pathways to autoimmunity. *Nat Immunol* 18: 716–724.
19. Janda, A., et al., 2016. Disturbed B-lymphocyte selection in autoimmune lymphoproliferative syndrome. *Blood* 127: 2193–2202.
20. Teshima, T., et al., 2003. Impaired thymic negative selection causes autoimmune graft-versus-host disease. *Blood* 102: 429–435.
21. Guerau-de-Arellano, M., et al., 2009. Neonatal tolerance revisited: A perinatal window for Aire control of autoimmunity. *J Exp Med* 206: 1245–1252.
22. Ohashi, P. S. 1996. T cell selection and autoimmunity: flexibility and tuning. *Curr Opin Immunol* 8: 808–814.
23. Biswas, S. K., and E. Lopez-Collazo. 2009. Endotoxin tolerance: new mechanisms, molecules and clinical significance. *Trends Immunol* 30: 475–487.
24. Lv, S., et al., 2017. A negative feedback loop of ICER and NF- $\kappa$ B regulates TLR signaling in innate immune responses. *Cell Death Differ* 24: 492–499.
25. Yoo, S. A., et al., 2019. Placental growth factor regulates the generation of TH17 cells to link angiogenesis with autoimmunity. *Nat Immunol* 20: 1348–1359.
26. Beyer, C., and G. Schett. 2011. A duet of bone and the immune system. *The Rheumatologist*. [cited 02/25/2021]; Available from: <https://www.the-rheumatologist.org/article/a-duet-of-bone-and-the-immune-system/>
27. Dinse, G. E., et al., 2020. Increasing prevalence of antinuclear antibodies in the United States. *Arthritis Rheumatol* 72: 1026–1035.
28. Uramoto, K. M., et al., Trends in the incidence and mortality of systemic lupus erythematosus, 1950-1992. *Arthritis Rheum* 42: 46–50.
29. Paz García. 2018. *Report for parliamentarians into autoimmune conditions*,. [cited 02/13/2021]; Available from: <https://www.immunology.org/news/report-reveals-the-rising-rates-autoimmune-conditions>

30. Grimaldi, L. M. E., et al., 2007. High prevalence and fast rising incidence of multiple sclerosis in Caltanissetta, Sicily, southern Italy. *Neuroepidemiology* 28: 28–32.
31. National Institutes of Health. 2002. *National Institutes of Health Autoimmune Disease Coordinating committee report*,. Bethesda (MD).
32. AARDA. 2018. Autoimmune Disease Statistics. *AARDA* . [cited 02/13/2021]; Available from: <https://www.aarda.org/news-information/statistics/>
33. Nielen, M. M. J., et al., 2004. Specific autoantibodies precede the symptoms of rheumatoid arthritis: a study of aerial measurements in blood donors. *Arthritis Rheum* 50: 380–386.
34. Arbuckle, M. R., et al., 2003. Development of autoantibodies before the clinical onset of systemic Lupus erythematosus. *N Engl J Med* 349: 1526–1533.
35. DeHoratius, R. J., et al., 1975. Anti-nucleic acid antibodies in systemic lupus erythematosus patients and their families. Incidence and correlation with lymphocytotoxic antibodies. *J Clin Invest* 56: 1149–1154.
36. Steiner, G., and J. Smolen. 2002. Autoantibodies in rheumatoid arthritis and their clinical significance. *Arthritis res* 4 Suppl 2: S1.
37. Liao, K. P., et al., 2013. Associations of autoantibodies, autoimmune risk alleles, and clinical diagnoses from the electronic medical records in rheumatoid arthritis cases and non-rheumatoid arthritis controls. *Arthritis Rheum* 65: 571–581.
38. Ali, Y. 2018. Rheumatologic tests: a primer for family physicians. *Am Fam Physician* 98: 164–170.
39. Kaipainen-Seppanen, O., and H. Kautiainen. 2006. Declining trend in the incidence of rheumatoid factor-positive rheumatoid arthritis in Finland 1980-2000. *J Rheumatol* 33.
40. Doran, M. F., et al., 2002. Trends in incidence and mortality in rheumatoid arthritis in Rochester, Minnesota, over a forty-year period. *Arthritis Rheum* 46: 625–631.
41. Aletaha, D., et al., 2010. 2010 Rheumatoid arthritis classification criteria: An American College of Rheumatology/European League Against Rheumatism collaborative initiative. *Ann Rheum Dis* 69: 1580–1588.
42. Hunter, T. M., et al., 2017. Prevalence of rheumatoid arthritis in the United States adult population in healthcare claims databases, 2004–2014. *Rheumatol Int* 37: 1551–1557.

43. Symmons, D., et al., 2002. The prevalence of rheumatoid arthritis in the United Kingdom: new estimates for a new century. *Rheumatology* 41: 793–800.
44. Silman, A. J., et al., 1993. Absence of rheumatoid arthritis in a rural Nigerian population. *J Rheumatol* 20: 618–622.
45. Moolenburgh, J. D., H. A. Valkenburg, and P. B. Fourie. 1986. A population study on rheumatoid arthritis in Lesotho, southern Africa. *Ann Rheum Dis* 45: 691–695.
46. Lau, E., et al., 1993. Low prevalence of rheumatoid arthritis in the urbanized Chinese of Hong Kong. *J Rheumatol* 20: 1133–1137.
47. Darmawan, J., et al., 1993. The epidemiology of rheumatoid arthritis in Indonesia. *Rheumatology* 32: 537–540.
48. McDougall, C., K. Hurd, and C. Barnabe. 2017. Systematic review of rheumatic disease epidemiology in the indigenous populations of Canada, the United States, Australia, and New Zealand. *Semin Arthritis Rheum* 46: 675–686.
49. Crowson, C. S., et al., 2011. The lifetime risk of adult-onset rheumatoid arthritis and other inflammatory autoimmune rheumatic diseases. *Arthritis Rheum* 63: 633–639.
50. Fairweather, D. L., et al., 2004. Women and autoimmune diseases. *Emerg Infect Dis* 10: 2005–2011.
51. Beeson, P. B. 1994. Age and sex associations of 40 autoimmune diseases. *Am J Med* 96: 457–462.
52. Begovich, A. B., et al., 2004. A missense single-nucleotide polymorphism in a gene encoding a protein tyrosine phosphatase (PTPN22) is associated with rheumatoid arthritis. *Am J Hum Genet* 75: 330–337.
53. Yamamoto, K., et al., 2015. Genetics of rheumatoid arthritis in Asia - present and future. *Nat Rev Rheumatol* 11: 375–379.
54. Walsh, A. M., et al., 2016. Integrative genomic deconvolution of rheumatoid arthritis GWAS loci into gene and cell type associations. *Genome Biol* 17: 79.
55. Holoshitz, J. 2010. The rheumatoid arthritis HLA-DRB1 shared epitope. *Curr Opin Rheumatol* 22: 293–298.
56. Leng, R. X., et al., 2020. Identification of new susceptibility loci associated with rheumatoid arthritis. *Ann Rheum Dis* 79: 1565–1571.
57. Ramos, P. S., A. M. Shedlock, and C. D. Langefeld. 2015. Genetics of autoimmune diseases: Insights from population genetics. *J Hum Genet* 60: 657–664.

58. Gregersen, P. K., J. Silver, and R. J. Winchester. 1987. The shared epitope hypothesis. an approach to understanding the molecular genetics of susceptibility to rheumatoid arthritis. *Arthritis Rheum* 30: 1205–1213.
59. Gibofsky, A., et al., 1978. Disease associations of the Ia-like human alloantigens: Contrasting patterns in rheumatoid arthritis and systemic lupus erythematosus\*. *J Exp Med* 148: 1728–1732.
60. Stastny, P. 1978. Association of the B-cell alloantigen DRw4 with rheumatoid arthritis. *N Engl J Med* 298: 869–871.
61. Stastny, P. 1976. Mixed lymphocyte cultures in rheumatoid arthritis. *J Clin Invest* 57: 1148–1157.
62. Tiwari, J. L., and P. I. Terasaki. 1985. *HLA and disease associations*,. Springer New York, New York, NY.
63. Vyse, T. J., and J. A. Todd. 1996. Genetic analysis of autoimmune disease. *Cell* 85: 311–318.
64. Deighton, C. M., et al., 1992. Contribution of inherited factors to rheumatoid arthritis. *Ann Rheum Dis* 51: 182–185.
65. Cooper, G. S., F. W. Miller, and J. P. Pandey. 1999. The role of genetic factors in autoimmune disease: Implications for environmental research. In *Environ Health Perspect* vol. 107. Public Health Services, US Dept of Health and Human Services. 693–700.
66. Silman, A. J., et al., 1993. Twin concordance rates for rheumatoid arthritis: results from a nationwide study. *Rheumatology* 32: 903–907.
67. Bellamy, N., et al., 1992. Rheumatoid arthritis in twins: a study of aetiopathogenesis based on the Australian Twin Registry. *Ann Rheum Dis* 51: 588–593.
68. Padyukov, L., et al., 2004. A gene-environment interaction between smoking and shared epitope genes in HLA-DR provides a high risk of seropositive rheumatoid arthritis. *Arthritis Rheum* 50: 3085–3092.
69. Costenbader, K. H., et al., 2006. Smoking intensity, duration, and cessation, and the risk of rheumatoid arthritis in women. *Am J Med* 119: 503.e1-503.e9.
70. Office of the Surgeon General, 1964. *Smoking and health: report of the advisory committee to the Surgeon General of the Public Health Service*.

71. Talhout, R., et al., 2011. Hazardous compounds in tobacco smoke. *Int J Environ Res Public Health* 8: 613–628.
72. Kobayashi, S., et al., 2008. A role for the aryl hydrocarbon receptor and the dioxin TCDD in rheumatoid arthritis. *Rheumatology* 47: 1317–1322.
73. Fu, J., et al., 2018. Shared epitope–aryl hydrocarbon receptor crosstalk underlies the mechanism of gene–environment interaction in autoimmune arthritis. *Proc Natl Acad Sci U S A* 115: 4755–4760.
74. Talbot, J., et al., 2018. Smoking-induced aggravation of experimental arthritis is dependent of aryl hydrocarbon receptor activation in Th17 cells. *Arthritis Res Ther* 20: 119.
75. Mayeux, J. M., et al., 2018. Silicosis and silica-induced autoimmunity in the diversity outbred mouse. *Front Immunol* 9: 26.
76. Gonzalez-Quintial, R., et al., 2019. Silica exposure and chronic virus infection synergistically promote lupus-like systemic autoimmunity in mice with low genetic predisposition. *Clin Immunol* 205: 75–82.
77. Pollard, K. M., et al., 2017. Induction of systemic autoimmunity by a xenobiotic requires endosomal TLR trafficking and signaling from the late endosome and endolysosome but not type I IFN. *J Immunol* 199: 3739–3747.
78. Roudier, J., et al., 1989. Susceptibility to rheumatoid arthritis maps to a T-cell epitope shared by the HLA-Dw4 DR  $\beta$ -1 chain and the Epstein-Barr virus glycoprotein gp110. *Proc Natl Acad Sci U S A* 86: 5104–5108.
79. Moudgil, K. D., et al., 2001. Environmental modulation of autoimmune arthritis involves the spontaneous microbial induction of T cell responses to regulatory determinants within heat shock protein 65. *J Immunol* 166: 4237–4243.
80. Harley, J. B., et al., 2018. Transcription factors operate across disease loci, with EBNA2 implicated in autoimmunity. *Nat Genet* 50: 699–707.
81. Lacerte, P., et al., 2016. Overexpression of TLR2 and TLR9 on monocyte subsets of active rheumatoid arthritis patients contributes to enhance responsiveness to TLR agonists. *Arthritis Res Ther* 18.
82. Strachan, D. P. 1989. Hay fever, hygiene, and household size. *BMJ* 299: 1259–1260.
83. Sheikh, A., and D. P. Strachan. 2004. The hygiene theory: Fact or fiction? *Curr Opin Otolaryngol Head Neck Surg* 12: 232–236.

84. Stiemsma, L., et al., 2015. The hygiene hypothesis: current perspectives and future therapies. *ImmunoTargets Ther* 4: 143.
85. Okada, H., et al., 2010. The ‘hygiene hypothesis’ for autoimmune and allergic diseases: an update. *Clin Exp Immunol* 160: 1–9.
86. Langan, D., E. Y. Kim, and K. D. Moudgil. 2019. Modulation of autoimmune arthritis by environmental ‘hygiene’ and commensal microbiota. *Cell Immunol* 339.
87. Dourado, E., et al., 2020. Diet as a modulator of intestinal microbiota in rheumatoid arthritis. *Nutrients* 12: 1–19.
88. Wang, D. D., et al., 2021. The gut microbiome modulates the protective association between a Mediterranean diet and cardiometabolic disease risk. *Nat Med* 27: 333–343.
89. Claesson, M. J., et al., 2012. Gut microbiota composition correlates with diet and health in the elderly. *Nature* 488: 178–184.
90. Daily, J. W., M. Yang, and S. Park. 2016. Efficacy of turmeric extracts and curcumin for alleviating the symptoms of joint arthritis: a systematic review and meta-analysis of randomized clinical trials. *J Med Food* 19: 717–729.
91. Norris, P. C., and E. A. Dennis. 2012. Omega-3 fatty acids cause dramatic changes in TLR4 and purinergic eicosanoid signaling. *Proc Natl Acad Sci U S A* 109: 8517–8522.
92. Dennis, E. A., and P. C. Norris. 2015. Eicosanoid storm in infection and inflammation. *Nat Rev Immunol* 15: 511–523.
93. Scher, J. U., et al., 2013. Expansion of intestinal *Prevotella copri* correlates with enhanced susceptibility to arthritis. *ELife* 2: e01202.
94. Pianta, A., et al., 2017. Evidence for immune relevance of *Prevotella copri*, a gut microbe, in patients with rheumatoid arthritis. *Arthritis Rheumatol* 69: 964-975.
95. 2010. No need to avoid healthy omega-6 fats - Harvard Health. *Harvard Health Publishing*. [accessed 4/22/2021]; Available from: [https://www.health.harvard.edu/newsletter\\_article/no-need-to-avoid-healthy-omega-6-fats](https://www.health.harvard.edu/newsletter_article/no-need-to-avoid-healthy-omega-6-fats)
96. Innes, J. K., and P. C. Calder. 2018. Omega-6 fatty acids and inflammation. *Prostaglandins Leukot Essent Fatty Acids* 132: 41–48.
97. Kleinewietfeld, M., et al., 2013. Sodium chloride drives autoimmune disease by the induction of pathogenic TH 17 cells. *Nature* 496: 518–522.

98. Hernandez, A. L., et al., 2015. Sodium chloride inhibits the suppressive function of FOXP3<sup>+</sup> regulatory T cells. *J Clin Invest* 125: 4212–4222.
99. Astry, B., S. H. Venkatesha, and K. D. Moudgil. 2015. Involvement of the IL-23/IL-17 axis and the Th17/Treg balance in the pathogenesis and control of autoimmune arthritis. *Cytokine* 74: 54–61.
100. Aletaha, D., and J. S. Smolen. 2018. Diagnosis and management of rheumatoid arthritis: a review. *JAMA* 320: 1360–1372.
101. Kalden, J. R., and H. Schulze-Koops. 2017. Immunogenicity and loss of response to TNF inhibitors: implications for rheumatoid arthritis treatment. *Nat Rev Rheumatol* 13: 707–718.
102. Mayo Clinic. Rheumatoid arthritis - symptoms and causes - Mayo Clinic. *Mayo Clinic* [accessed 03/01/2021]; Available from: <https://www.mayoclinic.org/diseases-conditions/rheumatoid-arthritis/symptoms-causes/syc-20353648>.
103. Theis, K. A., T. J. Brady, and C. G. Helmick. 2017. No one dies of old age anymore: a coordinated approach to comorbidities and the rheumatic diseases. *Arthritis Care Res (Hoboken)* 69: 1–4.
104. Dadoun, S., et al., 2013. Mortality in rheumatoid arthritis over the last fifty years: systematic review and meta-analysis. *Joint Bone Spine* 80: 29–33.
105. D. Smith, M. 2012. The normal synovium. *Open Rheumatol J* 5: 100–106.
106. Huang, Q. Q., et al., 2007. Increased macrophage activation mediated through toll-like receptors in rheumatoid arthritis. *Arthritis Rheum* 56: 2192–2201.
107. Schrijver, I. A., et al., 2000. Antigen-presenting cells containing bacterial peptidoglycan in synovial tissues of rheumatoid arthritis patients coexpress costimulatory molecules and cytokines. *Arthritis Rheum* 43: 2160–2168.
108. van der Heijden, et al., 2000. Presence of bacterial DNA and bacterial peptidoglycans in joints of patients with rheumatoid arthritis and other arthritides. *Arthritis Rheum* 43: 593–598.
109. Raijmakers, R., et al., 2012. Elevated levels of fibrinogen-derived endogenous citrullinated peptides in synovial fluid of rheumatoid arthritis patients. *Arthritis Res Ther* 14: R114.
110. Sacre, S. M., et al., 2007. The toll-like receptor adaptor proteins MyD88 and Mal/TIRAP contribute to the inflammatory and destructive processes in a human model of rheumatoid arthritis. *Amer J Pathol* 170: 518–525.

111. Astry, B., E. Harberts, and K. D. Moudgil. 2011. A cytokine-centric view of the pathogenesis and treatment of autoimmune arthritis. *J Interferon Cytokine Res* 31: 927–940.
112. Brennan, F. M., and I. B. McInnes. 2008. Evidence that cytokines play a role in rheumatoid arthritis. *J Clin Invest* 118: 3537–3545.
113. Murray, P. J., et al., 2014. Macrophage activation and polarization: nomenclature and experimental guidelines. *Immunity* 41: 14–20.
114. Stein, M., et al., 1992. Interleukin 4 potently enhances murine macrophage mannose receptor activity: A marker of alternative immunologic macrophage activation. *J Exp Med* 176: 287–292.
115. Martinez, F. O., and S. Gordon. 2014. The M1 and M2 paradigm of macrophage activation: Time for reassessment. *F1000Prime Reports* 6.
116. Tardito, S., et al., 2019. Macrophage M1/M2 polarization and rheumatoid arthritis: a systematic review. *Autoimmun Rev* 18.
117. Tardito, S., et al., 2019. Macrophage M1/M2 polarization and rheumatoid arthritis: a systematic review. *Autoimmun Rev* 18: 102397.
118. Han, S., et al., 2018. Liver X receptor agonist therapy prevents diffuse alveolar hemorrhage in murine lupus by repolarizing macrophages. *Front Immunol* 9: e135.
119. Han, S., et al., Reeves. 2017. A novel subset of anti-inflammatory CD138 + macrophages is deficient in mice with experimental lupus. *J Immunol* 199: 1261–1274.
120. Aronoff, D. M., et al., 2005. Cutting edge: macrophage inhibition by cyclic AMP (cAMP): differential roles of protein kinase A and exchange protein directly activated by cAMP-1. *J Immunol* 174: 595–599.
121. Aarvak, T., and J. B. Natvig. 2001. Cell-cell interactions in synovitis: Antigen presenting cells and T cell interaction in rheumatoid arthritis. *Arthritis Res* 3: 13–17.
122. Weinberg, J., et al., 1995. Human mononuclear phagocyte inducible nitric oxide synthase (iNOS): analysis of iNOS mRNA, iNOS protein, biopterin, and nitric oxide production by blood monocytes and peritoneal macrophages. *Blood* 86: 1184–1195.
123. Lee, J. H., et al., 2017. Pathogenic roles of CXCL10 signaling through CXCR3 and TLR4 in macrophages and T cells: relevance for arthritis. *Arthritis Res Ther* 19: 163.
124. Lee, J. H., et al., 2012. CXCL10 promotes osteolytic bone metastasis by enhancing cancer outgrowth and osteoclastogenesis. *Cancer Res* 72: 3175–3186.

125. Athreya, B. H., and W. W. Nichols. 1974. Basophilia in juvenile rheumatoid arthritis. *Pediatr Res* 8: 397–397.
126. Zhang, N., Z. Zhang, and X. Wang. 2018. Correlation analysis between peripheral blood basophils and disease activity in patients with rheumatoid arthritis. *Eur J Inflamm* 16: 1–7.
127. Rivellese, F., et al., 2019. Mast cells in early rheumatoid arthritis. *Int J Mol Sci* 20: 2040.
128. Beringer, A., and P. Miossec. 2019. Systemic effects of IL-17 in inflammatory arthritis. *Nat Rev Rheumatol* 15: 491–501.
129. Taams, L. S. 2020. Interleukin-17 in rheumatoid arthritis: trials and tribulations. *J Exp Med* 217: e20192048.
130. Chen, W., et al., 2018. Neutrophil function in an inflammatory milieu of rheumatoid arthritis. *J Immunol Res* 2018.
131. Miyabe, Y., C. Miyabe, and A. D. Luster. 2017. LTB4 and BLT1 in inflammatory arthritis. *Semin Immunol* 33: 52–57.
132. Kim, N. D., et al., 2006. A unique requirement for the leukotriene B4 receptor BLT1 for neutrophil recruitment in inflammatory arthritis. *J Exp Med* 203: 829–835.
133. Burkett, P. R., et., 2019. T cells and their subsets in autoimmunity. *The Autoimmune Diseases*. Ed 6:91–116.
134. Liu, X., et al., 2019. T cell receptor  $\beta$  repertoires as novel diagnostic markers for systemic lupus erythematosus and rheumatoid arthritis. *Ann Rheum Dis* 78: 1070–1078.
135. Wagner, U. G., et al., 1998. Perturbation of the T cell repertoire in rheumatoid arthritis. *Proc Natl Acad Sci U S A* 95: 14447–14452.
136. Sakurai, K., et al., 2018. HLA-DRB1 shared epitope alleles and disease activity are correlated with reduced T Cell receptor repertoire diversity in CD4+ T cells in rheumatoid arthritis. *J Rheumatol* 45: 905–914.
137. Schulze-Koops, H., and J. R. Kalden. 2001. The balance of Th1/Th2 cytokines in rheumatoid arthritis. *Best Pract Res: Clin Rheumatol* 15: 677–691.
138. Miltenburg, A. M. M., et al., 1992. T Cells cloned from human rheumatoid synovial membrane functionally represent the Th 1 subset. *Scand J Immunol* 35: 603–610.

139. Harrington, L. E. et al., 2005. Interleukin 17-producing CD4<sup>+</sup> effector T cells develop via a lineage distinct from the T helper type 1 and 2 lineages. *Nat Immunol* 6: 1123–1132.
140. Cua, D. J., et al., 2003. Interleukin-23 rather than interleukin-12 is the critical cytokine for autoimmune inflammation of the brain. *Nature* 421: 744–748.
141. Aggarwal, S., et al., 2003. Interleukin-23 promotes a distinct CD4 T cell activation state characterized by the production of interleukin-17. *J Biol Chem* 278: 1910–1914.
142. Chen, Z., et al., 2007. Distinct regulation of interleukin-17 in human T helper lymphocytes. *Arthritis Rheum* 56: 2936–2946.
143. Zhou, L., et al., 2007. IL-6 programs TH-17 cell differentiation by promoting sequential engagement of the IL-21 and IL-23 pathways. *Nat Immunol* 8: 967–974.
144. Acosta-Rodriguez, E., et al., 2007. Interleukins 1beta and 6 but not transforming growth factor- $\beta$  are essential for the differentiation of interleukin 17-producing human T helper cells. *Nat Immunol* 8: 942–949.
145. Zhou, L., et al., 2008. TGF-B-induced Foxp3 inhibits TH17 cell differentiation by antagonizing ROR $\gamma$ t function. *Nature* 453: 236–240.
146. Veldhoen, M., et al., 2006. TGF $\beta$  in the context of an inflammatory cytokine milieu supports de novo differentiation of IL-17-producing T cells. *Immunity* 24: 179–189.
147. Bettelli, E., et al., 2006. Reciprocal developmental pathways for the generation of pathogenic effector TH17 and regulatory T cells. *Nature* 441: 235–238.
148. Quintana, F. J., et al., 2008. Control of Treg and TH17 cell differentiation by the aryl hydrocarbon receptor. *Nature* 453: 65–71.
149. Veldhoen, M., et al., 2008. The aryl hydrocarbon receptor links TH17-cell-mediated autoimmunity to environmental toxins. *Nature* 453: 106–109.
150. Quintana, F. J., et al., 2010. An endogenous aryl hydrocarbon receptor ligand acts on dendritic cells and T cells to suppress experimental autoimmune encephalomyelitis. *Proc Natl Acad Sci U S A* 107: 20768–20773.
151. Symons, A., A. L. Budelsky, and J. E. Towne. 2012. Are Th17 cells in the gut pathogenic or protective. *Mucosal Immunol* 5: 4–6.
152. Hubbard, T. D., I. A. Murray, and G. H. Perdew. 2015. Indole and tryptophan metabolism: Endogenous and dietary routes to ah receptor activation. *Drug Metab Dispos* 43: 1522–1535.

153. Roager, H. M., and T. R. Licht. 2018. Microbial tryptophan catabolites in health and disease. *Nat Commun* 9.
154. Maeda, Y., et al., 2016. Dysbiosis contributes to arthritis development via activation of autoreactive T cells in the intestine. *Arthritis Rheumatol* 68: 2646–2661.
155. Xu, Y. Z., et al., 2013. Orally available and efficacious  $\alpha 4\beta 1/\alpha 4\beta 7$  integrin inhibitors. *Bioorg Med Chem Lett* 23: 4370–4373.
156. Lazarovits, A. I., and J. Karsh. 1993. Differential expression in rheumatoid synovium and synovial fluid of alpha 4 beta 7 integrin. A novel receptor for fibronectin and vascular cell adhesion molecule-1. *J Immunol* 151: 165–172.
157. Shlomchik, M. J. 2008. Sites and stages of autoreactive B cell activation and regulation. *Immunity* 28: 18–28.
158. Rudnicka, W., et al., 2009. Functional TLR9 modulates bone marrow B cells from rheumatoid arthritis patients. *Eur J Immunol* 39: 1211–1220.
159. Kim, H. J., and C. Berek. 2000. B cells in rheumatoid arthritis. *Arthritis Res* 2: 126–131.
160. Schellekens, G. A., et al., 2000. The diagnostic properties of rheumatoid arthritis antibodies recognizing a cyclic citrullinated peptide. *Arthritis Rheum* 43: 155–163.
161. Rantapää-Dahlqvist, S., et al., 2003. Antibodies against cyclic citrullinated peptide and IgA rheumatoid factor predict the development of rheumatoid arthritis. *Arthritis Rheum* 48: 2741–2749.
162. Benoist, C., and D. Mathis. 2000. A revival of the B cell paradigm for rheumatoid arthritis pathogenesis? *Arthritis Res* 2: 90–94.
163. Feng, X., and J. M. McDonald. 2011. Disorders of bone remodeling. *Annu Rev Pathol* 6: 121–145.
164. Bahney, C. S., et al., 2019. Cellular biology of fracture healing. *J Orthop Res* 37: 35–50.
165. Carmeliet, P. 2003. Angiogenesis in health and disease. *Nature Medicine* 9: 653–660.
166. Harada, K., et al., 2013. Polyphosphate-mediated inhibition of tartrate-resistant acid phosphatase and suppression of bone resorption of osteoclasts. *PLoS ONE* 8:e78612
167. Shim, J. hyuck, Z. Stavre, and E. M. Gravallesse. 2018. Bone loss in rheumatoid arthritis: basic mechanisms and clinical implications. *Calcif Tissue Int* 102: 533–546.

168. Udagawa, N., et al., 1990. Origin of osteoclasts: Mature monocytes and macrophages are capable of differentiating into osteoclasts under a suitable microenvironment prepared by bone marrow-derived stromal cells. *Proc Natl Acad Sci U S A* 87: 7260–7264.
169. Asagiri, M., et al., 2005. Autoamplification of NFATc1 expression determines its essential role in bone homeostasis. *J Exp Med* 202: 1261–1269.
170. Yang, Q., et al., 2008. VEGF enhancement of osteoclast survival and bone resorption involves VEGF receptor-2 signaling and  $\beta$ 3-integrin. *Matrix Biol* 27: 589–599.
171. Cackowski, F. C., et al., 2010. Osteoclasts are important for bone angiogenesis. *Blood* 115: 140–149.
172. Taylor, P. C., and B. Sivakumar. 2005. Hypoxia and angiogenesis in rheumatoid arthritis. *Curr Opin Rheumatol* 17: 293–298.
173. Walsh, D. A. 1999. Angiogenesis and arthritis. *Rheumatology* 38: 103–112.
174. Lund-Olesen, K. 1970. Oxygen tension in synovial fluids. *Arthritis Rheum* 13: 769–776.
175. Falchuk, K. H., E. J. Goetzl, and J. P. Kulka. 1970. Respiratory gases of synovial fluids. An approach to synovial tissue circulatory-metabolic imbalance in rheumatoid arthritis. *Amer J Med* 49: 223–231.
176. Etherington, P. J., et al., 2002. VEGF release is associated with reduced oxygen tensions in experimental inflammatory arthritis. *Clin Exp Rheumatol* 20: 799–805.
177. Tang, N., et al., 2004. Loss of HIF-1 $\alpha$  in endothelial cells disrupts a hypoxia-driven VEGF autocrine loop necessary for tumorigenesis. *Cancer Cell* 6: 485–495.
178. Durai, M., H. R. Kim, and K. D. Moudgil. 2004. The regulatory c-terminal determinants within mycobacterial heat shock protein 65 are cryptic and cross-reactive with the dominant self homologs: implications for the pathogenesis of autoimmune arthritis. *J Immunol* 173: 181–188.
179. Moudgil, K. D., et al., 1997. Diversification of T cell responses to carboxy-terminal determinants within the 65-kD heat-shock protein is involved in regulation of autoimmune arthritis. *J Exp Med* 185: 1307–1316.
180. Sudoł-Szopińska, I., et al., 2012. The pathogenesis of rheumatoid arthritis in radiological studies. Part I: formation of inflammatory infiltrates within the synovial membrane. *J Ultrason* 12: 202–213.

181. Garcia-Morteo, O., et al., 1988. Tarsal ankylosis in juvenile and adult onset rheumatoid arthritis. *J Rheumatol* 15: 298–300.
182. Smolen, J. S., et al., 2010. Treating rheumatoid arthritis to target: recommendations of an international task force. *Ann Rheum Dis* 69: 631–637.
183. Chan, E. S. L., and B. N. Cronstein. 2010. Methotrexate how does it really work? *Nat Rev Rheumatol* 6: 175–178.
184. Hench, P. S. 1949. The potential reversibility of rheumatoid arthritis. *Ann Rheum Dis* 8: 90–96.
185. Hench, P. S., et al., 1950. Effects of cortisone acetate and pituitary ACTH on rheumatoid arthritis, rheumatic fever and certain other conditions: a study in clinical physiology. *Arch Intern Med* 85: 545–666.
186. Ricciotti, E., and G. A. Fitzgerald. 2011. Prostaglandins and inflammation. *Arterioscler Thromb Vasc Biol* 31: 986–1000.
187. Crofford, L. J., et al., 1994. Cyclooxygenase-1 and -2 expression in rheumatoid synovial tissues. Effects of interleukin-1 $\beta$ , phorbol ester, and corticosteroids. *J Clin Invest* 93: 1095–1101.
188. Rouzer, C. A., and L. J. Marnett. 2009. Cyclooxygenases: structural and functional insights. *J Lipid Res* 50: S29.
189. Fattahi, M. J., and A. Mirshafiey. 2012. Prostaglandins and rheumatoid arthritis. *Arthritis* 2012: 1–7.
190. Hata, A. N., and R. M. Breyer. 2004. Pharmacology and signaling of prostaglandin receptors: multiple roles in inflammation and immune modulation. *Pharmacol Ther* 103: 147–166.
191. Shimizu, T. 2009. Lipid mediators in health and disease: enzymes and receptors as therapeutic targets for the regulation of immunity and inflammation. *Annu Rev Pharmacol Toxicol* 49: 123–150.
192. Masclee, G. M. C., et al., 2014. Risk of upper gastrointestinal bleeding from different drug combinations. *Gastroenterology* 147: 784-792.e9.
193. Wolfe, M. M., D. R. Lichtenstein, and G. Singh. 1999. Gastrointestinal toxicity of nonsteroidal antiinflammatory drugs. *N Engl J Med* 340: 1888–1899.
194. FitzGerald, G. A., and C. Patrono. 2001. The coxibs, selective inhibitors of cyclooxygenase-2. *N Engl J Med* 345: 433–442.

195. FitzGerald, G. A. 2004. Coxibs and cardiovascular disease. *N Engl J Med* 351: 1709–1711.
196. Trelle, S., et al., 2011. Cardiovascular safety of non-steroidal anti-inflammatory drugs: Network meta-analysis. *BMJ* 342: 154.
197. Farber, S., et al., 1947. The action of pteroylglutamic conjugates on man. *Science* 106: 619–621.
198. Jolivet, J., et al., 1983. The pharmacology and clinical use of methotrexate. *N Engl J Med* 309: 1094–1104.
199. Gubner, R., S. August, and V. Ginsberg. 1951. Therapeutic suppression of tissue reactivity. II. Effect of aminopterin in rheumatoid arthritis and psoriasis. *Am J Med Sci* 221: 176–182.
200. van der Heijde, D., et al., 2019. Tofacitinib in combination with Methotrexate in patients with rheumatoid arthritis: clinical efficacy, radiographic, and safety outcomes from a twenty-four-month, phase III study. *Arthritis Rheumatol* 71: 878–891.
201. Lipsky, P. E., et al., 2000. Infliximab and Methotrexate in the treatment of rheumatoid arthritis. *N Engl J Med* 343: 1594–1602.
202. Burmester, G. R., et al., 2017. Treatment efficacy and methotrexate-related toxicity in patients with rheumatoid arthritis receiving methotrexate in combination with adalimumab. *RMD Open* 3: 465: e000465.
203. Huttenhower, C., D. et al., 2012. Structure, function and diversity of the healthy human microbiome. *Nature* 486: 207–214.
204. Foster, K. R., et al., 2017. The evolution of the host microbiome as an ecosystem on a leash. *Nature* 548: 43–51.
205. Olszak, T., et al., 2012. Microbial exposure during early life has persistent effects on natural killer T cell function. *Science* 336: 489–493.
206. Ma, Y., et al., 2014. Oral administration of recombinant *Lactococcus lactis* expressing HSP65 and tandemly repeated P277 reduces the incidence of type I diabetes in non-obese diabetic mice. *PLoS ONE* 9: 105701.
207. Gomes-Santos, A. C., et al., 2017. Hsp65-producing *Lactococcus lactis* prevents inflammatory intestinal disease in mice by IL-10- and TLR2-dependent pathways. *Front Microbiol* 8: 30.
208. Wen, L., et al., 2008. Innate immunity and intestinal microbiota in the development of Type 1 diabetes. *Nature* 455: 1109–1113.

209. Lyons, A., et al., 2010. Bacterial strain-specific induction of Foxp3<sup>+</sup> T regulatory cells is protective in murine allergy models. *Clin Exp Allergy* 40: 811–819.
210. Secher, T., et al., 2017. Oral administration of the probiotic strain *Escherichia coli* Nissle 1917 reduces susceptibility to neuroinflammation and repairs experimental autoimmune encephalomyelitis-induced intestinal barrier dysfunction. *Front Microbiol* 8: 1096.
211. Nanda Kumar, N. S., et al., 2008. Probiotic administration alters the gut flora and attenuates colitis in mice administered dextran sodium sulfate. *J Gastroenterol Hepatol* 23: 1834–1839.
212. Calcinaro, F., et al., 2005. Oral probiotic administration induces interleukin-10 production and prevents spontaneous autoimmune diabetes in the non-obese diabetic mouse. *Diabetologia* 48: 1565–1575.
213. Valladares, R., et al., 2010. *Lactobacillus johnsonii* N6.2 mitigates the development of type 1 diabetes in BB-DP rats. *PLoS ONE* 5: e10507.
214. So, J. S., et al., 2008. *Lactobacillus casei* potentiates induction of oral tolerance in experimental arthritis. *Mol Immunol* 46: 172–180.
215. Mazmanian, S. K., J. L. Round, and D. L. Kasper. 2008. A microbial symbiosis factor prevents intestinal inflammatory disease. *Nature* 453: 620–625.
216. Ochoa-Repáraz, J., et al., 2010. A polysaccharide from the human commensal *Bacteroides fragilis* protects against CNS demyelinating disease. *Mucosal Immunol* 3: 487–495.
217. Maslowski, K. M., et al., 2009. Regulation of inflammatory responses by gut microbiota and chemoattractant receptor GPR43. *Nature* 461: 1282–1286.
218. Schuijjs, M. J., et al., 2015. Farm dust and endotoxin protect against allergy through A20 induction in lung epithelial cells. *Science* 349: 1106–1110.
219. McInnes, I. B., et al., 2003. A novel therapeutic approach targeting articular inflammation using the filarial nematode-derived phosphorylcholine-containing glycoprotein ES-62. *J Immunol* 171: 2127–2133.
220. Peón, A. N., et al., 2017. Helminth products potently modulate experimental autoimmune encephalomyelitis by downregulating neuroinflammation and promoting a suppressive microenvironment. *Mediators Inflamm* 2017: 1–16.
221. Finlay, C. M., et al., 2016. Helminth products protect against autoimmunity via innate type 2 cytokines IL-5 and IL-33, which promote eosinophilia. *J Immunol* 196: 703–714.

222. Eissa, M. M., et al., 2016. Anti-arthritic activity of *Schistosoma mansoni* and *Trichinella spiralis* derived-antigens in adjuvant arthritis in rats: tol<sub>r</sub> of FOXP3<sup>+</sup> treg cells. *PLoS ONE* 11: e0165916.
223. Grainger, J. R., et al., 2010. Helminth secretions induce de novo T cell Foxp3 expression and regulatory function through the TGF- $\beta$  pathway. *J Exp Med* 207: 2331–2341.
224. Tran, G. T., et al., 2017. Interleukin-5 mediates parasite-induced protection against experimental autoimmune encephalomyelitis: association with induction of antigen-specific CD4<sup>+</sup>CD25<sup>+</sup> T regulatory cells. *Front Microbiol* 8: 1453.
225. Zaccone, P., et al., 2009. *Schistosoma mansoni* egg antigens induce Treg that participate in diabetes prevention in NOD mice. *Eur J Immunol* 39: 1098–1107.
226. Hübner, M. P., et al., 2012. Helminth protection against autoimmune diabetes in nonobese diabetic mice is independent of a type 2 immune shift and requires TGF- $\beta$ . *J Immunol* 188: 559–568.
227. Hübner, M. P., J. Thomas Stocker, and E. Mitre. 2009. Inhibition of type 1 diabetes in filaria-infected non-obese diabetic mice is associated with a T helper type 2 shift and induction of FoxP3<sup>+</sup> regulatory T cells. *Immunology* 127: 512–522.
228. Mishra, P. K., et al., 2013. Prevention of type 1 diabetes through infection with an intestinal nematode parasite requires IL-10 in the absence of a Th2-type response. *Mucosal Immunol* 6: 297–308.
229. Liu, Q., et al., 2009. Helminth infection can reduce insulinitis and type 1 diabetes through CD25- and IL-10-independent mechanisms. *Infect Immun* 77: 5347–5358.
230. Salinas-Carmona, M. C., et al., 2009. Spontaneous arthritis in MRL/lpr mice is aggravated by *Staphylococcus aureus* and ameliorated by *Nippostrongylus brasiliensis* infections. *Autoimmunity* 42: 25–32.
231. Wilson, M. S., et al., 2005. Suppression of allergic airway inflammation by helminth-induced regulatory T cells. *J Exp Med* 202: 1199–1212.
232. Song, X., et al., 2011. Impact of *Schistosoma japonicum* infection on collagen-induced arthritis in DBA/1 mice: a murine model of human rheumatoid arthritis. *PLoS ONE* 6: e23453.
233. Kitagaki, K., et al., 2006. Intestinal helminths protect in a murine model of asthma. *J Immunol* 177: 1628–1635.
234. Mangan, N. E., 2004. Helminth infection protects mice from anaphylaxis via IL-10-producing B cells. *J Immunol* 173: 6346–6356.

235. Kitagaki, K., et al., 2006. Intestinal helminths protect in a murine model of asthma. *J Immunol* 177: 1628–1635.
236. Wilson, M. S., et al., 2005. Suppression of allergic airway inflammation by helminth-induced regulatory T cells. *J Exp Med* 202: 1199–1212.
237. Osada, Y., et al., 2009. Schistosoma mansoni infection reduces severity of collagen-induced arthritis via down-regulation of pro-inflammatory mediators. *Int J Parasitol* 39: 457–464.
238. Abdollahi-Roodsaz, S., S. B. Abramson, and J. U. Scher. 2016. The metabolic role of the gut microbiota in health and rheumatic disease: Mechanisms and interventions. *Nat Rev Rheumatol* 12: 446–455.
239. Scher, J. U., D. R. Littman, and S. B. Abramson. 2016. Microbiome in inflammatory arthritis and human rheumatic diseases. *Arthritis Rheumatol* 68: 35–45.
240. Meisel, M., et al., 2018. Microbial signals drive pre-leukaemic myeloproliferation in a Tet2-deficient host. *Nature* 557: 580–584.
241. Ma, C., et al., 2018. Gut microbiome-mediated bile acid metabolism regulates liver cancer via NKT cells. *Science* 360.
242. Scher, J. U., et al., 2012. Periodontal disease and the oral microbiota in new-onset rheumatoid arthritis. *Arthritis Rheum* 64: 3083–3094.
243. Hayashi, C., et al., 2010. Pathogen-mediated inflammatory atherosclerosis is mediated in part via toll-like receptor 2-induced inflammatory responses. *J Innate Immun* 2: 334–343.
244. Marchant, C., M. D. Smith, S. Proudman, D. R. Haynes, and P. M. Bartold. Et al., 2013. Effect of Porphyromonas gingivalis on citrullination of proteins by macrophages in vitro. *J Periodontol* 84: 1272–1280.
245. Maresz, K. J., et al., 2013. Porphyromonas gingivalis facilitates the development and progression of destructive arthritis through its unique bacterial peptidylarginine deiminase (PAD). *PLoS Pathog* 9: e1003627.
246. Vossenaar, E. R., et al., 2004. Expression and activity of citrullinating peptidylarginine deiminase enzymes in monocytes and macrophages. *Ann Rheum Dis* 63: 373–381.
247. Marietta, E., et al., 2016. Suppression of inflammatory arthritis by human gut-derived Prevotella histicola in humanized mice. *Arthritis Rheumatol* 68: 2878–2888.

248. Sakaguchi, S., et al., 2003. SKG mice, a new genetic model of rheumatoid arthritis. *Arthritis Res Ther* 5: 10–10.
249. Lucas, S., et al., 2018. Short-chain fatty acids regulate systemic bone mass and protect from pathological bone loss. *Nat Commun Commun* 9: 55.
250. Ivanov, I. I., et al., 2009. Induction of intestinal Th17 cells by segmented filamentous bacteria. *Cell* 139: 485–498.
251. Wu, H. J., et al., 2010. Gut-residing segmented filamentous bacteria drive autoimmune arthritis via T helper 17 cells. *Immunity* 32: 815–827.
252. Chen, B., et al., 2018. Presence of segmented filamentous bacteria in human children and its potential role in the modulation of human gut immunity. *Front Microbiol* 9: 1403.
253. Chen, J., et al., 2016. An expansion of rare lineage intestinal microbes characterizes rheumatoid arthritis. *Genome Med* 8: 43.
254. Baunwall, S. M. D., et al., 2020. Faecal microbiota transplantation for recurrent *Clostridioides difficile* infection: an updated systematic review and meta-analysis. *EClinicalMedicine* 29–30: 100642.
255. Zhang, X., et al., 2015. The oral and gut microbiomes are perturbed in rheumatoid arthritis and partly normalized after treatment. *Nat Med* 21: 895–905.
256. Picchianti-Diamanti, A., et al., 2018. Analysis of gut microbiota in rheumatoid arthritis patients: disease-related dysbiosis and modifications induced by etanercept. *Int J Mol Sci* 19: 2938.
257. Baharav, E., et al., 2004. Lactobacillus GG bacteria ameliorate arthritis in Lewis rats. *J Nutr* 134: 1964–1969.
258. Yamashita, M., et al., 2017. Preventive Effect of Lactobacillus helveticus SBT2171 on Collagen-Induced Arthritis in Mice. *Front Microbiol* 8: 1159.
259. Mohammed, A. T., et al., 2017. The therapeutic effect of probiotics on rheumatoid arthritis: a systematic review and meta-analysis of randomized control trials. *Clin Rheumatol* 36: 2697–2707.
260. Aqaiezhad Rudbane, S. M., et al., 2018. The efficacy of probiotic supplementation in rheumatoid arthritis: a meta-analysis of randomized, controlled trials. *Inflammopharmacology* 26: 67–76.

261. Brown, A. J., et al., 2003. The orphan G protein-coupled receptors GPR41 and GPR43 are activated by propionate and other short chain carboxylic acids. *J Biol Chem* 278: 11312–11319.
262. Maslowski, K. M., et al., 2009. Regulation of inflammatory responses by gut microbiota and chemoattractant receptor GPR43. *Nature* 461: 1282–1286.
263. Hui, W., et al., 2019. Butyrate inhibit collagen-induced arthritis via Treg/IL-10/Th17 axis. *Int Immunopharmacol* 68: 226–233.
264. Mizuno, M., et al., 2017. The dual role of short fatty acid chains in the pathogenesis of autoimmune disease models. *PLoS ONE* 12: e0173032.
265. Park, J., et al., 2019. Bidirectional regulatory potentials of short-chain fatty acids and their G-protein-coupled receptors in autoimmune neuroinflammation. *Sci Rep* 9: 1–13.
266. Flinn, J. H., et al., 1964. Excretion of tryptophan metabolites by patients with rheumatoid arthritis. *Arthritis Rheum* 7: 201–210.
267. Schroecksnadel, K., et al., 2006. Tryptophan degradation increases with stage in patients with rheumatoid arthritis. *Clin Rheumatol* 25: 334–337.
268. Schroecksnadel, K., et al., 2003. Increased degradation of tryptophan in blood of patients with rheumatoid arthritis. *J Rheumatol* 30: 1935–1939.
269. Wikoff, W. R., et al., 2009. Metabolomics analysis reveals large effects of gut microflora on mammalian blood metabolites. *Proc Natl Acad Sci U S A* 106: 3698–3703.
270. Brown, J., B. Robusto, and L. Morel. 2020. Intestinal dysbiosis and tryptophan metabolism in autoimmunity. *Front Immunol* 11: 1741.
271. Fan, Z., et al., 2020. The prophylactic effects of different Lactobacilli on collagen-induced arthritis in rats. *Food Funct* 11: 3681–3694.
272. Jin, U. H., et al., 2017. Short chain fatty acids enhance aryl hydrocarbon (Ah) responsiveness in mouse colonocytes and Caco-2 human colon cancer cells. *Sci Rep* 7: 10163.
273. Romagnoli, P. A., et al., 2016. Commensal metabolite indol-3-propionic acid promotes gut barrier function by regulating IL-22 production during intestinal inflammatory conditions. *J Immunol* 196.
274. Venkatesh, M., et al., 2014. Symbiotic bacterial metabolites regulate gastrointestinal barrier function via the xenobiotic sensor PXR and toll-like receptor 4. *Immunity* 41: 296–310.

275. Rothhammer, V., et al., 2016. Type I interferons and microbial metabolites of tryptophan modulate astrocyte activity and central nervous system inflammation via the aryl hydrocarbon receptor. *Nat Med* 22: 586–597.
276. Isawa, K., et al., 2002. Isolation and identification of a new bifidogenic growth stimulator produced by *Propionibacterium freudenreichii* ET-3. *Biosci Biotechnol Biochem* 66: 679–681.
277. Kang, J., T. Kim, and G. Moon. 2015. A novel *Lactobacillus casei* LP1 producing 1,4-dihydroxy-2-naphthoic acid, a bifidogenic growth stimulator. *Rev Nutr Food Sci* 20: 78–81.
278. Okamoto, H., et al., 2007. Anti-arthritis effects of vitamin K2 (menaquinone-4) - A new potential therapeutic strategy for rheumatoid arthritis. *FEBS Journal* 274: 4588–4594.
279. Ebina, K., et al., 2013. Vitamin K2 administration is associated with decreased disease activity in patients with rheumatoid arthritis. *Mod Rheumatol* 23: 1001–1007.
280. Abdel-Rahman, M. S., E. A. M. Alkady, and S. Ahmed. 2015. Menaquinone-7 as a novel pharmacological therapy in the treatment of rheumatoid arthritis: a clinical study. *Eur J Pharmacol* 761: 273–278.
281. Strandwitz, P. 2018. Neurotransmitter modulation by the gut microbiota. *Brain Res* 1693: 128–133.
282. Tian, J., et al., 2011. Oral GABA treatment downregulates inflammatory responses in a mouse model of rheumatoid arthritis. *Autoimmunity* 44: 465–470.
283. Bhat, R., et al., 2010. Inhibitory role for GABA in autoimmune inflammation. *Proc Natl Acad Sci U S A* 107: 2580–2585.
284. Tian, J., et al.,.  $\gamma$ -Aminobutyric acid inhibits T cell autoimmunity and the development of inflammatory responses in a mouse type 1 diabetes model. *J Immunol* 173: 5298–5304.
285. Poland, A., E. Glover, and A. S. Kende. 1976. Stereospecific, high affinity binding of 2,3,7,8-tetrachlorodibenzo-p-dioxin by hepatic cytosol. Evidence that the binding species is receptor for induction of aryl hydrocarbon hydroxylase. *J Biol Chem* 251: 4936–4946.
286. Denison, M. S., and S. R. Nagy. 2003. Activation of the aryl hydrocarbon receptor by structurally diverse exogenous chemicals. *Annu Rev Pharmacol Toxicol* 43: 309–343.

287. Vogel, C. F. A., and F. Matsumura. 2009. A new cross-talk between the aryl hydrocarbon receptor and RelB, a member of the NF- $\kappa$ B family. *Biochem Pharmacol* 77: 734–745.
288. Kimura, A., et al., 2009. Aryl hydrocarbon receptor in combination with Stat1 regulates LPS-induced inflammatory responses. *J Exp Med* 206: 2027–2035.
289. Itoh, K., et al., 1999. Keap1 represses nuclear activation of antioxidant responsive elements by Nrf2 through binding to the amino-terminal Neh2 domain. *Genes Dev* 13: 76–86.
290. West, A. P., et al., 2011. TLR signalling augments macrophage bactericidal activity through mitochondrial ROS. *Nature* 472: 476–480.
291. Kaul, N., and H. J. Forman. 1996. Activation of NF $\kappa$ B by the respiratory burst of macrophages. *Free Radic Biol Med* 21: 401–405.
292. Zhang, Y., et al., 2013. ROS play a critical role in the differentiation of alternatively activated macrophages and the occurrence of tumor-associated macrophages. *Cell Research* 23: 898–914.
293. Agidigbi, T. S., and C. Kim. 2019. Reactive oxygen species in osteoclast differentiation and possible pharmaceutical targets of ROS-mediated osteoclast diseases. *Int J Mol Sci* 20: 3576.
294. Kim, J., et al., 2019. Synergistic oxygen generation and reactive oxygen species scavenging by manganese ferrite/ceria co-decorated nanoparticles for rheumatoid arthritis treatment. *ACS Nano* 13: 3206–3217.
295. Sekine, H., et al., 2009. Hypersensitivity of Aryl hydrocarbon receptor-deficient mice to lipopolysaccharide-induced septic shock. *Mol Cell Biol* 29: 6391–6400.
296. Palatnik, A., H. Xin, and E. J. Su. 2016. Dichotomous effects of aryl hydrocarbon receptor (AHR) activation on human fetoplacental endothelial cell function. *Placenta* 44: 61–68.
297. Jia, Y., et al., 2019. Tetrandrine enhances the ubiquitination and degradation of Syk through an AhR-c-src-c-Cbl pathway and consequently inhibits osteoclastogenesis and bone destruction in arthritis. *Cell Death Dis* 10.
298. Kobayashi, E. H., et al., 2016. Nrf2 suppresses macrophage inflammatory response by blocking proinflammatory cytokine transcription. *Nat Commun* 7.
299. Kanzaki, H., et al., 2013. The Keap1/Nrf2 protein axis plays a role in osteoclast differentiation by regulating intracellular reactive oxygen species signaling. *J Biol Chem* 288: 23009–23020.

300. Nezu, M., et al., 2017. Nrf2 inactivation enhances placental angiogenesis in a preeclampsia mouse model and improves maternal and fetal outcomes. *Sci Signal* 10.
301. Zhao, M., et al., 2016. Nuclear Factor Erythroid 2-related Factor 2 Deficiency Exacerbates Lupus Nephritis in B6/lpr mice by Regulating Th17 Cell Function. *Sci Rep* 6.
302. Holtzclaw, W. D., A. T. Dinkova-Kostova, and P. Talalay. 2004. Protection against electrophile and oxidative stress by induction of phase 2 genes: The quest for the elusive sensor that responds to inducers. *Adv Enzy Regul* vol. 44. 335–367.
303. Hayes, J. D., A. T. Dinkova-Kostova, and M. McMahon. 2009. Cross-talk between transcription factors AhR and Nrf2: lessons for cancer chemoprevention from dioxin. *Toxicol Sci* 111: 199–201.
304. Miao, W., et al., 2005. Transcriptional regulation of NF-E2 p45-related factor (NRF2) expression by the aryl hydrocarbon receptor-xenobiotic response element signaling pathway: Direct cross-talk between phase I and II drug-metabolizing enzymes. *J Biol Chem* 280: 20340–20348.
305. Shin, S., et al., 2007. NRF2 modulates aryl hydrocarbon receptor signaling: influence on adipogenesis. *Mol Cell Biol* 27: 7188–7197.
306. Dudics, S., S. H. Venkatesha, and K. D. Moudgil. 2018. The micro-RNA expression profiles of autoimmune arthritis reveal novel biomarkers of the disease and therapeutic response. *Int J mol* 19.
307. McIntire, F. C., et al., 1967. Chemical, physical, and biological properties of a lipopolysaccharide from *Escherichia coli* K-235. *Biochemistry* 6: 2363–2372.
308. van Meerloo, J., G. J. L. Kaspers, and J. Cloos. 2011. Cell sensitivity assays: The MTT assay. *Methods Mol Biol* 237–245.
309. Livak, K. J., and T. D. Schmittgen. 2001. Analysis of relative gene expression data using real-time quantitative PCR and the 2- $\Delta\Delta$ CT method. *Methods* 25: 402–408.
310. Perkins, D. J., et al., 2018. Autocrine–paracrine prostaglandin E 2 signaling restricts TLR4 internalization and TRIF signaling. *Nat Immunol* 19: 1309–1318.
311. J, Nguyen., and A. Nohe. 2017. Factors that affect the osteoclastogenesis of RAW264.7 cells. *J Biochem Anal Stud* 2.
312. Kim, T. K., et al., 2018. Inhibition of VEGF-dependent angiogenesis and tumor angiogenesis by an optimized antibody targeting CLEC14a. *Mol Oncol* 12: 356–372.

313. Venkatesha, S. H., et al., 2011. Celastrus-derived celastrol suppresses autoimmune arthritis by modulating antigen-induced cellular and humoral effector responses. *J Biol Chem* 286: 14138–14146.
314. Langan, D., et al., 2021. Microbiota-derived metabolites, indole-3-aldehyde and indole-3-acetic acid, differentially modulate innate cytokines and stromal remodeling processes associated with autoimmune arthritis. *Int J Mol Sci* 22: 2017.
315. Means, T. K., et al., 2001. Differential effects of a toll-Like receptor antagonist on Mycobacterium tuberculosis -induced macrophage responses. *J Immunol* 166: 4074–4082.
316. Kong, L., W. Smith, and D. Hao. 2019. Overview of RAW264.7 for osteoclastogenesis study: phenotype and stimuli. *J Cell Mol Med* 23: 3077–3087.
317. Elshabrawy, H. A., et al., 2015. The pathogenic role of angiogenesis in rheumatoid arthritis. *Angiogenesis* 18: 433–448.
318. Xue, P., et al., 2019. CDDO-Me, Sulforaphane and tBHQ attenuate the RANKL-induced osteoclast differentiation via activating the NRF2-mediated antioxidant response. *Biochem Biophys Res Commun* 511: 637–643.
319. Dorożyńska, I., M. et al., 2014. Partial depletion of natural gut flora by antibiotic aggravates collagen induced arthritis (CIA) in mice. *Pharmacol Rep* 66: 250–255.
320. Lin, L., and J. Zhang. 2017. Role of intestinal microbiota and metabolites on gut homeostasis and human diseases. *BMC Immunology* 18.
321. Muszer, M., et al., 2015. Human microbiome: when a friend becomes an enemy. *Arch Immunol Ther Exp* 63: 287–298.
322. Blanco-Míguez, A., et al., 2017. MAHMI database: A comprehensive MetaHitbased resource for the study of the mechanism of action of the human microbiota. *Database* 2017.
323. de Oliveira, G. L. V., et al., 2017. Intestinal dysbiosis and probiotic applications in autoimmune diseases. *Immunology* 152: 1–12.
324. Xu, H., et al., 2020. Interactions between gut microbiota and immunomodulatory cells in rheumatoid arthritis. *Mediators Inflamm* .
325. Sittipo, P., J. W. Shim, and Y. K. Lee. 2019. Microbial metabolites determine host health and the status of some diseases. *Int J Mol Sci* 20.
326. Sanna, S., et al., 2019. Causal relationships among the gut microbiome, short-chain fatty acids and metabolic diseases. *Nat Genet* 51: 600–605.

327. Kang, K. Y., et al., 2015. Downregulation of tryptophan-related metabolomic profile in rheumatoid arthritis synovial fluid. *J Rheumatol* 42: 2003–2011.
328. Scott, D. L., F. Wolfe, and T. W. J. Huizinga. 2010. Rheumatoid arthritis. *The Lancet* 376: 1094–1108.
329. Noack, M., and P. Miossec. 2017. Selected cytokine pathways in rheumatoid arthritis. *Semin Immunopathol* 39: 365–383.
330. Amarasekara, D. S., et al., 2018. Regulation of osteoclast differentiation by cytokine networks. *Immune Netw* 18.
331. Yang, J., J. Yan, and B. Liu. 2018. Targeting VEGF/VEGFR to modulate antitumor immunity. *Front Immunol* 9: 978.
332. Kaur, S., et al., 2014. CD47 signaling regulates the immunosuppressive activity of VEGF in T cells. *J Immunol* 193: 3914–3924.
333. Huang, H. et al., 2015. VEGF suppresses T-lymphocyte infiltration in the tumor microenvironment through inhibition of NF- $\kappa$ B-induced endothelial activation. *FASEB Journal* 29: 227–238.
334. Abdel-Maged, A. E., et al., 2019. Efficacy and safety of Ramucirumab and methotrexate co-therapy in rheumatoid arthritis experimental model: involvement of angiogenic and immunomodulatory signaling. *Toxicol Appl Pharmac* 380: 114702.
335. Alexeev, E. E., et al., 2018. Microbiota-derived indole metabolites promote human and murine intestinal homeostasis through regulation of interleukin-10 receptor. *Am J Pathol* 188: 1183–1194.
336. Yu, J., et al., 2019. A tryptophan metabolite of the skin microbiota attenuates inflammation in patients with atopic dermatitis through the aryl hydrocarbon receptor. *J Allergy Clin Immunol* 143: 2108-2119.e12.
337. Swimm, A., et al., 2018. Indoles derived from intestinal microbiota act via type I interferon signaling to limit graft-versus-host disease. *Blood* 132: 2506–2519.
338. Waller, E. K., et al., 2014. Administration of a tryptophan metabolite, indole-3-carboxaldehyde, reduces graft versus host disease morbidity and mortality and enhances gastrointestinal barrier function in a murine model of allogeneic bone marrow transplantation. *Blood* 124: 2420–2420.
339. Cheng, Y., et al., Aryl Hydrocarbon Receptor Activity of Tryptophan Metabolites in Young Adult Mouse Colonocytes. *Drug Metab Dispos* 43: 1536–1543.

340. Jin, U. H., et al., 2014. Microbiome-derived tryptophan metabolites and their aryl hydrocarbon receptor-dependent agonist and antagonist activities. *Mol Pharmacol* 85: 777–788.
341. Cerezo, A. B., et al., 2019. Anti-VEGF signalling mechanism in HUVECs by melatonin, serotonin, hydroxytyrosol and other bioactive compounds. *Nutrients* 11.
342. Lin, X., et al., 2021. Nrf2 through aryl hydrocarbon receptor regulates IL-22 response in CD4<sup>+</sup> T cells. *J Immunol* 206: 1540–1548.
343. Liby, K. T., and M. B. Sporn. 2012. Synthetic oleanane triterpenoids: multifunctional drugs with a broad range of applications for prevention and treatment of chronic disease. *Pharmacol Rev* 64: 972–1003.
344. Powell, D. N., et al., 2020. Indoles from the commensal microbiota act via the AHR and IL-10 to tune the cellular composition of the colonic epithelium during aging. *Proc Natl Acad Sci U S A* 117: 21519–21526.
345. Hendriks, M., and S. K. Ramasamy. 2020. Blood vessels and vascular niches in bone development and physiological remodeling. *Front Cell Dev Biol* 8: 602278.
346. Nanjundaiah, S. M., et al., 2012. Celastrus and its bioactive celastrol protect against bone damage in autoimmune arthritis by modulating osteoimmune cross-talk. *J Biol Chem* 287: 22216–22226.
347. Alshammari, T. M., et al., 2015. Comparison of different serum sample extraction methods and their suitability for mass spectrometry analysis. *Saudi Pharm J* 23: 689–697.